VILNIUS GEDIMINAS TECHNICAL UNIVERSITY

Šarūnas MIKUČIONIS

MODELLING OF STRATIFIED DIELECTRIC MEDIUM STRIPLINE DELAY DEVICES

DOCTORAL DISSERTATION

TECHNOLOGICAL SCIENCES,
ELECTRICAL AND ELECTRONIC ENGINEERING (01T)

Vilnius LEIDYKLA TECHNIKA 2014

Doctoral dissertation was prepared at Vilnius Gediminas Technical University in 2010–2014.

Supervisor

Prof Dr Vytautas URBANAVIČIUS (Vilnius Gediminas Technical University, Electrical and Electronic Engineering – 01T).

The Dissertation Defense Council of Scientific Field of Electrical and Electronic Engineering of Vilnius Gediminas Technical Unive-rsity:

Chairman

Prof Dr Jurij NOVICKIJ (Vilnius Gediminas Technical University, Electrical and Electronic Engineering – 01T).

Members:

Prof Dr Romas BARONAS (Vilnius University, Informatics – 09P),

Dr Andrius KATKEVIČIUS (Vilnius Gediminas Technical University, Electrical and Electronic Engineering – 01T),

Dr Bartlomiej SALSKI (Warsaw University of Technology, Electrical and Electronic Engineering – 01T),

Dr Rimantas SIMNIŠKIS (State Research Institute Center for Physical Sciences and Technology, Electrical and Electronic Engineering – 01T).

The dissertation will be defended at the public meeting of the Dissertation Defense Council of Electrical and Electronic Engineering in the Senate Hall of Vilnius Gediminas Technical University at **2 p. m. on 16 January 2015**.

Address: Saulėtekio al. 11, LT-10223 Vilnius, Lithuania.
Tel.: +370 5 274 4956; fax +370 5 270 0112; e-mail: doktor@vgtu.lt

A notification on the intended defending of the dissertation was sent on 15 December 2014.

A copy of the doctoral dissertation is available for review at the Internet website http://dspace.vgtu.lt/ and at the Library of Vilnius Gediminas Technical University (Saulėtekio al. 14, LT-10223 Vilnius, Lithuania).

VGTU leidyklos TECHNIKA 2302-M mokslo literatūros knyga

ISBN 978-609-457-750-5

© VGTU leidykla TECHNIKA, 2014
© Šarūnas Mikučionis, 2014
sarunas.mikucionis@gmail.com

VILNIAUS GEDIMINO TECHNIKOS UNIVERSITETAS

Šarūnas MIKUČIONIS

SLUOKSNIUOTOS DIELEKTRINĖS TERPĖS JUOSTELINIŲ VĖLINIMO ĮTAISŲ MODELIAVIMAS

MOKSLO DAKTARO DISERTACIJA

TECHNOLOGIJOS MOKSLAI,
ELEKTROS IR ELEKTRONIKOS INŽINERIJA (01T)

VGTU
LEIDYKLA
TECHNIKA
Vilnius 2014

Disertacija rengta 2010–2014 metais Vilniaus Gedimino technikos universitete.

Vadovas

prof. dr. Vytautas URBANAVIČIUS (Vilniaus Gedimino technikos universitetas, elektros ir elektronikos inžinerija – 01T).

Vilniaus Gedimino technikos universiteto elektros ir elektronikos inžinerijos mokslo krypties disertacijos gynimo taryba:

Pirmininkas

prof. dr. Jurij NOVICKIJ (Vilniaus Gedimino technikos universitetas, elektros ir elektronikos inžinerija – 01T).

Nariai:

prof. dr. Romas BARONAS (Vilniaus universitetas, informatika – 09P),

dr. Andrius KATKEVIČIUS (Vilniaus Gedimino technikos universitetas, elektros ir elektronikos inžinerija – 01T),

dr. Bartlomiej SALSKI (Varšuvos technologijos universitetas, elektros ir elektronikos inžinerija – 01T),

dr. Rimantas SIMNIŠKIS (Valstybinis mokslinių tyrimų institutas Fizinių ir technologijos mokslų centras, elektros ir elektronikos inžinerija – 01T).

Disertacija bus ginama viešame Elektros ir elektronikos inžinerijos mokslo krypties disertacijos gynimo tarybos posėdyje **2015 m. sausio 16 d. 14 val.** Vilniaus Gedimino technikos universiteto senato posėdžių salėje.

Adresas: Saulėtekio al. 11, LT-10223 Vilnius, Lietuva.

Tel.: (8 5) 274 4956; faksas (8 5) 270 0112; el. paštas doktor@vgtu.lt

Pranešimai apie numatomą ginti disertaciją išsiusti 2014 m. gruodžio 15 d.

Disertaciją galima peržiūrėti interneto svetainėje http://dspace.vgtu.lt/ ir Vilniaus Gedimino technikos universiteto bibliotekoje (Saulėtekio al. 14, LT-10223 Vilnius, Lietuva).

Abstract

Problem of investigation of stripline delay devices in stratified dielectric medium is considered in the dissertation.

In the first chapter scientific publications regarding modelling of stripline delay devices and microwave devices in planar stratified dielectric medium, issued from 1976 to 2014 year are analytically reviewed. Areas of applications, methods of analysis and design and problems in modelling and design are analyzed.

In the second chapter models of coupled and multiconductor microstrip lines in nonhomogenous dielectric medium are analyzed. Conditions for ensuring normal wave propagation in the lines are researched. Such lines can serve as the basis for stripline meander delay line modelling. The possibilities of equalizing phase velocities for odd and even normal wave propagation in coupled striplines in stratified dielectric medium are analyzed. The effect of air microlayer in double shielded stripline devices is reseached by using the created model.

Techniques for synthesis, i.e. obtaining constructional parameters according to the desired electrical characteristics of multiconductor microstrip lines operating in even and odd normal mode have been created and researched. The proposed technique is based on iterative calculation of characterisitics by changing parameters, until the desired characteristic value is obtained.

Effect of equalizing phase velocities of electromagnetic wave in strips of microstrip meander delay line to frequency characteristics have been investigated. Meander delay line based on the multiconductor line operating in even mode was designed and its characteristics were calculated using commercial software.

Influence of air microlayer in packaged double shielded meander stripline delay line has been investigated. The delay line was designed and its characteristics were calculated by two different techniques – the proposed modelling technique combined with S-matrix method and modelled with comercial software based on the method of moments. A prototype double shielded meander delay line has been produced and its characteristics have been measured in order to check the correctness of the model. Comparisson of calculations and measurement differed by no more than 2%.

Reziumė

Disertacijoje nagrinėjama juostelinių mikrobangų vėlinimo įtaisų sluoksniuotoje dielektrinėje terpėje modeliavimo problema.

Pirmajame skyriuje analitiškai apžvelgtos 1974–2014 m. mokslinės publikacijos apie vėlinimo ir kitus mikrobangų įtaisus sluoksniuotame dielektrike. Išnagrinėtos tokių įtaisų taikymo sritys, analizės ir projektavimo metodai.

Antrajame skyriuje išanalizuoti susietųjų ir daugialaidžių juostelinių linijų nevienalyčiame dielektrike modeliai, išnagrinėtos normaliųjų bangų režimo sudarymo sąlygos jose. Šios linijos naudojamos kaip pagrindas meandrinių vėlinimo linijų modeliams. Išnagrinėtos galimybės suvienodinti lyginės ir nelyginės bangų sklidimo greičius susietosiose juostelinėse linijose, naudojant daugiasluoksnę dielektrinę terpę. Naudojant sukurtus modelius išnagrinėta oro mikrosluoksnio įtaka dviekranių juostelinių įtaisų elektrinėms charakteristikoms.

Sukurtos ir ištirtos daugialaidžių mikrojuostelinių linijų, veikiančių normaliųjų bangų režimu sintezės, t. y. konstrukcinių parametrų radimo pagal norimas elektrines charakteristikas radimo metodikos. Siūloma metodika grįsta iteraciniu charakteristikų skaičiavimu keičiant parametrus iki pasiekiamos norimos charakteristikos.

Išnagrinėtos elektromagnetinių bangų fazinių greičių suvienodinimo įtaka meandrinės mikrojuostelinės vėlinimo linijos charakteristikoms. Suprojektuota ir komercine programine įranga ištirta meandrinė mikrojuostelinė vėlinimo linija, grįsta daugialaidės mikrojuostelinė linijos veikiančios lyginės modes režimu, modeliu.

Išnagrinėta oro mikrosluoksnio įtaka dviekranės meandrinės juostelinės vėlinimo linijos charakteristikoms. Suprojektuota dviekranė meandrinė vėlinimo linija ir jos charakteristikos paskaičiuotos dviem metodais – hibridiniu metodu, grįstu baigtinių skirtumų ir S-parametrų matricų metodais, ir momentų metodu grįsta komercine programine įranga. Siekiant patikrinti kompiuterinio modeliavimo adekvatumą buvo pagamintas ir ekperimentiškai ištirtas dviekranės meandrinės vėlinimo linijos prototipas. Skirtumas tarp apskaičiuotų ir išmatuotų reikšmių neviršyjo 2%.

Notations

Symbols

C	–	capacitance
c_0	–	velocity of the electromagnetic wave in free space (vacuum), 299792458 m/s
C_1	–	unit length capacitance
G	–	Green's function
L_1	–	unit length inductance
q	–	electric charge
S	–	gap size between adjacent conductors
V	–	voltage
v_p	–	phase velocity
W	–	width of the conductor
Z	–	characteristic impedance
λ	–	wavelength
ε_0	–	the electric constant, $8.854\,187\,817 \times 10^{-12}$ F/m
$\varepsilon_{r\,eff}$	–	effective relative dielectric permittivity
ε_r	–	relative dielectric permittivity
Ω	–	ohm

Abbreviations

BEM	–	boundary element method
CML	–	coupled microstrip line
CMOS	–	complementary metal-oxide-semiconductor structure
DD	–	delay device
DL	–	delay line
DSM	–	double shielded microstrip
FDTD	–	finite difference time domain
FEM	–	finite element method
IC	–	integrated circuit
IEM	–	inverted embedded microstrips
LTCC	–	low temperature co-fired ceramics
MCL	–	multiconductor line
MCML	–	multiconductor microstrip line
MIMI	–	metal-insulator-metal-insulator
MIS	–	metal insulator semiconductor
MoM	–	method of moments
PCB	–	printed circuit board
PEC	–	perfect electric conductor
PEMC	–	perfect electromagnetic conductor
SW	–	slow-wave
SWD	–	slow-wave device
TFMSL	–	thin film microstrip line
VLSI	–	very large scale of integration

Contents

Introduction

Problem Formulation

Slow wave devices are widely used in modern electronic equipment. The structure of such devices, as of most other integrated electronic devices until the beginning of the 21st century used to be planar – signal conductors were placed in a single plane. In the last two decades however, structure of modern electronic devices and microwave equipment in general is undergoing a transformation from planar to 3D structure. The reasons for that change are the need to reduce the volume and mass of the devices, improve characteristics by shortening signal paths and/or gain new functionality of devices.

In case of 3D structures, signal conductors are embedded between dielectric layers in various patterns, thus the stratified structure of dielectrics and conductors is created.

Interaction between signal conductors in different layers, and effect of stratified medium on the propagation of electromagnetic waves is poorly investigated.

Slow wave devices in stratified dielectric medium have not been investigated in detail and no technique for synthesis of multiconductor lines, in which electromagnetic waves propagate with equal phase velocities, has been presented. Such lines can be used as basis for design of slow wave devices.

Therefore the hypothesis is formulated in the dissertation, that by applying numerical EM modeling techniques it is possible:

- to find the conditions which cause equal phase velocities along the conductors of the non-uniform dielectric delay devices;
- to calculate electrical characteristics of the delay device in the stratified dielectric medium by utilizing the quasi-TEM approach;
- to evaluate the effect of the stratified dielectric medium on the frequency characteristics of the delay devices.

Relevance of the Thesis

In the field of electronics, delay devices are used in various electronic circuits. It might be used in a feedback path of a generator. Delay lines are critical in phased antenna arrays in order to control their directivity. Particular types of digital signal communications rely heavily on precise arrival of signals, therefore, if electrical lenghts of signal paths is different, delay line is necessary to synchronize signals on input.

Various types of delay lines exist. One way of delay line classification is dividing into two categories: active and electrodynamic. Active delay lines are based on active components (transistors, amplifiers) to delay an electrical signal. Electrodynamic delay lines are based on signal electrical path. The simplest case of such delay line is a transmission line of particular non-zero length. It is shaped into more compact shape – in most cases meander or helical. The electrodynamic delay lines are simpler and cheaper to produce and have very low energy consumption.

Due to constantly arising new applications of delay devices it is necessary to create efficient design technique for the new structures of the delay devices. Those can be in PCBs, packaged electronics or inside IC topology.

Synthesis techniques for finding constructional parameters by the given required electrical characteristics are required for design. If straightforward synthesis procedures are unavailable, analysis of the model is repeated iteratively, and parameters of the model are varied until the constructional parameters to meet the required characteristics are found.

In most cases, structure of the delay devices is planar. However in recent years, 3D stratified structures are also designed. Therefore due to wide application of delay devices it is necessary to create models for 3D stratified structures.

The Object of Research

The main object of investigation is multiconductor stripline and microstrip structures in stratified dielectric medium, and meander delay line in stratified dielectric medium based on the model of a multiconductor stripline or multiconductor microstrip line.

The Aim of the Thesis

The main goal of this thesis is to investigate dependencies of electrical characteristics of the delay devices in stratified dielectric medium by creating and utilizing models based on numerical techniques.

The Objectives of the Thesis

The following objectives have been set in order to achieve the defined aim of the thesis:

1. To investigate the conditions needed to excite normal wave propagation in multiconductor microstrip lines and a possibility to equalize phase velocities for even and odd normal modes in stratified dielectric coupled lines by creating a mathematical model and implementing it in software.
2. To find dependencies of electrical characteristics of microstrip multiconductor lines on their constructional parameters by creating a synthesis technique of multiconductor microstrip lines, operating in normal mode, and implementing it in software.
3. To analyze the characteristics of the meander microstrip delay line based on the model of multiconductor microstrip line operating in even normal mode.
4. To investigate influence of air gap on the characteristics of the double shielded (“sandwich” type) meander stripline delay line.

Research Methodology

The research technique used in this dissertation is numerical modelling of electromagnetic fields in the analyzed structure. Two numerical methods are

incorporated – the method of moments (MoM) and the finite difference (FD) method. Quasi-TEM approach is utilized in order to simplify the task from 3D to 2D, thereby reducing computational requirements. Conditions of normal modes in coupled and multiconductor striplines are analyzed and applied for meander stripline design. Additionally, S-matrix method and commercial MoM software (Sonnet®) is used for analysis of the created models of delay lines. The designed and produced delay device prototype was measured using sampling oscilloscope PicoScope 9312 from Pico Technology Ltd. The results of modelling are compared to the published ones achieved by other researchers, and in one case – compared to the experimental data.

Scientific Novelty of the Thesis

Despite the fact, that planar slow wave device is not a new concept in the field of microwave electronics, application of modern design and production technologies require incorporating of the well-known devices into new designs. The mentioned tasks require an efficient and accurate design technique, which, because of complicated stratified dielectric structures is not readily available. In this dissertation new methods of evaluating effect of the stratified medium on the electrical characteristics of delay devices are introduced.

Research performed in this dissertation led to the following results, new in the scientific field of Electrical and electronic engineering:

1. New mathematical model for analysis of the multiconductor microstrip line in stratified dielectric has been presented.
2. A technique for synthesis of the multiconductor microstrip line, operating in even or odd normal mode has been created.
3. A technique for finding the conditions of equal phase velocities for even and odd normal modes in coupled lines in stratified dielectric has been presented.

Practical Value of the Research Findings

Modern communications equipment relies on complex interaction between various microwave devices. Signal delay devices play significant role in microwave circuitry. Since most modern devices are constructed in ICs and PCBs (cases of stratified medium), deeper knowledge about delay devices in stratified medium can help design more efficient devices.

1. Technique for synthesis of multiconductor microstrip lines operating in normal mode has been created. Results of the synthesis can be used in design of slow-wave devices.
2. Technique for modelling of coupled striplines in stratified dielectric medium, for which phase velocities for even and odd mode are equal. Such transmission lines have reduced crosstalk. In addition, slow-wave devices based on such coupled striplines have lower phase distortion and hence potentially wider frequency band. Moreover, such properties are also useful in designing filters, couplers and similar microwave devices.
3. The influence of air microlayer in double shielded stripline meander delay line on its electrical characteristics has been investigated.

The created models of coupled, multiconductor and delay lines can be used in CAD software for designing DLs in stratified medium.

The Defended Statements

1. By applying iterative analysis algorithm based on the Newton-Rapson method, widths of the conductors can be altered to ensure even or odd normal mode propagation along the line, so the modal voltages differ by no more than 2%, and phase velocities differ by no more than 3%.
2. Particular combination of thicknesses of dielectric layers of different dielectric permittivities can be used to equalize phase velocities for even and odd normal modes in coupled stripline in stratified dielectric medium.
3. Phase distortions can be reduced by 2% creating a meander microstrip delay line based on the model of the multiconductor microstrip line operating in even normal mode.
4. Increase of the normalized thickness of the air microlayer, occurring as a result of non-zero conductor thickness, from 0 to 0.1 in a double shielded stripline meander delay line can reduce phase velocity by up to 5%. Increase of the normalized thickness of the air microlayer, occurring as a result of imprecise placement of the shield, from 0 to 0.05 can reduce phase velocity by up to 20%

Approval of the Research Findings

Results of research have been published in 10 articles: 4 articles in Thomson Reuters ISI Web of Science database journals with impact factor (Martavičius *et al*. 2007; Mikučionis, Urbanavičius 2010a; Mikučionis, Urbanavičius 2011, Krukonis *et al.* 2013), 6 articles in journals referenced and abstracted in other international databases: (Mikučionis 2012; Krukonis, Mikučionis 2013) are indexed/abstracted in ICONDA, Gale®: Academic OneFile, InfoTrac Custom; ProQuest: Ulrichsweb™, Summon™; EBSCOhost: Academic Search Complete; IndexCopernicus databases; (Mikučionis *et al.* 2014) is indexed in INSPEC and SCOPUS databases; (Mikučionis, Urbanavičius 2010b) is indexed in IEEE database.

Results have also been presented in 10 conferences: 1 in international conference abroad (Warsaw,Poland), 5 in international conferences in Lithuania and 4 in local conferences.

List of conferences:

- Š. Mikučionis. 2007. Surištųjų linijų modelis/Model of Coupled Lines. Scientific conference "Science – Future of Lithuania: Electronics and Electrical Engineering". 2007. Vilnius, Lithuania.
- Š. Mikučionis. 2010. Normaliosios modos daugialaidėse mikrojuostelinėse linijose/Normal Modes in Multiconductor Microstrip Lines. International scientific conference "Electronics' 2010". Vilnius, Kaunas, Lithuania.
- Š. Mikučionis, V. Urbanavičius. 2010. Investigation of Normal Modes in Microstrip Multiconductor Line Using MoM. 18th International Conference on Microwave, Radar and Communications (Mikon 2010). Vilnius, Lithuania.
- Š. Mikučionis. 2011. Normaliųjų bangų sužadinimo sąlygos daugialaidėse mikrojuostelinėse linijose/Conditions of Normal Modes Excitation in Multiconductor Microstrip Lines. Scientific conference "Science – Future of Lithuania: Electronics and Electrical Engineering 2010". Vilnius, Lithuania.
- Š. Mikučionis, V. Urbanavičius. 2011. Synthesis of Multiconductor Line using the Method of Moments. International scientific conference "Electronics' 2011". Vilnius, Kaunas, Lithuania.
- Š. Mikučionis. 2011. Synthesis of Multiconductor Microstrip lines Operating in Normal Mode. International conference "Young Scientist Towards the Chalanges of Modern Technology 2011". Warsaw. Poland

- Krukonis, Š. Mikučionis. 2012. Susietųjų linijų nevienalytėje terpėje modelis, grįstas BSLS metodu/FDTD Based Model of Coupled Lines in a Non-Uniform Dielectric Medium. Scientific conference "Science – Future of Lithuania: Electronics and Electrical Engineering 2012". Vilnius, Lithuania.
- Mikučionis, Šarūnas, Urbanavičius, Vytautas. 2012. Quasi-tem analysis of coupled microstrip lines on multilayered dielectric. The 22nd International Conference "Electromagnetic Disturbances EMD'2012"Vilnius, Lithuania.
- Mikučionis Šarūnas. 2013. Fazinių greičių netolygumo įtaka mikrojuostelinių meandrinių vėlinimo linijų charakteristikoms/Influence of Phase Velocity on the Characteristics of the Meander Microstrip Delay Lines. Scientific conference "Science – Future of Lithuania: Electronics and Electrical Engineering 2013". Vilnius, Lithuania.

Dissertation Structure

Dissertation consists of introduction, 4 chapters, general conclusions, references list, list of author's scientific publications on the topic of the dissertation and summary in Lithuanian.

Volume of the dissertation is 119 pages excluding annexes. Dissertation contains 47 figures, 8 tables, 62 numbered formulas, 70 references are used.

1

Overview of Stripline Slow Wave and Other Microwave Devices in Stratified Dielectric Medium and Their Research Techniques

Overview of stripline slow wave devices and similar microwave devices in stratified dielectric medium is presented in this chapter. Examples of the devices and their applications are presented. Examples of modelling techniques are mentioned. Conclusions of overview are drawn and aims of the thesis are set.

1.1. Microwave Devices in Stratified Dielectric Medium

Only in very rare, almost exceptional cases scientists and engineers deal with uniform dielectric medium when designing electronic devices. The majority of modern devices include various structures consisting of conductors, semiconductors, dielectrics and other materials of various complexities. Even the simplest of semiconductor devices might be produced using several types of

semiconductor materials, dielectrics and conductors, properties of which can be significantly different and therefore influence the electrical characteristics of the device.

In the field of microwave design, particular role belongs to stratified dielectric medium. Integrated circuits (IC) are always produced in layers (Evans *et al.* 2012), larger scale microwave devices in most case have at least two dielectric layers – the dielectric substrate, on which the device is formed, and the surrounding air (Xu & Chen 2011). In practice, however, much more complicated structures are not uncommon.

Such device structure plays a major role for signal and wave propagation in the device, therefore structure of medium has to be taken into account when designing a device.

In this thesis devices having stratified dielectric medium are investigated. General structure of such device is composed of arbitrary number of dielectric layers, having arbitrary parameters (thickness, dielectric permittivity), and conductors situated in that dielectric structure (Fig. 1.1).

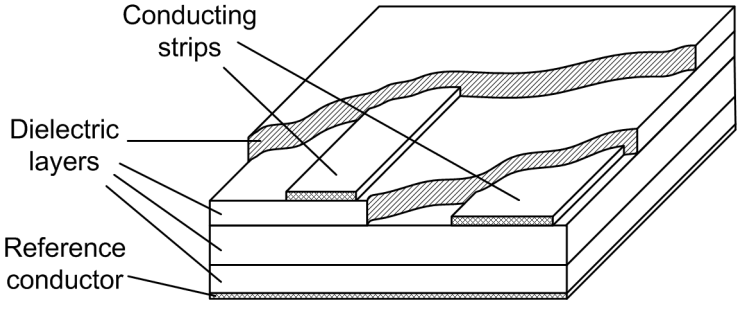

Fig. 1.1. General structure of the conductors in the stratified dielectric medium

The aforementioned structure may also have ground (reference conductor) planes on top and sides of the structure. Conductors can also be situated between different layers of dielectrics and can be interconnected in different ways (Musa & Sadiku 2008).

Various strip-like conductor devices in stratified dielectric medium have been researched by scientist throughout the world in the past half-century. The simplest case of the considered structures is a microstrip transmission line in a stratified dielectric (Bauer & Menzel 2010). However, these also differ in structure. Layer of air between a suspended substrate and reference conductor shield introduces layered medium effect (Awasthi *et al.* 2005). Very thin layers like bonding materials for adhering conductors to a PCB substrate also create

multilayer structure, effect of which has to be taken into account for higher frequencies (Vo *et al.* 2002). Multilayer transmission structures widely used in ICs like thin film-microstrip line (TFMSL), metal-insulator-metal-insulator (MIMI) structures or inverted embedded microstrips (IEM) are also cases of stratified medium (Zhang & Song 2007). Another type of popular stratified medium is low temperature co-fired ceramics (Bauer & Menzel 2010).

Properties of stratified dielectric structures also allow to design microwave devices like filters (Kim & Myoung 2005), couplers (Yang & Jeong 2006). Radiative and resonant properties of striplines can be used for antennas (Wu *et al.* 2006; Braaten *et al.* 2009; Lucido 2012).

Stratified medium introduces additional complexity for analysis and design of the devices, however in most cases it is necessary to deal with it. Firstly, there might be a need to design a device in a predefined IC dielectric and/or semiconductor layer pattern (on-chip device). As an example, a transmission line for ultra-wideband pulse propagation on a 0.25 μm CMOS chip can be given (Liao & Nguyen 2007). By changing the structure of a stratified substrate, losses can be reduced and velocity improved for a 60 GHz suspended microstrip line in a CMOS chip by combining different thicknesses of Si_3N_2, polyimide and lossy Si layers (Prasad *et al.* 2008). High speed interconnects in multilayer packaged electronic systems were analyzed in order to improve their performance in mutigigaherz frequency range (Cangellaris & Wu 2008).

Additional layers of dielectric can also enhance particular characteristics of devices. Tightly coupled microstrip lines present a problem of cross-talk. One of the offered solutions for this issue is creating an overlay dielectric above the lines (Muthana & Kroger 2007). Usually a slow wave device is designed to have the least dispersion of characteristics, however, in some cases, as e.g. analog signal processing frequency selective delay time is required. Size of the device can be reduced and its characteristics improved by using multilayered structure (Gupta & Sounas 2012). Higher order mode leakage in microstrip transmission line is a common problem in high frequency circuits. It might case crosstalk and undesired coupling between circuits. It has been shown, that, introduction of an additional dielectric layer with particular properties, and additional conductor can reduce this problem significantly (Zhou & Xu 2005).

Research of stratified dielectric medium is not only limited to microwave devices, its effects are also important for digital electronic equipment, like noise coupling in multilayer computing PCBs like computer mainboards or graphics cards (Engin *et al.* 2006).

Due to wide application potential and simplicity of production, strip-like conductor structures in general have been researched widely in recent decades. CAD tools for full wave modelling of 2D and 3D planar microwave devices on high temperature superconductor including material losses and anisotropy were

created (Vendik *et al.* 2003). Slow wave microstrip line in multilayer insulator and semiconductor structure was modeled using quasi-TEM approach and single layer reduction technique. Such structures are common in CMOS and high-electron-mobility transistor (HEMT) structures (Verma & Sharma 2004).

General study of dispersion characteristics of multilayer microstrip lines on SiO_2-Si-SiO_2 substrate with thin metal ground in VLSI semiconductor chips was performed by using spectral domain approach (Zhang & Song 2005). Shielded microstrips on stratified dielectric were analyzed in full-wave (Gnilenko 2007).

Importance of stratified dielectric medium is not only limited to characteristics of electronic devices. The analysis of stratified dielectric medium is also useful in non destructive material analysis application (Aschen 2011) or measurement of dielectric layer thickness (Ghasr & Zoughi 2008).

Particular combinations of dielectric layers can reduce electromagnetic wave reflections from surfaces, which can be used for radome design (Fitzek & Rasshofer 2009), frequency selective reflection and transmission surfaces (Choubani *et al.* 2006), and applied in areas of geophysical probing, material science and biological research (Zeng & Delisle 2010).

Stratified medium also includes biological medium. This has to be taken into account when designing spiral microstrip antenna for a microwave therapy (Hou & Gao 2009).

1.2. Slow Wave Devices in Stratified Dielectric Medium

1.2.1. Slow Wave Devices

For certain electronic devices it is necessary to have a particular delay of a propagating signal (wave). Such properties can be used in various electronic systems like antennas (Park & Jeon 2013), analog to digital converters (Li *et al.* 2009), phase shifters (Wei *et al*. 2013), time synchronization (Hsu & Wen 2007) and other applications for analog time domain signal processing (Xiang *et al*. 2012). It is commonly called a delay line. The two main characteristics for a delay line are delay time, measured in time units, and bandwidth, which indicates the frequency range, in which the signal is delayed by a specified time, and is not distorted. In addition to that, physical size of the device is also important. Reduction of size of the delay line, while keeping the delay time and bandwidth unchanged can be done by altering the surrounding dielectric medium of the device.

1.2.2. Effects and Usage of Stratified Medium

The effects of stratified dielectric on the characteristics of the meander line are poorly investigated.

Other approaches have been made to reduce the size of the delay line without reducing delay time and/or bandwidth. One of them was making meander 3-dimensional (situated in space rather than in one plane) (Jiang & Ruimin 2009). Another was also making a structure 3-dimensional and creating quasi-coaxial interconnections between the layers (Kim 2008). However no publications of investigating the effect of stratified dielectric medium for planar meander delay line were found.

1.3. Analysis Techniques of Microwave Devices in Stratified Dielectric Medium

In this chapter, brief description of methods of analysis of microwave devices in stratified dielectric medium is given.

1.3.1. Quasi-TEM Approach

In this subsection basic principles of applying the quasi-TEM mode are described.

In general case, electromagnetic waves of various configurations propagate in microstrip lines at various phase velocities. However influence of longitudinal electromagnetic field components on general wave configuration can be neglected in a wide frequency range, for cases when dimensions of a cross section of the microstrip line are significantly smaller than the wavelength (Pozar 2011). Thus quasi-TEM approach can be used in the analysis of microstrip lines.

By utilizing the quasi-TEM approach, dynamic characteristics of the system can be expressed from static parameters, and significant part of 3D problems can be solved as 2D ones. Such approach simplifies the calculations and reduces requirements for computational resources with little loss of accuracy.

In case of non-magnetic materials, phase velocities and characteristic impedances can be calculated by knowing unit length capacitances of the conductors (Han *et al.* 2009).

The stripline structure can be considered infinitely long and can be modeled by only investigated cross-section of the structure (Bhadauria & Kumar 2010).

It is known (Nannapaneni Narayana Rao 2004) that, in case of TEM mode, characteristic impedance of the line is expressed as:

$$Z = \sqrt{\frac{L_1}{C_1}}, \tag{1.1}$$

where L_1 is a unit length inductance and C_1 is a unit length capacitance of the conductor. In case of such line the following is correct:

$$L_1 C_1 = \mu\varepsilon = \mu_0 \mu_r \varepsilon_0 \varepsilon_r, \tag{1.2}$$

where μ_r is relative magnetic permeability of the dielectric, ε_r is relative dielectric permittivity of the dielectric, μ_0 is the magnetic constant and ε_0 is the electric constant. According to the Equation (1.2), $L_1 = \mu\varepsilon / C_1$, in that case Equation (1.1) can be rewritten as:

$$Z = \frac{\sqrt{\mu\varepsilon}}{C_1}. \tag{1.3}$$

In this thesis, only non-magnetic dielectrics, i.e. $\mu_r = 1$, are considered since these are the most common in microwave devices. Equation (1.3) is modified to:

$$Z = \frac{\sqrt{\varepsilon_r}}{c_0 C_1}, \tag{1.4}$$

where $c_0 = 1/\sqrt{\mu_0 \varepsilon_0}$ is the velocity of the electromagnetic wave in vacuum (and air).

It is clear that by utilising the quasi-TEM approach, it is sufficient to analyse only the cross-section of the structure, and in case of non-magnetic matereials, it is sufficient to find the capacitances of the conductors.

Equation (1.4) can be applied in case of uniform dielectric medium. In case the dielectric medium is not uniform, the concept of the effective relative dielectric permittivity $\varepsilon_{r\,eff}$ is applied. The system with arbitrary dielectric medium is modelled as if the dielectric medium was a uniform dielectric with particular relative dielectric permittivity $\varepsilon_{r\,eff}$. It is calculated by:

$$\varepsilon_{r\,eff} = \frac{C_1}{C_1^{(a)}}, \tag{1.5}$$

where C_1 is the unit length capacitance of the investigated line, and $C_1^{(a)}$ is the unit length capacitance of the same line, with all dielectrics replaced by air. By utilising this value, Equation (1.4) is expressed as:

$$Z = \frac{1}{c_0 \sqrt{C_1 C_1^{(a)}}}. \tag{1.6}$$

Therefore, in order to find the effective dielectric permittivity $\varepsilon_{r\,eff}$, and characteristic impedance Z, by applying the quasi-TEM approach it is sufficient to calculate two capacitances of the line.

1.3.2. Analysis Techniques

All analysis methods of microwave devices can be divided into four categories: analytic, numeric, hybrid and empirical.

Analytical methods are based on mathematical closed form expressions. These are simple to implement and usually have low demand in computational recources. The main drawback of these methods is their applicability only to the simple structures. Yet analytical methods are applicable for the microwave devices in stratified medium. Analytical methods for modelling of planar windings in stratified medium for induction heating applications have been created (Acero & Alonso 2006). Circuit model of a multilayer semiconductor slow-wave microstrip line in metal-insulator-semiconductor (MIS) and Schottky contact structures has been also published (Verma & Sharma 2004). Analytical expressions have been derived for evaluating of reflection from stratified dielectrics, backed by perfect electromagnetic conductor (PEMC) layer (Nayyeri *et al.* 2011).

Numerical methods incorporate numerical solutions of differential and/or integral field equations (Štaras 2008). Analytical problems, which are very complex or impossible to solve otherwise, are turned into series of simple arithmetic operations, which are usually performed on a computer (Steer *et al.* 2002). One of the widely used techniques for analysis of planar microstrip and stripline structures is the method of moments (MoM)(Khalil *et al.* 1999; Urbanavičius & Martavičius 2006). The basis for the MoM is the Green's function. Expression of Green's function for stratified medium is very complicated due to Sommerfeld integrals involved, and much effort has been made to simplify the procedure. One of the most frequently mentioned is the discrete complex image method (Ling & Jin 2000; Ge & Esselle 2002; Karan *et al.* 2009; Su *et al.* 2012). Vector transform solution procedure for finding Green's functions (Weiss & Kilic 2010), Equivalent Medium Approach (Bianconi *et al.* 2010).

However, the MoM is not the only tool used for analysis of electromagnetic wave propagation in stratified medium. The finite difference time domain (FDTD) method has been found useful for stratified medium. It was used for

modelling of reflection of incident plane wave to stratified lossy dispersive medium (Liang *et al.* 2009; Chen & Xu 2012). It has also been used for modelling of aperture coupled microstrip antennas in stratified cylindrical medium (He 2006). The more exotic case – microwave emission from stratified and non-uniform lunar surface has been modeled by the finite element method (FEM) (Jin & Fa 2010).

Finite difference and finite elements have also been employed in modelling of electrodynamic delay devices (Šileikis *et al*. 2000), (Urbanavičius & Pomarnacki 2008).

Hybrid methods are some combination of both – analytic and numerical methods. In fact, most numerical techniques can be considered hybrid, since it takes analytical manipulations of expressions until numerical methods can be applied. Usage of these methods is also common in electrodynamics (Scarlatos *et al.* 2005)

Empirical methods are usually interpolated and/or extrapolated experiment results. Empirical methods are very reliable, however, precise devices have to be made, and measurements must also be of very high accuracy, therefore the cost of obtaining data is also high. Experiments regarding wave propagation in stratified media have been performed. Radio wave propagation has been measured over ice-salt water (Dembelov *et al.* 2012). Ultrawideband pulse propagation in microstrip structures in stratifiedd CMOS structure have been measured (Chirala & Nguyen 2006).

At the time of writing the thesis, numerical and hybrid techniques were used the most. Increasing computational capabilities of computers have further increased popularity of numerical techniques.

The first attempts to model the effect of stratified medium for the characteristics of microwave devices have been described in publications in 1970s (Itoh & Mittra 1974), and were still developed to the time of writing this dissertation (Ye *et al.* 2013).

1.3.3. Method of Moments

In this subchapter fundamentals of the method of moments (MoM) are presented. The MoM is applied for investigation of normal modes in stratified dielectric medium in this dissertation. It is used for calculation of the charge distribution in the cross-section of the conductors in stripline structures.

The MoM, also known as the boundary element method (BEM), is the numerical technique for solving linear partial differential equations, which have been formulated as integral equations. It is applicable to problems, for which Green's functions can be calculated. Greens function in case of electromagnetic

modelling is an expression of potential at a particular point in space in terms of unit point charge at some other point and distance between the two points.

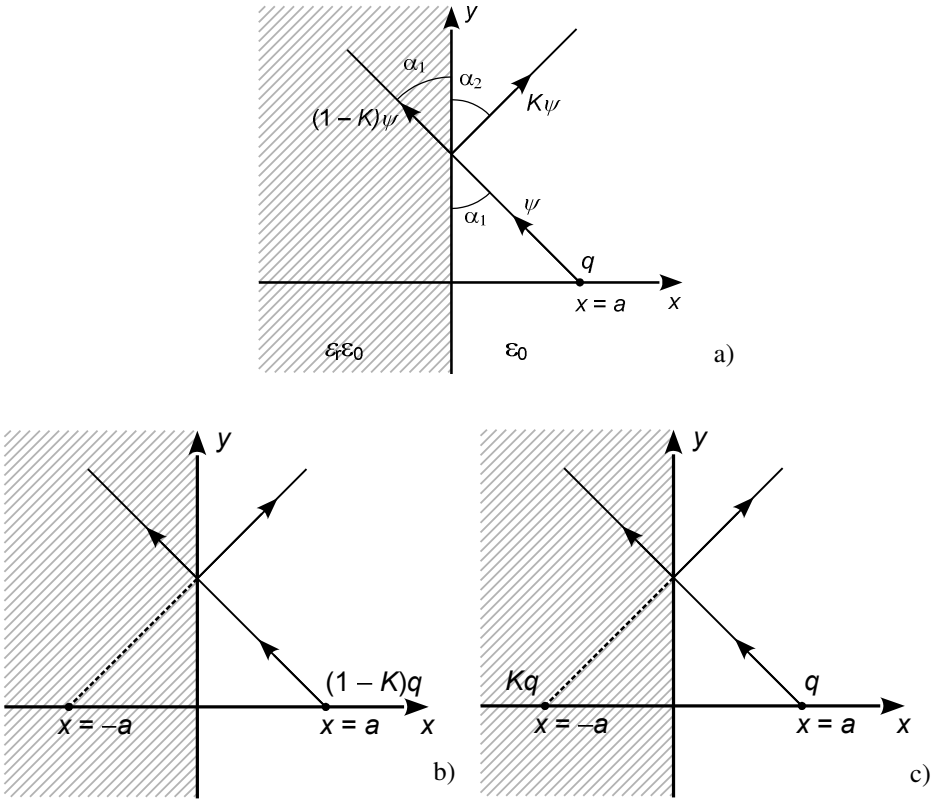

Fig. 1.2. Principles of the partial images technique: a) line charge near dielectric boundary, b) modeling of the electric field in the region of the dielectric, c) modeling of the electric field in the region of air

Partial Images Technique

In calculations used in this thesis, the technique of partial images applied, in order to be able to apply the MoM. The technique is described in detail in (Silvester & Ferrari 1996).

The basis for the partial images technique is presented in this subsection. The simplest case of stratified medium is two dielectric layers, or half-spaces. One half space is air, another – dielectric with relative dielectric permittivity ε_r.

Infinitely long line charge q is present near the dielectric boundary, parellel to z axis (Fig. 1.2 (a)). Electric field flux ψ is emanating in all directions from the line charge. Consider one line of the flux passing the dielectric interface. Some part – $(1 - K)\psi$ passes through the dielectric boundary, the remaining part $-K\psi$ is reflected back. By applying a boundary condition, that the normal component of the electric flux must be continuous at the dielectric interface:

$$(1-K)\psi\sin\alpha_1 = \psi\sin\alpha_1 - K\psi\sin\alpha_2, \tag{1.7}$$

it is obvious, that $\alpha_1 = \alpha_2$.

By applying another boundary condition, that parallel component of the electric flux must also be continuous through the dielectric boundary:

$$\frac{1}{\varepsilon_r\varepsilon_0}(1-K\psi\cos\alpha_1) = \frac{1}{\varepsilon_0}(\psi\cos\alpha_1 - K\psi\cos\alpha_1), \tag{1.8}$$

then:

$$K = -\frac{\varepsilon_r - 1}{\varepsilon_r + 1}. \tag{1.9}$$

The coefficient K is independent on incident angle, and can have values from −1 to 0. It can be similarly shown, that if flux from dielectric into air is analysed, coefficient K has the same but opposite in sign value.

This case can be modelled in the following way. The reflection of the charge is modelled by the point charge, situated symmetrically to the original point charge, with respect to the dielectric boundary plane. Therefore, when modelling in the region of the dielectric (left half-space) (Fig. 1.2 (b)), the electric field is modelled by the point charge in place of the original one in the point $(a,0)$, with charge of $(1 - K)q$. In the other half space (Fig. 1.2 (c)), electric field is modelled as a superposition of two charges – the original one in the point $(a,0)$, and its mirror charge (with respect to boundary plane) of magnitude q in the point $(-a,0)$.

Therefore, the Green's function in the dielectric region is expressed:

$$G(P_j : P_i) = -\frac{1-K}{4\pi\varepsilon_0\varepsilon_r}\ln\left[(x_j - a)^2 + y_j^2\right], \tag{1.10}$$

and Green's function in air region:

$$G(P_j : P_i) = -\frac{1}{4\pi\varepsilon_0}\left\{\ln\left[(x_j - a)^2 + y_j^2\right] + K\ln\left[(x_j + a)^2 + y_j^2\right]\right\}. \tag{1.11}$$

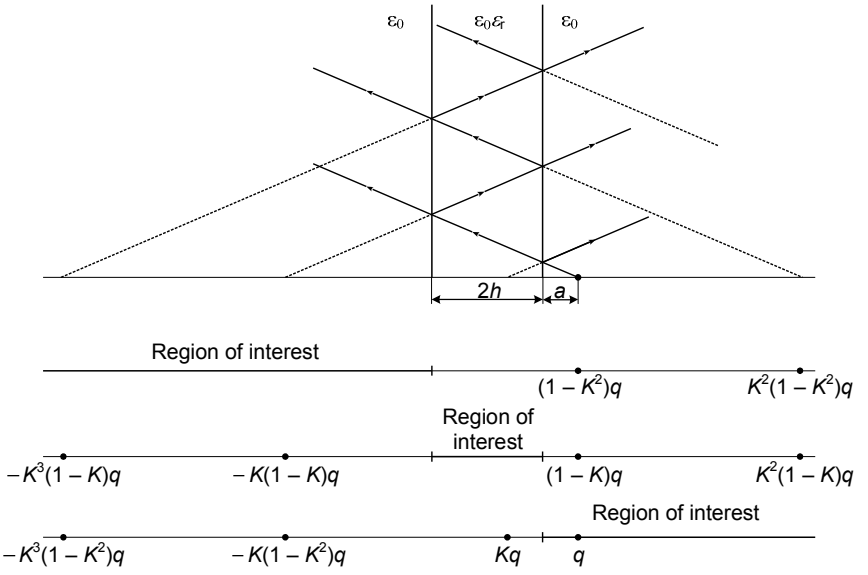

Fig. 1.3. A line charge near the dielectric slab, and its partial images

In order to have a structure more similar to the real microstrip line, a reference conductor plate should be present under the dielectric layer. The presence of such layer can be modeled by mirror charges, i.e. charges of the same magnitude, but opposite polarity situated symmetrically to the plane of the reference conductor.

Consider a line charge, near a dielectric slab of finite thickness $2h$ (Fig. 1.3). By applying the same analysis as in the example above, it is seen that multiple reflections of electric field flux are present, which can be modelled by series of partial charge images. Depending on the region of interest, i.e. the region, in which electric field is being expressed, partial charge images are positioned according to the reflection lines.

Such technique can be applied for modelling of planar microstrip structures. The influence of the reference conductor of the microstrip line can be modelled by making the mirror image of the line with respect to the reference conductor plane.

Microstrip line is a basic part of stripline devices, therefore, its model is used as basis for all other microstrip device models.

In order to apply the method of moments for the microstrip line, cross section of the line of width W is divided into N smaller sub-strips or segments. Charge of every segment is said to be concentrated in the center of each segment

of width ΔW, and is considered as a point charge in a cross-section of the microstrip line (Fig. 1.4). Potentials at the centers of every segment are expressed as a superposition of all point charges of the analyzed system. This way the system of linear equations is made, which can be further solved by any known technique for the purpose.

The solution of the system of linear equations is the discrete charge distribution in the cross section of the line.

According to this technique, influence on potential of point of every charge is expressed in 6 steps:

Step 1. Potential at point P_j created by the charge of the same point q_j and it's first partial image Kq_j is expressed by:

$$\varphi\left(P_j : P_j\right) = -\frac{\left(1+K\right)q_i}{2\pi\varepsilon_0}\left[\ln\left(\frac{\Delta W}{2}\right)-1\right], \tag{1.12}$$

where $K = -\dfrac{\varepsilon_r - 1}{\varepsilon_r + 1}$ – reflection coefficient, ε_0 – dielectric constant.

Step 2. Potential at point P_j created by all remaining charges of q_j is expressed by:

$$\varphi\left(P_j : P_j\right) = \frac{K\left(1-K^2\right)q_j}{2\pi\varepsilon_0}\sum_{n=1}^{\infty} K^{2(n-1)}\ln\left(4nh\right). \tag{1.13}$$

Step 3. Potential at point P_j, created by mirror charge $-q_j$ and all its partial images is expressed by:

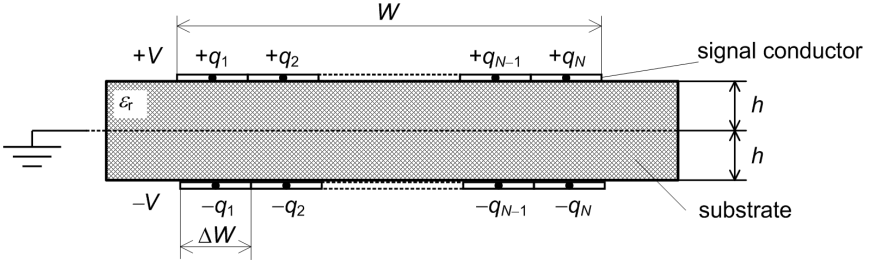

Fig. 1.4. Modelling of microstrip line

$$\varphi\left(P_j : P_{j'}\right) = \frac{K\left(1-K^2\right)q_j}{2\pi\varepsilon_0}\sum_{n=1}^{\infty} K^{2(n-1)} \ln\left[\left(4n-2\right)h\right]. \quad (1.14)$$

Step 4. Potential at point P_j, created by charges q_i situated in all points P_i ($1 \le i \le N$ and $i \ne j$, where $N = N_1 + N_2$ – number of all unknown charges), and their first partial images Kq_j is expressed by:

$$\varphi\left(P_j : P_i\right) = -\frac{\left(1+K\right)q_i}{2\pi\varepsilon_0} \ln\left(\Delta W \cdot \left|i-j\right|\right). \quad (1.15)$$

Step 5. Potential at point P_j, created by all reaming partial charges of q_i situated in all points P_i, is expressed by:

$$\varphi\left(P_j : P_i\right) = \frac{K\left(1-K^2\right)q_i}{4\pi\varepsilon_0}\sum_{n=1}^{\infty} K^{2(n-1)} \ln\left[\left(\Delta W \cdot \left|i-j\right|\right)^2 + \left(4nh\right)^2\right]. \quad (1.16)$$

Step 6. Potential at point P_j, created by mirror charges $-q_i$ at points $P_{i'}$ and all their partial images is expressed by:

$$\varphi\left(P_j : P_i\right) = \frac{\left(1-K^2\right)q_i}{4\pi\varepsilon_0}\sum_{n=1}^{\infty} K^{2(n-1)} \ln\left\{\left(\Delta W \cdot \left|i-j\right|\right)^2 + \left[\left(4n-2\right)h\right]^2\right\}. \quad (1.17)$$

Full potential at point P_j is expressed by summing all components of potential at that point. Expressions of full potentials of all points are found and equation system is built.

It is seen from formulas, that in most cases summing goes to infinity, however implementing infinite sum is impossible on a computer. Therefore in software implementation a limited number of additions is chosen.

By designating potential of the n^{th} conductor as V_n:

$$\begin{cases} V_1 = & G_{11}q_1 + G_{12}q_2 + & \ldots & + G_{1N}q_N \\ V_2 = & G_{21}q_1 + G_{22}q_2 + & \ldots & + G_{2N}q_N \\ \ldots & \ldots & \ldots & \ldots \\ V_N = & G_{N1}q_1 + G_{N2}q_2 + & \ldots & + G_{NN}q_N \end{cases}, \quad (1.18)$$

or in matrix form:

$$[\mathbf{V}] = [\mathbf{G}] \times [\mathbf{q}]. \quad (1.19)$$

Coefficients G_{ij} define potential at point P_i created by charge q_j in Equation (1.18). In case under consideration, coefficients G_{ij} are expressed by adding potentials, expressed by Equations (1.12) to (1.17), and dividing by charge q_j:

$$G_{ij} = \sum_{j=1}^{N} \phi\left(P_i : P_j\right). \tag{1.20}$$

Column-matrix of unknown charges is calculated by solving linear equation system (1.19).

Capacitances per unit length of conducting strips at particular voltages are determined by summing all unit length charges of sub-strips:

$$C_1 = \sum_{i=1}^{N_1} q_i \,, C_2 = \sum_{i=N_1+1}^{N_2} q_i \,, \ldots C_N = \sum_{i=N_{N-1}+1}^{N_N} q_i \,. \tag{1.21}$$

Characteristic impedances and effective relative dielectric permittivity are calculated by Equations (1.5)–(1.6).

1.3.4. The Finite Difference Method

In this subchapter basics of the finite difference (FD) method are presented. This method is used for analysis of the layered dielectric medium in this thesis.

Basics of the Finite Difference Method

In general, the FD method is a numerical technique for obtaining approximate solution of the differential equations.

Electrostatic problems are solved by using:

$$\operatorname{div} \vec{D} = \rho(x, y, z) \,, \tag{1.22}$$

where $\operatorname{div} \vec{D}$ is the divergence of the electric displacement field (electric inductance), ρ is the charge density at coordinates x, y and z. Noting that

$$\vec{D} = \varepsilon_0 \varepsilon_r \vec{E} \,, \tag{1.23}$$

and

$$\vec{E} = -\operatorname{grad} \varphi \,, \tag{1.24}$$

equation (1.22) can be rearranged to:

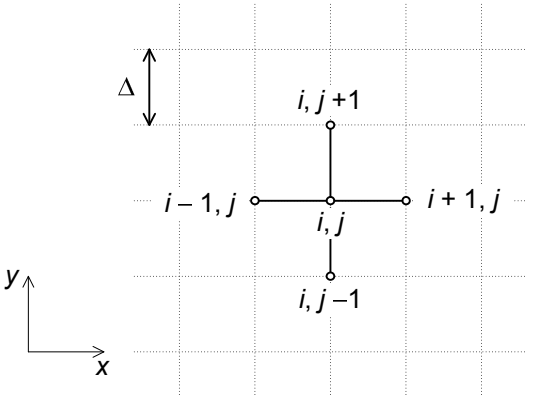

Fig. 1.5. Finite difference mesh

$$\text{div grad}\,\varphi = -\frac{\rho(x,y,z)}{\varepsilon_0 \varepsilon_r}, \tag{1.25a}$$

where φ is the electric potential, ε_0 is the dielectric constant and ε_r is the relative dielectric permittivity.

The last equation (Eq. 1.25a) is also known as the Poisson's equation. When applied in Cartesian coordinate system, it can be expressed as:

$$\frac{\partial^2 \varphi}{\partial x^2} + \frac{\partial^2 \varphi}{\partial y^2} + \frac{\partial^2 \varphi}{\partial z^2} = -\frac{\rho(x,y,z)}{\varepsilon_0 \varepsilon_r}, \tag{1.25b}$$

or

$$\nabla^2 \varphi = -\frac{\rho(x,y,z)}{\varepsilon_0 \varepsilon_r}, \tag{1.25c}$$

where $\varepsilon = \varepsilon_0 \varepsilon_r$ is the absolute dielectric permittivity, and ∇^2 is the Laplace operator, given by:

$$\nabla^2 = \frac{\partial^2}{\partial x^2} + \frac{\partial^2}{\partial y^2} + \frac{\partial^2}{\partial z^2}. \tag{1.26}$$

If no free charges are present, the Poisson equation can be simplified to Laplace equation and in two-dimensional case it becomes:

$$\frac{\partial^2 \varphi}{\partial x^2} + \frac{\partial^2 \varphi}{\partial y^2} = 0 . \tag{1.27}$$

The second order partial derivatives can be expressed using finite differences.

Two dimensional space is divided into elementary cells by uniform Cartesian mesh. Integers i and j denote the numbers of mesh nodes, and mesh step is constant:

$$x_{i+1} - x_i = x_i - x_{i-1} = \Delta x , \tag{1.28a}$$

$$y_{i+1} - y_i = y_i - y_{i-1} = \Delta y , \tag{1.28b}$$

where $\Delta x = \Delta y = \Delta$.

The first order derivative of potential in the space between the nodes with indices i, j, and $i + 1, j$ is expressed as

$$\frac{\partial \varphi}{\partial x} \cong \frac{\varphi_{i+1,j} - \varphi_{i,j}}{\Delta} , \tag{1.29a}$$

and the first derivative between points i, j, and $i - 1, j$ is expressed as:

$$\frac{\partial \varphi}{\partial x} \cong \frac{\varphi_{i,j} - \varphi_{i-1,j}}{\Delta} . \tag{1.29b}$$

Then approximate second order derivative is expressed as:

$$\frac{\partial^2 \varphi}{\partial x^2} \cong \frac{\left(\varphi_{i+1,j} - \varphi_{i,j}\right)/\Delta - \left(\varphi_{i,j} - \varphi_{i-1,j}\right)/\Delta}{\Delta} = \frac{\varphi_{i+1,j} + \varphi_{i-1,j} - 2\varphi_{i,j}}{\Delta^2} . \tag{1.29c}$$

The second order partial derivative in y direction is expressed in the similar way:

$$\frac{\partial^2 \varphi}{\partial y^2} \cong \frac{\varphi_{i,j+1} + \varphi_{i,j-1} - 2\varphi_{i,j}}{\Delta^2} . \tag{1.30}$$

By substituting Equations (1.29c) and (1.30) into the Laplacian equation (Eq. 1.20), it becomes:

$$\varphi_{i+1,j} + \varphi_{i-1,j} + \varphi_{i,j+1} + \varphi_{i,j-1} - 4\varphi_{i,j} = 0 , \tag{1.31a}$$

and can be further modified to:

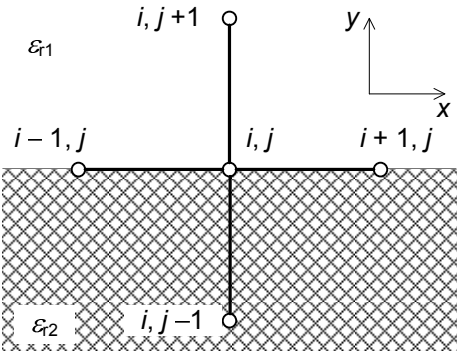

Fig. 1.6. Finite difference mesh at the boundary of dielectrics

$$\varphi_{i,j} = \frac{\varphi_{i+1,j} + \varphi_{i-1,j} + \varphi_{i,j+1} + \varphi_{i,j-1}}{4}. \tag{1.31b}$$

Equation (1.31b) is an expression of a numerical second order derivative in a uniform dielectric medium.

In this thesis, nonuniform dielectric medium is considered. In case of non-uniform dielectric medium, the mesh is created so, that the nodes are exactly on the boundary between the dielectric materials.

According to Gauss law, in the absence of free charges:

$$\frac{\partial D_x}{\partial x} + \frac{\partial D_y}{\partial y} = 0, \tag{1.32}$$

where D_x and D_y are component of the electric displacement field.

At known potentials of the adjacent nodes, first order derivatives of D_x and D_y are given by:

$$\frac{\partial D_y}{\partial y} = \frac{D_{i,j+1/2} - D_{i,j-1/2}}{\Delta} = -\frac{\varepsilon_0}{\Delta^2}\left[\varepsilon_{r1}\left(\varphi_{i,j+1} - \varphi_{i,j}\right) - \varepsilon_{r2}\left(\varphi_{i,j} - \varphi_{i,j-1}\right)\right], \tag{1.33a}$$

and similarly

$$\frac{\partial D_x}{\partial x} = \frac{\varepsilon_0 \varepsilon_{r3}}{\Delta^2}\left(\varphi_{i+1,j} + \varphi_{i-1,j} - 2\varphi_{i,j}\right), \tag{1.33b}$$

where ε_{r3} is the relative effective dielectric permittivity at the boundary of dielectrics.

By substituting Equations (1.33a) and (1.33b) into (1.32), the potential of the node on the boundary of dielectric materials is expressed:

$$\varphi_{i,j} = \frac{\varepsilon_{r1}\varphi_{i,j+1} + \varepsilon_{r2}\varphi_{i,j-1} + \varepsilon_{r3}\left(\varphi_{i+1,j} + \varphi_{i-1,j}\right)}{\varepsilon_{r1} + \varepsilon_{r2} + \varepsilon_{r3}}. \tag{1.34}$$

Then the value of the relative effective dielectric permittivity ε_{r3} can be found assuming that potentials $\varphi_{i-1,j}$, $\varphi_{i+1,j}$ and $\varphi_{i,j}$ are related as:

$$\varepsilon_{r1}\varphi_{i,j+1} + \varepsilon_{r2}\varphi_{i,j-1} = \varepsilon_{r3}\left(\varphi_{i-1,j} + \varphi_{i+1,j}\right). \tag{1.35}$$

Thus,

$$\varepsilon_{r3} = \frac{\varepsilon_{r1}\varphi_{i,j+1} + \varepsilon_{r2}\varphi_{i,j-1}}{\varphi_{i-1,j} + \varphi_{i+1,j}}, \tag{1.36a}$$

which, in case of close values of potentials can be expressed as:

$$\varepsilon_{r3} \cong \frac{\varepsilon_{r1} + \varepsilon_{r2}}{2}. \tag{1.36b}$$

In such way values of the relative dielectric permittivity at dielectric boundaries can be replaced by value calcultaed by Equation (1.36b) and perform iterations using Equation (1.34).

It is seen, that despite the fact that FD method is iterative, and all region must be discretised, as opposed to the MoM, simplicity of handling non-uniform dielectric media makes it a favourable method for the tasks of this thesis.

1.4. Normal Modes in Stratified Dielectric Medium

Definition of modes in case of multiconductor structures is quite complicated and ambiguous. In case of multiconductor systems, normal mode (or normal wave) is the ratio of amplitudes of voltages (or currents), for which velocities of a propagating waves along every conductor are equal.

Consider any infinitely long system of multiple conductors. In case the surrounding medium is uniform, wave propagation phase velocities in all conductors are equal. In case the surrounding medium is non uniform, electromagnetic field is distributed in materials with different properties, intensities of the field are different, therefore phase velocities of waves, travelling along the conductors in general case are different.

The main parameter, which determines the velocity of wave propagation, is the effective dielectric permittivity $\varepsilon_{\mathrm{r\,eff}}$. According to the quasi-TEM approach, distribution of the electric field depends on the structure of the system investigated, and voltages of the conductors.

The effective dielectric permittivity indicates the ratio of capacities of the system of conductors (Eq. 1.5).

In case of stripline structures, one of the main characteristics of every conducting strip is its unit length capacitance C_1, by calculating the unit length capacitance of the same conducting strip, with all dielectrics replaced by air $C_1^{(\mathrm{a})}$, the effective dielectric permittivity can be calculated. In case of non magnetic materials (relative magnetic permeability $\mu_{\mathrm{r}} = 1$), phase velocity v_{p} of the wave travelling along the conductor can be expressed as

$$v_{\mathrm{p}} = \frac{\mathrm{c}_0}{\sqrt{\varepsilon_{\mathrm{r\,eff}}}}, \tag{1.37}$$

where c_0 – is the velocity of the electromagnetic wave in air (vacuum).

Effective dielectric permittivity is highly dependent upon the structure of the surrounding medium of the conductors and the distribution of the electromagnetic field.

The structure of electromagnetic field depends on the amplitude ratios of waves, travelling along the conductors.

In general, in a system consisting of *N* signal conductors and a reference conductor, there can exist *N* modes. Each mode is defined by *N* amplitude values, and the corresponding phase velocity value, for which phase velocities of the propagating wave are equal along every conductor.

These modes are referred to as normal modes, or, with a reference to mathematical terms, eigenmodes, and the corresponding phase velocity as the corresponding eigenvalue.

Normal mode in case of milticonductor lines (MCL) is achieved when phase velocities $v_{\mathrm{p}i}$ of the electromagnetic wave along *i*-th microstrip conductor are the same:

$$v_{\mathrm{p}1} = v_{\mathrm{p}2} = \ldots = v_{\mathrm{p}N}, \tag{1.38}$$

where $v_{\mathrm{p}i}$ is calculated by Equation (1.37). Since c_0 is constant, $\varepsilon_{\mathrm{r\,eff}}$ must be the same for all microstrip conductors in order to excite a normal mode. Modal voltages in an MCL are calculated using partial capacitance matrices $[\mathbf{C}_1]$ and $\left[\mathbf{C}_1^{(\mathrm{a})}\right]$. The matrix $[\mathbf{C}_1]$ is a square $N \times N$ matrix, where *N* is the number of

microstrip conductors of an MCL, and each element of the matrix C_{1ij} is capacitance per unit length of *j*-th microstrip conductor, when voltage of *i*-th microstrip conductor equals to 1 V, and voltages of other conductors are equal to 0. $\left[\mathbf{C}_1^{(a)}\right]$ is the similar matrix of the same MCL with free space in place of the dielectric substrate. When both matrices are known, modal voltages can be found by calculating eigenvalues of the relative effective dielectric permittivity vector by solving generalized eigenvalue equation:

$$[\mathbf{C}_1][\mathbf{V}] = [\varepsilon]\left[\mathbf{C}_1^{(a)}\right][\mathbf{V}]. \tag{1.39}$$

The resulting matrix $[\mathbf{V}]$ is matrix, rows of which correspond to voltages of different modes, and $[\varepsilon]$ is a column-matrix, members of which are effective dielectric permittivities for each mode.

The concept of modes is applied to the multiconductor systems in stratified dielectric medium as well as for any other multiconductor system with non-uniform dielectric medium. As mentioned before, in general case, *N* modes can exist. But in case of planar multiconductor lines, two modes are of primary importance – odd mode and even mode. When voltage values of all conductors are of the same polarity (but not necessarily of the same value), and phase velocities are equal – *c* mode. When voltages of adjacent conductors are of opposite polarities, and the condition of equal phase velocities is satisfied, it is referred to as the π mode.

Modal voltages can be calculated by using static analysis, which is used in quasi-TEM mode.

It should also be noted, that characteristic impedances of the conductors are also different for different modes. This has to be taken into account when modelling devices based on multiconductor line model (such as meander delay line) in order to evaluate the matching of characteristic impedances along the path of electromagnetic wave.

In order to increase the delay time of a slow wave device (SWD), the path of wave propagation is increased. Conductor of the SWD is shaped into meander (serpentine) or spiral (helical) (Guo & Shiue 2006). In such case, structure of the SWD becomes periodic or quasi-periodic.

Periodic conductor system is effectively modeled by corresponding multiconductor line (MCL). When model of the MCL is created, it is necessary to find its effective dielectric permittivity $\varepsilon_{\text{reff}}$ and characteristic impedance Z_i of the conductors when even and odd normal waves propagate along the line.

1.5. Conclusions of Chapter 1 and Formulation of the Tasks

The following conclusions can be stated considering the overview of stripline slow-wave devices in stratified dielectric medium:

1. Effects of parameters of stratified dielectric medium on the electrical characteristics of stripline delay devices are not thoroughly investigated.
2. Numerical and hybrid techniques are mostly suitable and most widely used for modelling of stripline structures in stratified medium.
3. Normal waves (modes) are of particular significance in applying the multiconductor line method for modelling of periodic structures.
4. In some types of microstrip structures air microlayers are present creating a non-uniform stratified didelectric medium. Effects of such medium on the electrical characteristics on delay devices have not yet been thoroughly investigated.

Considering the above, the following tasks can be stated:

1. To investigate the conditions needed to excite normal wave propagation in multiconductor microstrip lines and a possibility to equalize phase velocities for even and odd normal modes in stratified dielectric coupled lines by creating a mathematical model and implementing it in software.
2. To find dependencies of electrical characteristics of microstrip multiconductor lines on their constructional parameters by creating a synthesis technique of multiconductor microstrip lines, operating in normal mode, and implementing it in software.
3. To analyze the characteristics of the meander microstrip delay line, based on the model of multiconductor microstrip line operating in even normal mode.
4. To investigate influence of air gap on the characteristics of the double shielded (“sandwich” type) meander stripline delay line.

2

Modelling of Stratified Medium Stripline Slow Wave Devices

In this chapter models for analysis of stripline slow-wave structures and results of modelling are presented. Two modelling techniques are described – the method of moments (MoM) using the partial images technique, and the finite difference (FD) method. The MoM was chosen for modelling of microstrip lines due to its high computational speed, simplicity of calculations and suitability for microstrip structures. However, in case of multilayer structures expression of the Green's function and hence the method of moments becomes complicated; therefore the method of finite differences was employed for modelling of stripline structures in stratified dielectric medium. FD method is well known and widely used for its simplicity of implementation and moderate computational requirements.

Calculations using the MoM were implemented in Matlab® environment. Calculations based on the FD method were implemented in Python scripting language. This language was picked for the availability of scientific calculation libraries (SciPy) and in order to avoid dependency on commercial software.

Four articles have been published on the subject of this chapter: (Martavičius *et al.* 2007; Mikučionis, Urbanavičius 2010b; Mikučionis, Urbanavičius 2012, Mikučionis *et al.* 2014).

2.1. Investigation of Normal Modes in Microstrip Structures

In this subchapter investigation of conditions of propagation of normal modes in coupled and multiconductor microstrip lines (CML and MCML) using the method of moments (MoM) is presented. Microstrip structures are the simplest case of microwave slow-wave devices in stratified dielectric medium.

2.1.1. Investigation of Normal Modes in Asymmetric Coupled Microstrip Lines

TEM waves in coupled lines are named in accordance with relation of conductors widths. In case of equal widths, electromagnetic waves can be either even-mode or odd-mode. Even-mode wave propagates in lines if voltages equal in magnitude and sign are applied to the signal strips. Odd-mode wave propagates in case voltages equal in magnitude and opposite in sign are applied.

If widths of signal strips are unequal, TEM waves are called c-mode and π-mode according to line excitation mode. It should be noted, that in case of unequal widths, voltages of signal strips can be different in sign and magnitude. Relation of voltages in case of c-mode and π-mode are denoted R_c and R_π respectively.

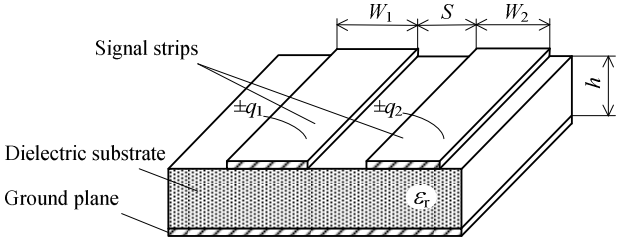

Fig. 2.1. Generalized structure of the coupled microstrip line

It is considered, that signal strips are infinitely long and the dielectric substrate is inifnitely wide, and quasi-TEM waves propagate along the strips. Thus, static analysis of cross-section of coupled microstrip line can be applied to determine line parameters (Fig. 2.1).

The main parameters of coupled microstrip lines operating in normal mode: characteristic impedance of signal strips $Z_{1,2,c,\pi}$, effective permittivity $\varepsilon_{r\,eff\,c,\pi}$, relation of voltages $R_{c,\pi}$ are found from capacitances of conductors:

$$Z_{1c,\pi} = \left[c_0 \sqrt{\left(C_{11}^{(a)} - R_{c,\pi} C_{12}^{(a)} \right) \left(C_{11} - R_{c,\pi} C_{12} \right)} \right]^{-1}, \tag{2.1}$$

$$Z_{2c,\pi} = \left[c_0 \sqrt{\left(C_{22}^{(a)} - C_{12}^{(a)} / R_{c,\pi} \right) \left(C_{22} - C_{12} / R_{c,\pi} \right)} \right]^{-1}, \tag{2.2}$$

$$\varepsilon_{r\,eff\,c,\pi} = \frac{C_{11} - R_{c,\pi} C_{12}}{C_{11}^{(a)} - R_{c,\pi} C_{12}^{(a)}} = \frac{C_{22} - \left(C_{12} / R_{c,\pi} \right)}{C_{22}^{(a)} - \left(C_{12}^{(a)} / R_{c,\pi} \right)}, \tag{2.3}$$

where subscripts 1 and 2 denote conductors, widths of which are W_1 and W_2 respectively; c and π subscripts denote of c-mode and π-mode; superscript (a) denotes capacitances of coupled microstrip line with same geometric properties but with no dielectric substrate (dielectric substrate is replaced with air).

Self capacitances C_{11}, C_{22}, $C_{11}^{(a)}$, $C_{22}^{(a)}$ and mutual capacitances C_{12}, $C_{12}^{(a)}$ are calculated by introducing so called *magnetic* and *electric* walls to the coupled microstrip line (Staras et al. 2012) or, in other words exciting signal strips in phase and out of phase respectively:

$$C_{11} = \frac{\left(C_{1o} + C_{1e} \right)}{2}, \tag{2.4}$$

$$C_{22} = \frac{\left(C_{2o} + C_{2e} \right)}{2}, \tag{2.5}$$

$$C_{12} = \frac{\left(C_{1o} - C_{1e} \right)}{2} = C_{21} = \frac{\left(C_{2o} - C_{2e} \right)}{2}, \tag{2.6}$$

$$C_{11}^{(a)} = \frac{\left(C_{1o}^{(a)} + C_{1e}^{(a)} \right)}{2}, \tag{2.7}$$

$$C_{22}^{(a)} = \frac{\left(C_{2o}^{(a)} + C_{2e}^{(a)} \right)}{2}, \tag{2.8}$$

where C_{1e} and C_{2e} – capacitances per unit length of signal strips with widths W_1 and W_2 respectively, when magnetic wall is introduced to the system (or when voltages of same sign are applied to the strips); C_{1o}, C_{2o} – capacitances of the same signal strips, when electric wall is introduced (or voltages different in sign are applied); superscript symbol (a) denotes capacitance calculated when dielectric substrate is replaced with air.

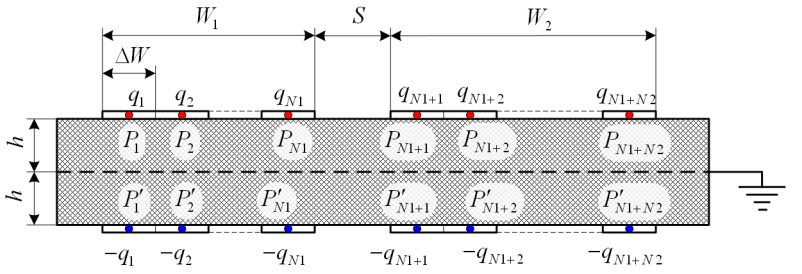

Fig. 2.2. Model of coupled microstrip lines

Unit length capacitances of the conductors are determined using the MoM. Unit length charge of the conductor is determined for a particular conductor voltage. Unit length capacitance is calculated by a well known relationship $C = Q/V$, where Q is total charge accumulated in the unit length of the conductor and V is the conductor voltage.

By applying the MoM, conductors in the cross section of coupled lines are divided into N equal sub-strips ΔW in width. Consider the model of coupled lines presented in Figure 2.2. It is assumed, that in every sub-strip *i*, charge is distributed uniformly with charge density ρ_{si}. For sake of simplicity, it is assumed, that charge of every sub-strip is concentrated in the string of infinitesimal thickness positioned in the center of the sub-strip, and charge per unit length of the *i*-th sub strip is expressed by:

$$q_i = \rho_{si} \cdot \Delta W \ . \tag{2.9}$$

Ground plane of the reference conductor is modeled by introducing mirror pair of conductors with respect to the reference conductor, and of opposite voltage, positioned at a distance 2*h* from the "real" pair of conductors (Fig. 2.2). An equipotential plane in place of the reference conductor is created that way.

Charge at point P_i and its potential, created in point P_j are expressed by Green's functions as describet in Chapter 1 (Equations (1.12) to (1.20))

In case of odd mode wave propagation, elements of respective conductor strips in potential matrix are changed to -1. Further calculation procedure remains the same as for even mode wave propagation.

Characteristic impedances and effective relative dielectric permittivity are calculated using Equations (1.5) and (1.6).

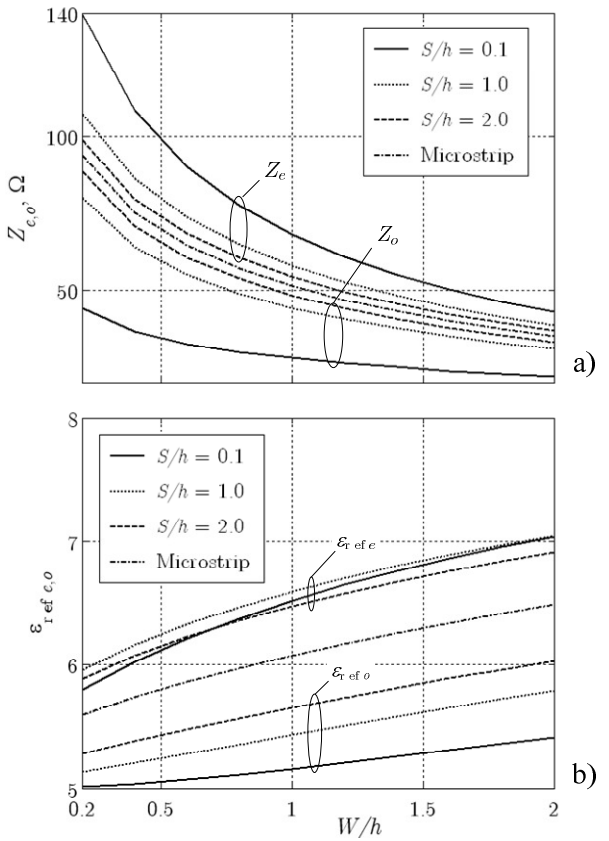

Fig. 2.3. Electrical characteristics of coupled microstrip lines a) characteristic impedance and b) effective permittivity, versus normalized width of the strips and space between them, when $\varepsilon_r = 9.6$

2.1.2. Results of Investigation of the Model of the Coupled Lines

Software tools have been developed according to the expressions in Equations (2.1) to (2.8) and (1.12) to (1.21). Normal mode parameters of symmetrically and asymmetrically coupled lines were calculated given various widths of gap between the strips and relations of strip widths. Calculation results were compared with published results worked out by other methods.

Dependence of characteristic impedance and effective permittivity on width of strips and gap width is presented in Figure 2.3. It is seen that characteristic

impedance decreases, and effective permittivity increases when width of strips increases for both – odd and even wave. Capacity per unit length of wider strips is higher, and more charge is accumulated in middle part of wider strips. This explains the dependencies presented in Figure 2.3. Capacitance per unit length when even-mode wave propagates is lower than that when odd-mode wave propagates. Hence characteristic impedance and effective permittivity in case of even-mode are always higher than in case of odd-mode. Strength of electric field in the gap between the strips is much higher in case of odd-mode, than in case of even-mode; therefore charge density at the inner edges of strips is higher for odd-mode. On the other hand, majority of electric field lines is concentrated in the air between the strips; consequently effective relative permittivity is lower for odd-mode.

It is known that, when the gap between the strips decreases, interaction between the charges in the strips increases – electric field strength for odd-mode increases (charge density at the inner edges of strips increases), and field strength decreases in case of even-mode (charge density at the inner edges of the strips decreases). Accordingly, when gap between the strips decreases, characteristic impedance increases for even-mode, and decreases for odd-mode. Dependence of effective relative permittivity on gap width for odd-mode is similar. In case of even-mode, dependence of effective relative permittivity on gap width is more complex. When gap width increases, the effective permittivity initially increases, and for higher values of gap width decreases (Fig. 2.4).

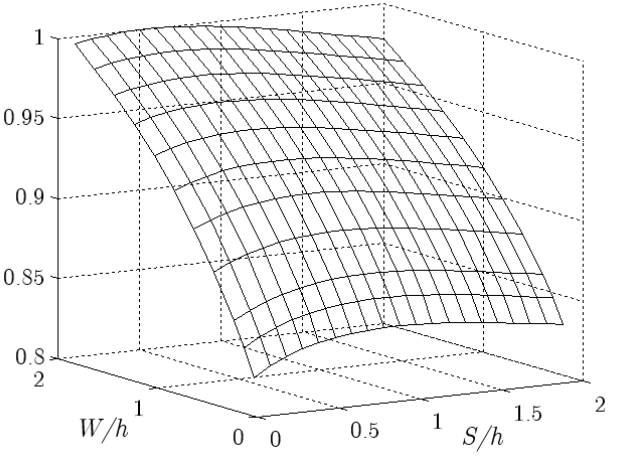

Fig. 2.4. Normalized effective permittivity of coupled microstrip lines as a function of normalized strip width and space between them at $\varepsilon_r = 9.6$

Table 2.1. Values of characteristic impedance of asymmetrically coupled lines calculated by various methods, when $W_1 = 0.6$ mm, $W_2 = 1.2$ mm, $h = 0.62$ mm, $\varepsilon_r = 9.7$. Column "Ref. 1" is data from (Bedair 1984), column "Ref. 2" is data from (Janhsen & Hansen 1991) and column "MoM" is data obtained using the described technique

S, mm	Ref. 1	Ref. 2	MoM
	Z_{c1}, Ω	Z_{c1}, Ω	Z_{c1}, Ω
0.1	74.50	75.50	72,78
0.2	70.81	71.43	69.57
0.3	68.04	68.57	67.02
0.4	65.90	66.43	64.96
0.5	64.28	64.29	63.29
0.6	62.99	63.21	61.91
	Z_{c2}. Ω	Z_{c2}. Ω	Z_{c2}. Ω
0.1	42.15	43.90	42.48
0.2	41.50	42.86	41.61
0.3	40.90	42.14	40.85
0.4	40.40	41.43	40.18
0.5	40.01	40.71	39.62
0.6	39.67	40.00	39.13

S, mm	Ref. 1	Ref. 2	MoM
	$Z_{\pi 1}$, Ω	$Z_{\pi 1}$, Ω	$Z_{\pi 1}$, Ω
0.1	34.45	35.00	34.63
0.2	38.85	39.64	39.10
0.3	41.58	42.82	41.89
0.4	43.51	44.29	43.87
0.5	44.96	46.43	45.34
0.6	46.10	47.50	46.48
	$Z_{\pi 2}$. Ω	$Z_{\pi 2}$. Ω	$Z_{\pi 2}$. Ω
0.1	19.49	20.70	20.21
0.2	22.77	24.30	23.39
0.3	25.05	26.43	25.53
0.4	26.69	27.86	27.14
0.5	27.99	29.29	28.38
0.6	29.04	30.35	29.38

This phenomenon is caused by the change of the charge distribution at the inner and outer edges of the strips, and in middle parts of strips when the gap width increases. When a relatively small gap between the strips increases (area in the graph in Figure 2.4, where S/h is close to zero), charge density at the outer edges of strips decreases, and more of the electric field lines cross the dielectric substrate, thus the effective permittivity increases.

Further increase of the gap width causes an increase of charge density at the inner edges of the strips; this in turn causes the increase of the part of the electric field in air at the gap between strips. Therefore, the effective permittivity decreases. It should be noted, that parameters of the strips, widhts of which are thinner, are more sensitive to the change of the gap width. This is due to higher relation between the charge accumulated at the edges of strips and in the middle part of the strips in case of thinner strips, than for the wider ones.

At the increase of the gap width, interaction between the strips decreases. It is seen in Figure 2.3 that when ratio *S*/*h* increases, parameters of coupled lines approach to parameters of a single microstrip line.

Comparison of characteristic impedance of coupled lines with same geometrical parameters determined by conformal mapping and spectral domain methods is presented in Table 2.1. It is seen that values of coupled lines characteristic impedance, determined by method under consideration (MoM) is almost always a bit lower than values calculated by other methods (except characteristic impedance of the wider strip in out of phase mode). Nevertheless, relative error with respect to conformal mapping method is below 3.7%, and with respect to results of the spectral domain method – below 3.8%. It must be noted, that values of characteristic impedance published in (Janhsen & Hansen 1991) are determined assuming signal of 10 GHz acts on a line, whereas influence of frequency is neglected in the model under consideration.

2.1.3. Investigation of Normal Modes in the Multiconductor Microstrip Line

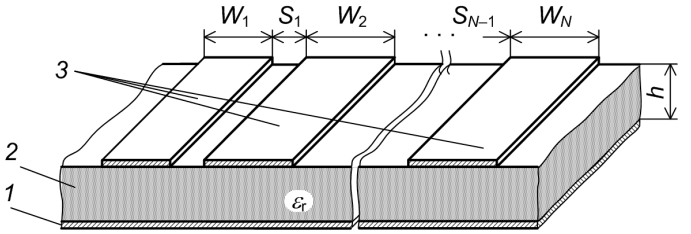

Fig. 2.5. Generalized structure of a multiconductor microstrip line

Multiconductor microstrip line (MCML), structure of which is shown in Figure 2.5, serves as a basic model for various common devices in microwave circuits, including slow-wave systems like meander and helical delay lines. When using models of such lines, modes of the multiconductor lines are of particular interest. In order to obtain and analyze normal waves in an MCML, modal voltages applied to the line conducting strips, and their corresponding effective dielectric permittivities should be known.

In order to calculate modal voltages and corresponding effective permittivities, partial capacitances of the conductors of the MCML must be known. Furthermore, partial capacitances of an MCML having exactly same dimensions, but all dielectrics replaced by air must also be calculated.

Method of moments and partial images technique is used to calculate partial capacitances of the conductors.

The algorithm of calculation of modal voltages of an MCML operating in normal mode (Fig. 2.6) is straightforward with no iteration loops or branching.

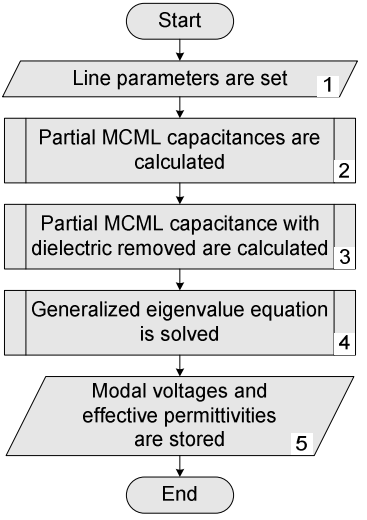

Fig. 2.6. Flowchart of the algorithm of the calculation of normal mode voltages in a multiconductor microstrip line

Description of the flowchart of the algorithm:

Step 1. Initial line parameters – widths of the conductors W_i and gap sizes S_i between them, thickness h and dielectric constant ε_r of the dielectric substrate are set.

Step 2. Partial unit-length capacitances C_i of the MCML are calculated using the chosen field solving technique.

Step 3. Partial unit-length capacitances $C_i^{(a)}$ of the same MCML with all dielectrics replaced by air are calculated.

Step 4. After obtaining matrices in steps 2 and 3, generalized eigenvalue Equation (1.39) is solved.

Step 5. The resulting characteristics values are output and/or stored for further processing (e.g. synthesis).

Steps 2 and 3 are performed by software tools, created for the research, while step 4 – solution of a generalized eigenvalue equation can be performed by any existing suitable tools.

The first step is straightforward and depends on the task to be performed. The second step is the most important and complicated. It requires modelling of the MCML and calculation of capacitances. In this thesis it is performed by using the method of moments and partial images technique as described in paragraph 1.3.3 and performed in 2.1.1. In this case for N conductor MCML, N calculations have to be performed. For every calculation voltage of one conductor should be set to 1 volt, and voltage of other conductors should be zero. Unit length charges accumulated in the conductors of an MCML are the rows of the capactance matrix.

The third step is the same procedure as in step 2. Capacitance matrix is calculated for the same MCML with dielectric layer replaced by air.

Then, when a corresponding capactince matrices are obtained, modal voltages and the corresponding effective permittivities are calculated by solving eigenvalue Equation (1.39).

2.1.4. Verification of the Model

In order to check if the model is adequate, three-conductor MCML was modelled and the results were compared to the ones published in (Awasthi et al. 2005), which were obtained using the spectral domain method (Table 2.2). The compared results in most cases agree within 3%.

Table 2.2. Comparison of parameters of the three-conductor asymmetrically coupled multiconductor microstrip line (W_1 = 0.3 mm, W_2 = 0.6 mm, W_3 = 1.2 mm, S_1 = 0.2 mm, S_2 = 0.4 mm, h = 0.63 mm, ε_r = 9.8). columns "Ref." denote the results published in (Awasthi et al. 2005)

Conductor number	Mode A		Mode B		Mode C	
	MoM	Ref.	MoM	Ref.	MoM	Ref.
Modal Voltages, V						
1	1	1	1	1	1	1
2	–0.9	–0.875	0.61	0.6	1.16	1.15
3	0.17	0.175	–0.66	–0.66	1.19	1.13
Effective Relative Dielectric Permittivity						
	5.51	5.55	6.1	6.15	7.58	7.6
Characteristic Impedance, Ω						
1	45	46.5	73.6	76	106	107
2	32.6	33	55.7	57	72.6	73.5
3	20	19.5	29	30	39.6	40

Further, the proposed technique was used for analysis of normal modes in symmetrically coupled four-conductor MCML. In case of four-conductor MCML four distinct modes are possible. Widths of the conductors W and gaps between the conductors S were equal. Mode voltage polarities and relation between them are presented in Table 2.3.

Table 2.3. Relations of modal voltages of four-conductor multiconductor microstrip line

Mode	Voltage polarity				Relations between voltages
	V_1	V_2	V_3	V_4	
A	+	+	+	+	$V_1 = V_4$, $V_2 = V_3$
B	+	+	–	–	$V_1 = -V_4$, $V_2 = -V_3$
C	+	–	–	+	$V_1 = V_4$, $V_2 = V_3$
D	+	–	+	–	$V_1 = -V_4$, $V_2 = -V_3$

Plus and minus signs in Table 2.3 specify the polarities, but not the magnitudes of modal voltages. It should also be noted that polarities of voltages are relative, i.e. for example polarities of voltages for mode A can all be negative. The calculation results of normal modes parameters versus normalized microstrip width W/h are shown in Figure 2.7.

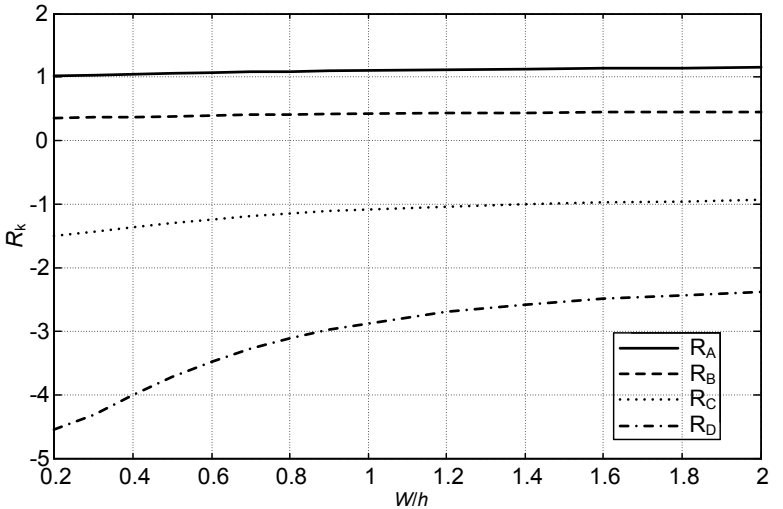

Fig. 2.7. Dependence of voltage ratios on normalized widths of the conductors of the symmetrically coupled multiconductor microstrip line

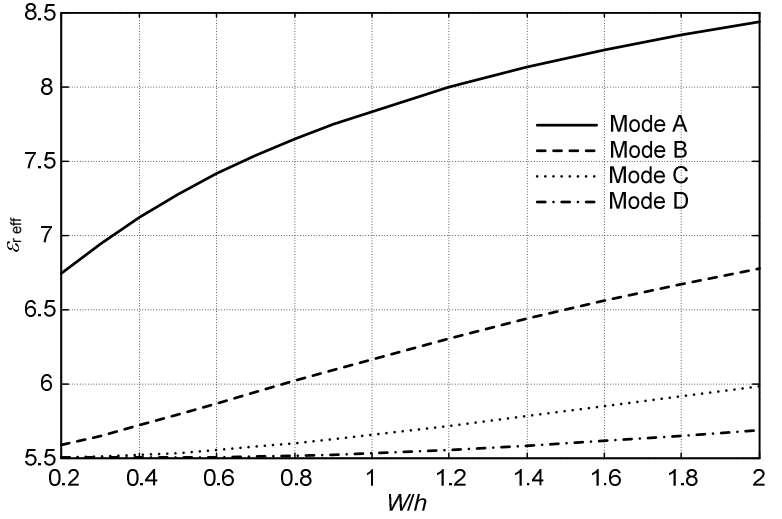

Fig. 2.8. Dependence of the effective permittivity on the normalized widths of conductors of the symmetrically coupled multiconductor microstrip line

It is seen in Figure 2.7 that in case of symmetrically coupled four-conductor MCML, there is only one distinct ratio of voltages of the adjacent strips for each mode:

$$R_k = V_2/V_1 = V_4/V_3 , \tag{2.10}$$

where k denotes the mode index. Therefore, for each mode, only two voltage magnitudes are distinct: $V_1 \neq V_2$, and $V_3 \neq V_4$.

At investigating dependences of normal waves parameters on the width of microstrips of the MCML, it was found that, in general, these dependences are similar to dependences for the microstrip coupled lines. Sending voltages of identical sign into all microstrips of the MMCL (mode A, or c-normal wave), the voltages ratio, at increasing *W*/*h*, varies insignificantly (Fig. 2.7). In the presented example, at tenfold increase of *W*/*h*, R_{A} increases only by 10 %. Similar dependence is observed for mode B when voltages of identical signs also are sent (into the pairs of external microstrips). Nevertheless, at the same variations of *W*/*h* for mode D (π-normal wave), R_{D} increases almost 2 times.

Effective permittivity $\varepsilon_{\mathrm{r\,eff}}$ also increases (Fig. 2.8) with the increase fo *W*/*h* for all modes. When the conductor is wider, greater part of the electric field is consentrated in the dielectric substrate, hence the increase of the effective permittivity $\varepsilon_{\mathrm{r\,eff}}$. But the degree of this increase is different for each mode. It is

seen that $\varepsilon_{r\,eff}$ for mode A varies most of all – by 24%, and $\varepsilon_{r\,eff}$ for mode D varies the least – only by 4%, correspondently $\varepsilon_{r\,eff}$ for modes B and C vary by 20% and 10%.

The characteristic impedance, in contrast, decreases with increasing *W*/*h*, for all modes (because the capacitances of conductors per unit length increase). For symmetrically coupled four-conductor MCML it was found that $Z_1 = Z_4$ and $Z_2 = Z_3$, where index denotes conductor number. Therefore it is enough to

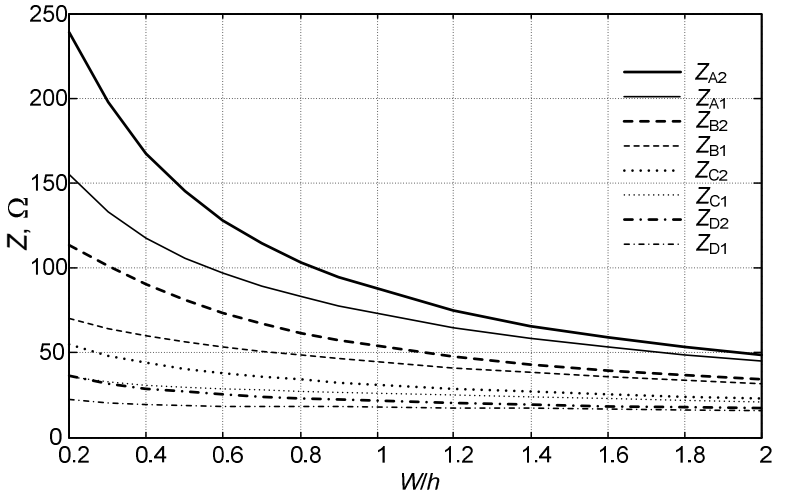

Fig. 2.9. Dependence of the characteristic impedance of the conductors on the normalized widths of conductors of the symmetrically coupled multiconductor microstrip line

present only eight dependencies of characteristic impedance on *W*/*h*.

In Figure 2.9 Z_{ki} denotes characteristic impedance of *i*-th conductor for mode *k*. It should be noted that for every mode internal microstrips of MCML (# 2 and # 3) have the greater characteristic impedance, and external microstrips (# 1 and # 4) have smaller impedance. The impedance of internal microstrips also changes, changing *W*/*h*, in the greater degree. It was found that as well as in case of $\varepsilon_{r\,eff}$ dependence on the widths of the conductors, mode A responds most sensitively to changing *W*/*h* – its impedances vary almost 5 times for internal microstrips and 3 times for external.

2.2. Modelling of Coupled Striplines in Stratified Dielectric Medium Using the Finite Difference Method

The MoM is known to be applied for more complex stratified medium, however derivation of initial equations require complex mathematical manipulations, which is undesirable, if thicknesses of layers are to be changed. Therefore the need for simpler numerical technique arises.

The finite difference (FD) method is a well known numerical technique for solving partial differential equations. It is simple to implement for inhomogeneous dielectric medium and requires moderate computational resources.

2.2.1. Calculation of Field and Conductor Capacitances

The FD method is applied on the cross-section of the stripline structure. Due to iterative nature of the method it takes significantly more operations to get the result. However the model itself is much simpler, therefore it takes less effort to implement it using programming tools. As in the case of method of moments modelling, quasi-TEM approach is applied and only static parameters are calculated. The finite difference method allows for more flexible dielectric composition of the area and/or volume investigated. Therefore it is easier adapted for stratified dielectric medium.

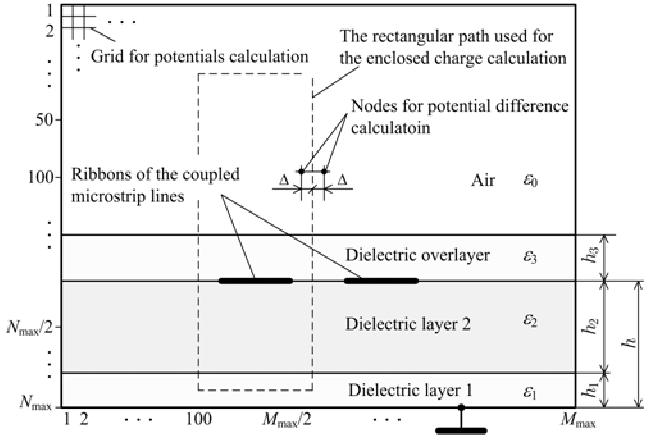

Fig. 2.10. Cross-section of the finite difference model of the coupled striplines

The modelling of the coupled lines was performed by utilizing the FD method in two dimensions (Fig. 2.10). The cross section of the coupled lines was enclosed in a rectangular contour with zero potential, and divided by a grid with

step Δ. Only potentials of the nodes of the grid are considered. Laplace equation is solved numerically for the cross-section of the line. As calculation proceeds, node voltages are compared to the previous result after each pass, and the highest difference of node voltages between successive iterations is checked. If the difference is lower, than the initially set, calculation stops, and the acquired node voltages are considered an approximation of the electric field in the cross section of the stripline.

As mentioned above, the initial value which needs to be calculated in order to calculate the needed characteristics is the unit length capacitance of the conductors C_{1i}. In case of the MoM, the solution was the unit length charge of the conductor, so capacitance could be calculated directly. In this case only distribution of the potential around the conductors is known. Therefore the unit length capacitance is calculated by integrating potential difference along the path around the conductor.

The effective permittivities for the even and odd modes are calculated by using technique described in 1.3.4 and by solving an eigenvalue equation (1.39).

2.2.2. Calculation of Partial Capacitances and Electrical Characteristics

Partial capacitance matrix is obtained by firstly setting the voltage of the first conductor to one, and voltage of the second one to zero, and calculating their unit length charge, thus obtaining C_{11} and C_{12}. Then, the first conductor voltage is set to zero, and that of the second – to one volt in order to calculate C_{21} and C_{22}.

In case of symmetric coupled lines (when widths of both conductors are equal), partial capacitance matrices are symmetric, i.e. $C_{11} = C_{22}$ and $C_{12} = C_{21}$. Therefore two calculation procedures need to be performed – first one is the modelling of the line with all dielectric layers in place and the second one with all dielectrics replaced by air.

2.2.3. Model Verification

In order to check the correctness of the model, the results of the calculations were compared to the results, obtained by other researchers using other methods (Elsherbeni *et al.* 1993).

The two layer dielectric line was modeled: dielectric constant of the first layer – ε_{r1} = 2.2, and that of the second – ε_{r2} = 9.6, normalized widths of the conductors: $W_1/h = W_2/h = 1$ and normalized gap between the conductors $S/h = 1$, overall thickness of the dielectric h.

The comparison of the results of the calculation, presented in Table 2.4, shows that the difference of the calculated effective dielectric constant in case of even mode was below 5%, and in case of odd mode was below 0.4%. This proves the model to be adequate.

Table 2.4. Comparison of the calculation results. "Ref." column denotes the results from (Elsherbeni et al. 1993)

h_1/h	Mode	$\varepsilon_{r\,eff}$		Δ, %
		Calculated	Ref.	
0.05	even	6.08	6.33	3.94
	odd	5.63	5.64	0.17
0.1	even	5.58	5.84	4.45
	odd	5.32	5.33	0.18
0.15	even	5.18	5.43	4.60
	odd	5.06	5.08	0.39
0.2	even	4.86	5.08	4.33
	odd	4.84	4.85	0.20
0.3	even	4.32	4.51	4.21
	odd	4.46	4.47	0.22
0.4	even	3.9	4.05	3.70
	odd	4.11	4.12	0.24
0.6	even	3.2	3.3	3.03
	odd	3.44	3.45	0.28
0.8	even	2.59	2.67	2.99
	odd	2.7	2.71	0.36

2.3. Characteristics of Coupled Striplines in a Multilayer Dielectric

The created model was further used to evaluate influence of the dielectric layer thickness and dielectric constants on the electrical characteristics of the coupled lines.

In the first set of analyses, coupled lines on two-layer dielectric were analyzed (Fig. 2.11). Starting with one layer of thickness h_1/h= 0.5, additional layer with different dielectric constant ε_{r2} was added and gradually increased to h_2/h_1 = 1.5.

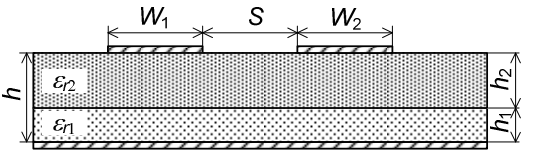

Fig. 2.11. Cross-section of the coupled stripline on a double layer dielectric

In the first case, the dielectric constant of the lower layer was set to $\varepsilon_{r1} = 9.6$, and that of the second layer was set to $\varepsilon_{r2} = 2.2$. In the second case, the dielectric constants were switched places. The dependence of the effective dielectric constant on the thickness of the upper dielectric layer and the overall dielectric thickness ratio is presented in Figure 2.12 a).

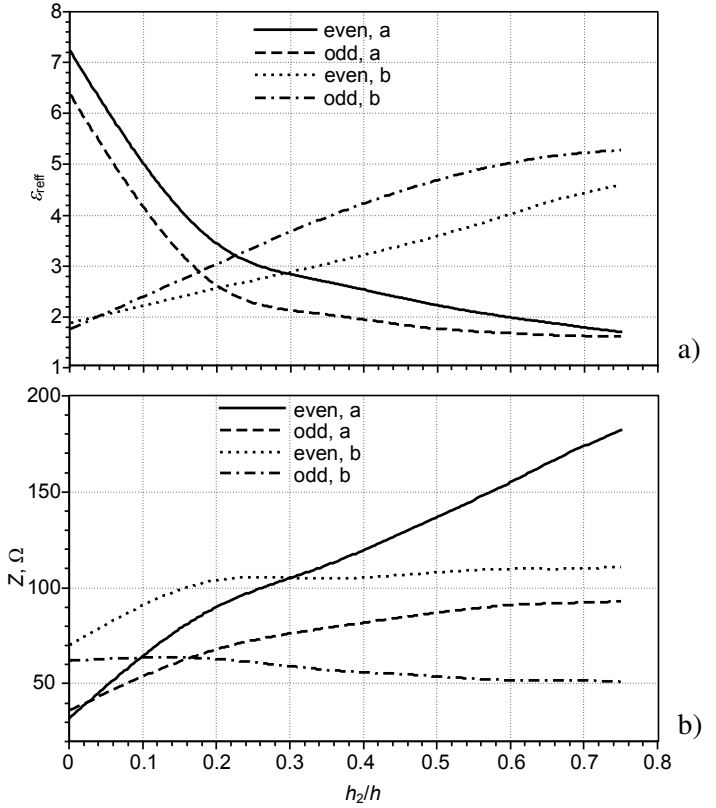

Fig. 2.12. Dependence of a) effective permittivity and b) characteristic impedance of the coupled striplines on the dielectric thickness ratio, when $h_1/h = 0.5$, curves a – $\varepsilon_{r1} = 9.6$, $\varepsilon_{r2} = 2.2$; curves b – $\varepsilon_{r1} = 2.2$, $\varepsilon_{r2} = 9.6$

In the first case (Fig. 2.12 a), curves a), effective permittivity is initially high, and then decreases, as the thickness of an additional layer having lower dielectric constant is increased. The effective permittivity for even mode remains higher than that in case of odd mode in the whole range.

In the second case (Fig. 2.12 a), curves b), where the dielectric constant of the lower layer is lower ($\varepsilon_{r1} = 2.2$), than that of the upper layer ($\varepsilon_{r2} = 9.6$), effective dielectric constant is initially low, and then gradually increases, as the thickness of an additional layer with higher dielectric constant is increased.

It can be noted, that when no upper layer is present, the effective dielectric constant in case of odd mode is slightly lower, than that in the case of even mode. As an additional layer is added, the effective dielectric constant in case of even mode is lower than that in case of odd mode. This can be explained by the influence of the upper layer with higher dielectric constant. In case of even mode, electric field concentrates between the conductors and the ground plane, therefore mostly in the dielectric. In case of odd mode, the majority of the electric field lines concentrate between the signal conductors – in the area of the dielectric and air between them.

Introduction of an additional layer with significantly higher dielectric constant right below the conductors causes higher concentration of electric field in the region between the conductors of an additional layer, therefore increasing the effective relative dielectric permittivity more noticably. In the case of even mode, significant part of the electric field lines is in both dielectric layers; therefore influence of the additional layer with higher dielectric constant is not that significant.

The dependence of the characteristic impedance of the lines on the dielectric thickness ratio is presented in Figure 2.12 b). The characteristic impedance of the lines in the first case ($\varepsilon_{r1} = 9.6$, $\varepsilon_{r2} = 2.2$) increases when the thickness of an additional layer is increased. Since overall thickness of the dielectric is increased, capacitances of the line decrease, therefore the characteristic impedance increases. In the second case ($\varepsilon_{r1} = 2.2$, $\varepsilon_{r2} = 9.6$), characteristic impedance in case of even mode initially increases, and then remains almost constant. As in the first case, when the overall thickness of the dielectric increases, capacitance decreases, but the higher dielectric constant of the additional layer compensates for that, and the change in the characteristic impedance is lower. In case of odd mode, the characteristic impedance slightly diminishes.

For the second set of modelling analyses, influence of the dielectric constants of different layers of the two-layer dielectric system was analyzed (Fig. 2.8). In the first case, the dielectric constant of the lower layer ε_{r1} was changed, and that of the second layer was fixed to $\varepsilon_{r2} = 9.6$. In the second case,

the dielectric constant of the second layer ε_{r2} was varied, and that of the lower was fixed to $\varepsilon_{r1} = 9.6$. The normalized widths of the conductors were chosen $W_1 / h = W_2 / h = 0.5$ and the normalized gap between the conductors $S / h = 0.5$.

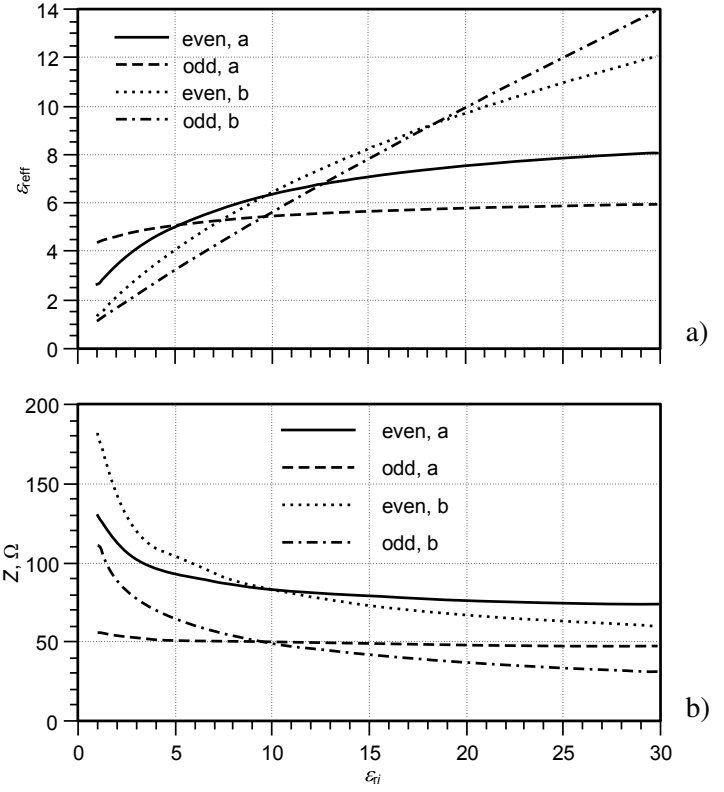

Fig. 2.13. Dependence of a) the effective permittivity and b) characteristic impedance of the coupled lines on the dielectric constant of a – lower layer ($\varepsilon_{r1} = \varepsilon_{ri}$), b – upper layer ($\varepsilon_{r2} = \varepsilon_{ri}$)

As it can be expected, the effective permittivity of the coupled lines increased as the dielectric constant of one of the layers increased for both – even and odd modes in both cases (Fig. 2.13 a)). The rate of change of the effective permittivity when increasing dielectric constant of one of the layers however was different. In the first case (Fig. 2.13 a), curves a), at dielectric constant of the lower layer being less than approximately 5, the effective permittivity in case of even mode was lower than that for the odd mode.

When dielectric constant of the lower layer is further increased, effective permittivity of the lines for the even mode becomes greater than that for the odd

mode. As mentioned earlier, the effective permittivity for the odd mode is mostly governed by the dielectric medium in the vicinity of the conductors. This is also proved by the slight change of the effective permittivity for the odd mode – from 4.39 to 5.95, only 36%, whereas for even mode, the change was higher – from 2.61 to 8.09 i.e. 210%.

In the second case (Fig. 2.13 a), curves b), when the dielectric constant of the upper layer ε_{r2} was varied, for its value between 1 and approximately 17, the effective permittivity was higher in case of the even mode, on the contrary to the first case. For values $\varepsilon_{r2} > 17$, the effective permittivity for odd mode was higher than that for the even mode. Also in this case the change of effective dielectric constant when changing the dielectric constant of the second dielectric layer ε_{r2} was higher for the odd mode (12.8 times), than that for the even mode (9.1 times), on the contrary to the results of the first case.

Very important results of the analyses are values of the dielectric constant of one of the layers, where effective permittivities are equal for both – even and odd modes. It means that for these values, phase velocities of the propagating wave are equal for both modes.

It can also be noted, that the influence of the dielectric constant of the dielectric layer closer to the conductors was significantly greater than that of the lower layer – 9.1 and 12.8 times vs. 3.1 and 1.36 times for even and odd modes respectively.

Characteristic impedances for all cases decreased (Fig. 2.13 b)), when dielectric constant of one of the layers was increased. This was due to increase of unit-length capacitances of the conductors caused by the increase of the effective permittivity. It should be noted, that the influence of the dielectric constant of the lower dielectric layer ε_{r1} to characteristic impedance in odd mode was very slight – only 16% decrease compared to the decrease for even mode – 43%. When the dielectric constant of the second layer ε_{r2} was changed, the difference between the changes of characteristic impedance was not that significant – 67% and 72% for even and odd modes respectively.

Further, the coupled line formed on a two-layer dielectric, and having an additional layer of dielectric above the conductors (overlayer) (Fig. 2.14) was investigated. The first set of analyses was investigation of influence of the thickness and dielectric constant of the third layer above the conductors on the electrical characteristics of the coupled line. The normalized thickness of the dielectric overlayer above the conductors h_3/h was chosen 0.125, 0.25 0.5 and 1, and the dielectric constant of the layer was increased from 1 to 30. The dielectric constants of the layers between the conductors and the shield conductor were $\varepsilon_{r1} = 9.6$ and $\varepsilon_{r2} = 2.2$ respectively. The results are presented in Figures 2.15 and 2.16.

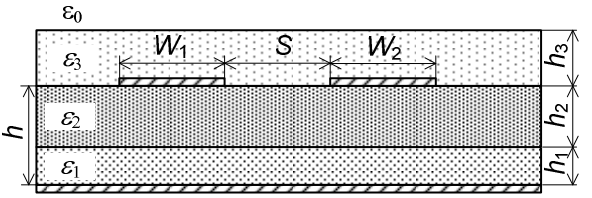

Fig. 2.14. Cross-section of the coupled line on a double layered dielectric, with additional overlayer

As it can be expected, increasing the thickness of the third layer and the dielectric constant caused the effective permittivity to increase (Fig. 2.15). At lower values of the dielectric constant of the overlayer ε_{r3}, the effective permittivity of the lines is higher for the even mode, than that for the odd mode. However, the effect of increasing the dielectric constant of the third layer ε_{r3} was greater for the effective permittivity in the odd mode, than that in the even mode. It is clearly seen in Figure 2.15, that for particular overlayer thickness h_3 and particular value of the dielectric permittivity of the overlayer ε_{r3}, effective permittivities for both, even and odd mode are equal.

As mentioned in the introduction, such property can be useful for reducing crosstalk between the transmittion lines. It is also worth noticing, that efective permittivities become equal at approximately the same value $\varepsilon_{reff} \approx 3.05$, at different thicknesses and dielectric constants of the overlayer.

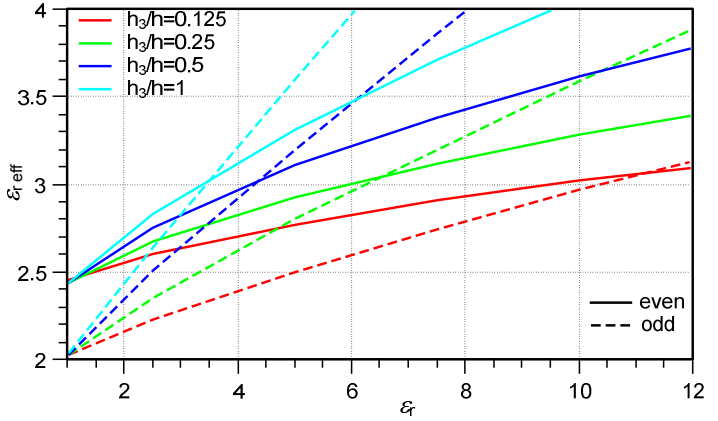

Fig. 2.15. Dependence of the effective permittivity of the coupled lines on the dielectric constant of the third layer, when $W_1/h = W_2/h = 1$, $S/h = 1$, $h_1/h = h_2/h = 0.5$, $\varepsilon_{r1} = 9.6$ and $\varepsilon_{r2} = 2.2$

The effective permittivity for different thicknesses of the third layer h_3 in the odd mode changed from 2.3 times to 6.1 times, while increasing the

dielectric constant of the third layer ε_{r3} from 1 to 30, whereas the same change in the case of even mode was from 1.5 times to 2.7 times.

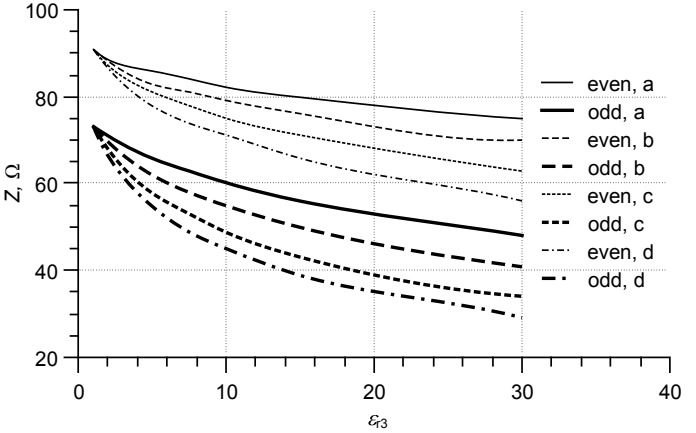

Fig. 2.16. Dependence of the characteristic impedance on the dielectric constant of the third layer, when $W_1/h = W_2/h = 1$, $S/h = 1$, $h_1/h = h_2/h = 0.5$, $\varepsilon_{r1} = 9.6$ and $\varepsilon_{r2} = 2.2$; a - $h_3/h = 0.125$, b – $h_3/h = 0.25$, c – $h_3/h = 0.5$, d – $h_3/h = 1$

It must also be noted, that for lower values of the dielectric constant of the third layer ε_{r3}, the effective permittivity for the even mode is higher than that for the odd mode. As the dielectric constant of the third layer ε_{r3} is increased, at some value, depending on the thickness of the layer h_3, the effective permittivity for the odd mode becomes higher than that of the even mode. Therefore there exists a range of dielectric thickness and dielectric constant values, for which the effective permittivities for both modes are equal.

Characteristic impedance (Fig. 2.16) of the lines decreased as both – thickness h_3 and dielectric constant of an additional layer ε_{r3} were increased. In all cases, even mode characteristic impedance was higher than odd mode characteristic impedance.

In further analysis, the effect of the thickness of the third layer h_3 having common values of dielectric constant ε_{r3} was investigated. Analysis was performed for a coupled line formed on two layer dielectric, and having additional layer of dielectric above the conductors.

For the first set of analyses dielectric constant of the first and second dielectric layers were $\varepsilon_{r1} = 9.6$ and $\varepsilon_{r2} = 2.2$ respectively. Dielectric constants of the third layer ε_{r3} were chosen 2.2, 4.7 and 16. For every dielectric constant value the normalized thickness of the third layer was varied between 0.1 and 4 (Fig. 2.17).

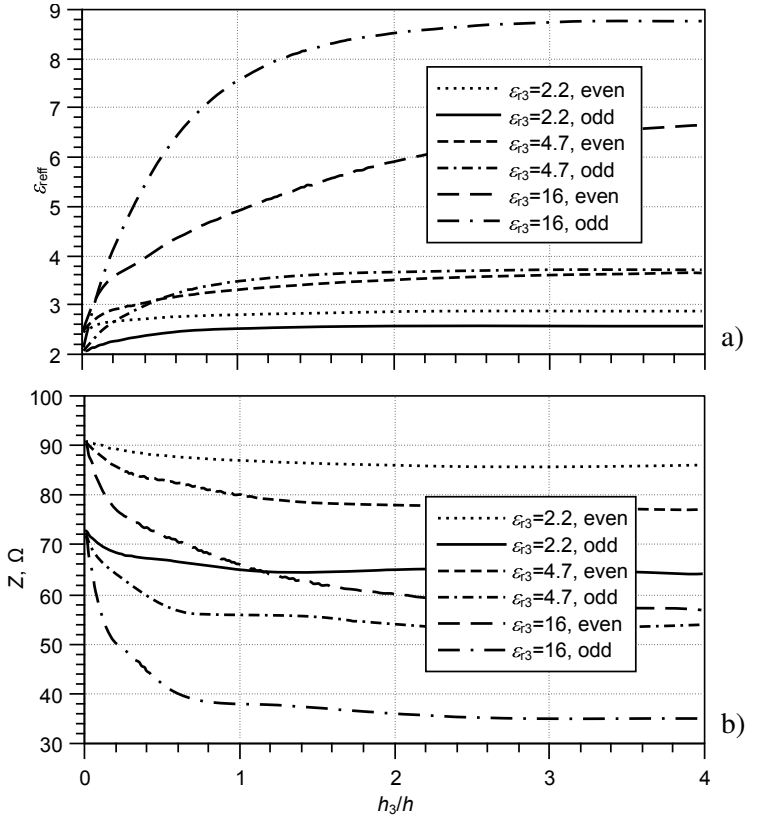

Fig. 2.17. Dependence of a) the effective permittivity and b) characteristic impedance on normalized thickness of the third layer h_3/h at different dielectric constants of the overlayer

It is seen from the graph in Figure 2.17 a) that, in case of dielectric constant of the overlayer $\varepsilon_{r3} = 2.2$, the effective permittivity of the even mode is higher than that of the odd mode throughout the range of thicknesses of the third layer. For other two cases ($\varepsilon_{r3} = 4.7$ and $\varepsilon_{r3} = 16$), however, effective permittivity for the even mode is higher than that of the odd mode for lower values of the thickness of the third layer h_3, as the thickness value is increased, the effective permittivity for the odd mode becomes higher than that of the even mode. In case when the dielectric constant of the third layer $\varepsilon_{r3} = 4.7$, this transition occurs at the normalized thickness of approximately $h_3/h = 0.5$, and in the case of $\varepsilon_{r3} = 16$, the same transition occurs when the normalized thickness of the third layer is approximately $h_3/h = 0.1$.

The second set of analyses was performed on coupled lines, for which the dielectric constants of the first and second layers were $\varepsilon_{r1} = 2.2$ and $\varepsilon_{r2} = 9.6$ respectively. Dielectric constants of the third layer ε_{r3} were chosen 4.7, 9.6 and 16. For every dielectric constant value ε_{r3} the normalized thickness of the third layer h_3/h was varied between 0.1 and 4. For this case, on the contrary to the previous analysis, the effective permittivity for the odd mode was higher than that for the even mode for all values of the dielectric constant ε_{r3} and normalized thickness of the third layer h_3/h (Fig. 2.18). Equal effective permittivities i.e. phase velocities for even and odd modes in this configuration were not obtained (Fig. 2.18).

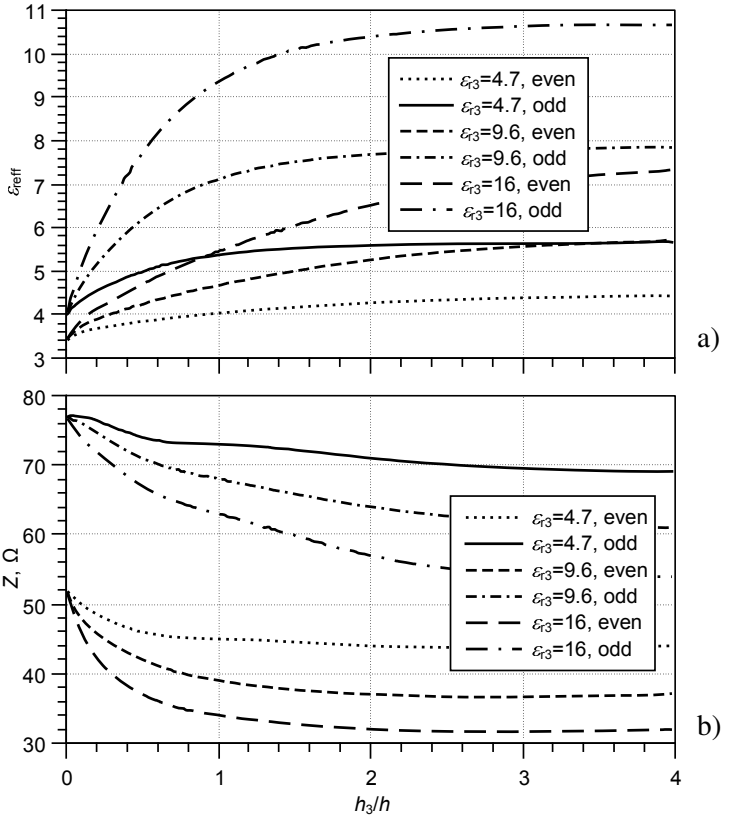

Fig. 2.18. Dependence of a) the effective permittivity and b) characteristic impedance on the normalized thickness of the third layer at different dielectric constants of the overlayer

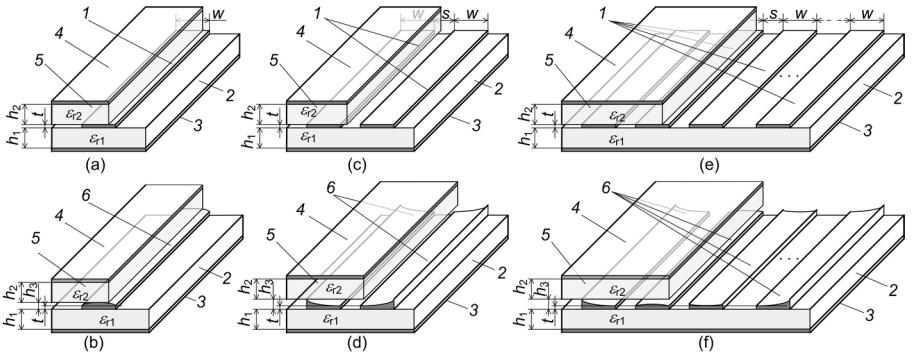

Fig. 2.19. The generalized structure of the double-shielded microstrip devices: transmission line a), and transmission line with non-rectangular conductor b), coupled microstrip lines c), and coupled lines with non-rectangular conductors d), multiconductor microstrip line e), and multiconductor line with non-rectangular conductors f) where 1 are rectangular microstrips; 2 and 5 are bottom and top dielectric substrates correspondently; 3 and 4 are bottom and top shields correspondently; 6 are the non-rectangular microstrips. Portion of the top dielectric plate and top shield are not shown here

2.4. Investigation of Air Microlayer Influence to the Characteristics of Multiconductor Lines

In this subsection model of double shielded microstrip line (DSML) with an air microlayer between the dielectric plates or between the conducting strips and one of the dielectrics is investigated. Occurrence and reasons of such phenomenon are explained, and results of the modelling are presented.

2.4.1. Origins of the Air Microlayer

One of the methods of construction of a double shielded stripline meander delay line is to etch the meander line on one double-sided copper laminated dielectric, and to use another dielectric plate with only a single copper layer as a cover. (Fig. 2.17). Since the thickness of the conductor is not infinitely small, and the surfaces are not perfect, air microlayer becomes present between the two plates. The effect of the mentioned air layer is not known; therefore the created model was used to research this effect.

2.4.2. Modelling of the Air Microlayer

As mentioned before, the FD method allows for easier implementation of complex dielectric medium. The main drawback of this method is that in order to model the effect of very thin layer, the dividing grid has to be more dense, hence significantly increasing computational requirements. However application of the MoM in case of stratified medium is mathematically more complex in this case, therefore the FD method was chosen, as described in Subchapter 2.2.

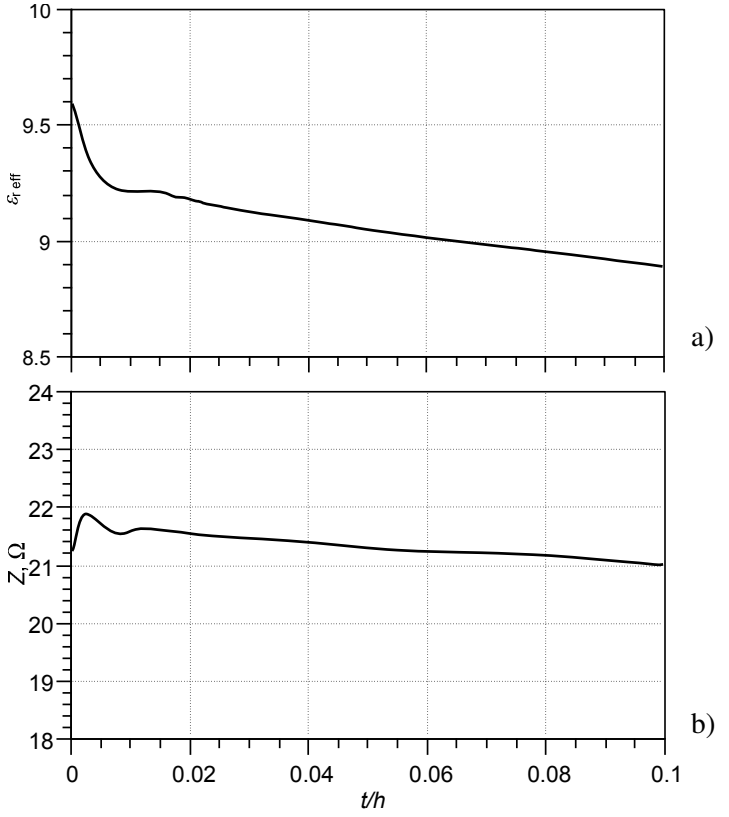

Fig. 2.20. Dependence of a) the effective permittivity and b) characteristic impedance of the double shielded transmission microstrip line on the normalized microstrip thickness t/h, when $h_1/h = 0.5$, $\varepsilon_r = 9.6$, $W/h = 1$

2.4.3. Results of the Modelling

Dependence of the effective permittivity $\varepsilon_{r\,eff}$, the characteristic impedance Z_0, and delay time t_d of the DSM devices on the air gap between top and bottom

dielectric substrates are investigated. Two cases were considered: when the gap is emerged due to the non-zero thickness of the microstrips, and when the gap is emerged due to inaccurate mounting the upper dielectric plate. In order to obtain better knowledge of the effect of the air microlayer, both cases were studied for three types of DSM devices: single microstrip line, coupled microstrip lines and six conductor microstrip lines.

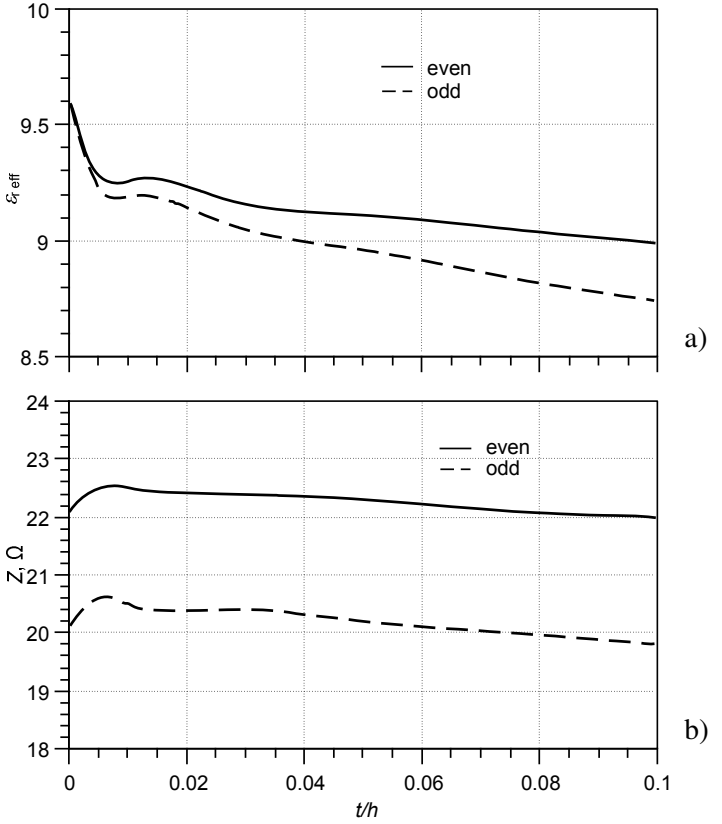

Fig. 2.21. Dependence of a) the effective permittivity and b) characteristic impedance of the coupled double shielded microstrip lines on normalized microstrip thickness t/h, when $h_1/h = 0.5$, $\varepsilon_r = 9.6$, $W/h = 1$, $S/h = 1$

Air Gap Due to non-zero Microstrip Thickness

Influence of the air gap, caused by the non-zero thickness of microstrips, on the effective permittivity and characteristic impedance of the DSM transmission line is presented in Figure 2.20 by corresponding curves. Two areas can be marked at

all the curves: the initial region where the air gap emerges ($0 < t/h_1 < 0.005$) and the region where it further increases ($t/h_1 > 0.005$). It is seen that with increasing microstrips thickness from 0 to $t/h_1 = 0.005$, all the curves change abruptly. Such a drastic change of the effective permittivity and the characteristic impedance is due to a shift of the distribution of the electric field in the cross-section of investigated devices.

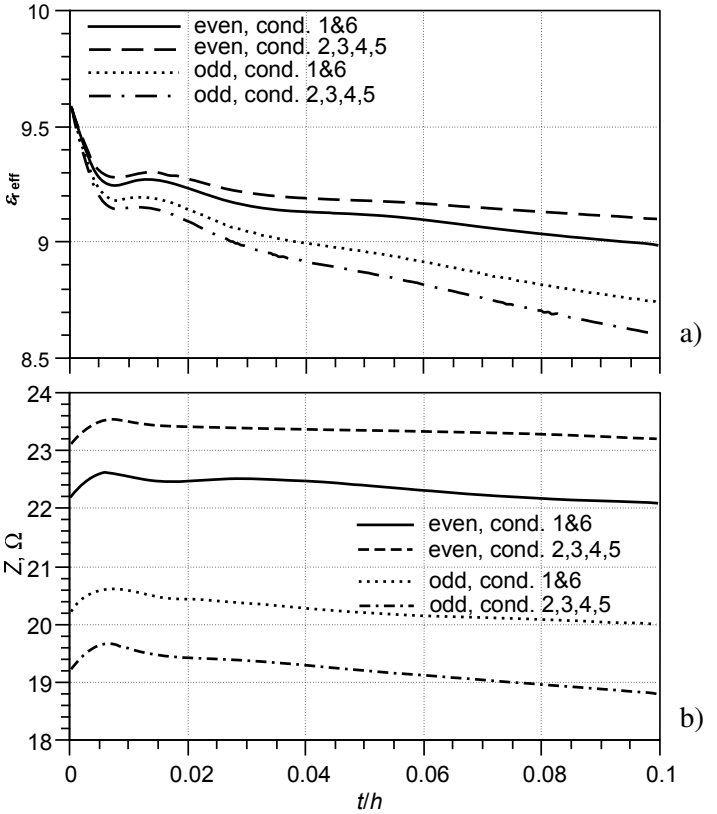

Fig. 2.22. Dependence of a) the effective permittivity and b) characteristic impedance of the six-conductor double shielded microstrip lines on normalized microstrip thickness t/h, when $h_1/h = 0.5$, $\varepsilon_r = 9.6$, $W/h = 1$, $S/h = 1$

When the air gap is absent, the structure of such devices corresponds to the stripline structure and the electric field is fully concentrated in the dielectric area. As a result, the effective permittivity is equal to the dielectric constant of the substrate, so unit length capacitance of the lines is relatively large and the characteristic impedance is therefore small.

As soon as a thin layer of air emerges ($0 < t/h_1 < 0.005$ in the considered case), the structure of the investigated device must be considered as double-shielded microstrip. Part of the electric field lines pass from the dielectric to the air, because of this there is a sharp decrease of the effective permittivity and lines unit-length capacitance and thus the impedance increases. With further increase of the microstrips thickness and the air gap ($t/h_1 > 0.005$), more and more electric field lines pass through the air and the effective permittivity decreases further (Figs. 2.20 a), 2.21 a) and 2.22 a)).

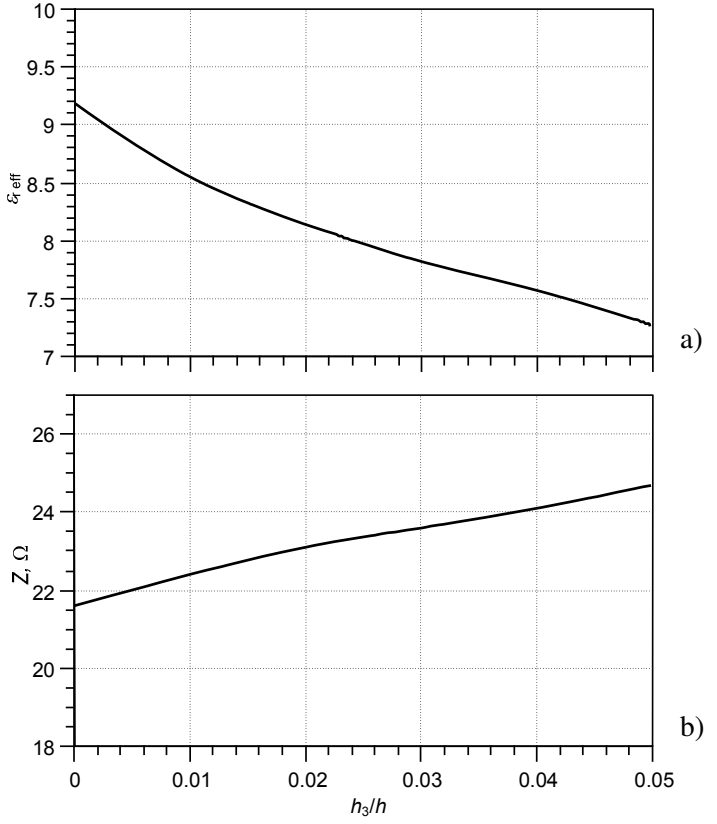

Fig. 2.23. Dependence of the a) effective permittivity and b) characteristic impedance of the double shielded microstrip transmission line on normalized air microlayer thickness h_3/h, where $h_1/h = 0.5$, $\varepsilon_r = 9.6$, $W/h = 1$

It should be noted that the expected increase of the characteristic impedance is not observed in this case. Moreover, the opposite is true – characteristic impedance is decreased. This decrement of the characteristic impedance can be

explained by accumulation of the additional electric charge on the increasing side walls of microstrips and, as a consequence, by increment of their unit length capacitance.

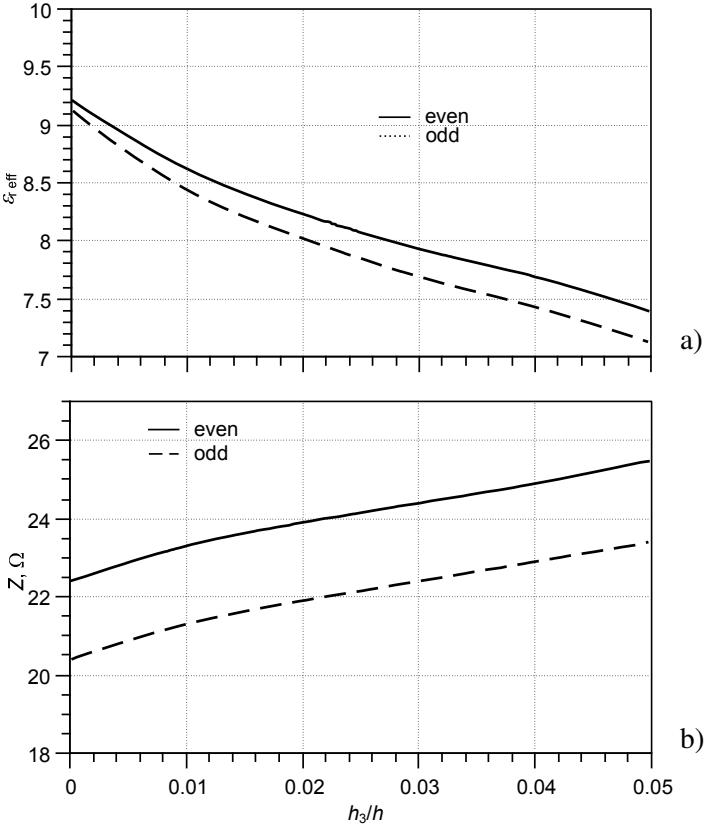

Fig. 2.24. Dependence of a) the effective permittivity and b) characteristic impedance of the double shielded coupled microstrip line on the normalized air microlayer thickness h_3/h, where $h_1/h = 0.5$, $\varepsilon_r = 9.6$, $W/h = 1$

Figures 2.21 and 2.22 show the change of effective permittivity and characteristic impedance of the coupled DSM lines and four-conductor multiconductor DSM line for the even and odd modes. It should be noted that the effective permittivity (Figs. 2.21 a) and 2.22 a)) of the odd mode is more sensitive to changes of the air gap due to the fact that more of the electric field lines are concentrated in this gap than in the even mode case.

Characteristic impedance (Figs. 2.21 b) and 2.22 b)) in this instance varies considerably less and almost in the same manner for the even and odd modes.

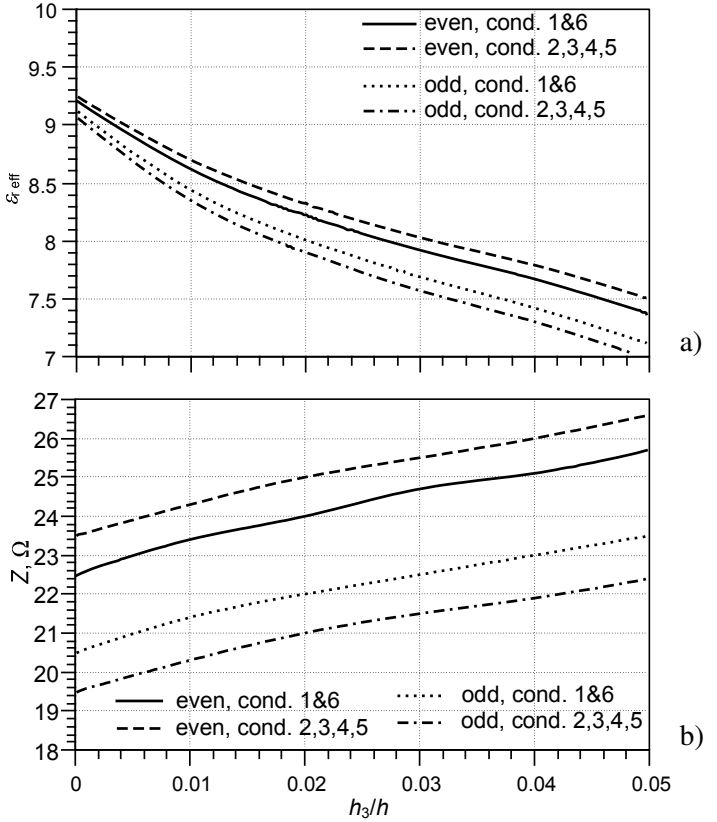

Fig. 2.25. Dependence of a) the effective permittivity and b) characteristic impedance of the double shielded six-conductor microstrip line on the normalized air microlayer thickness h_3/h, when $\varepsilon_r = 9.6$, $W/h = 1$, $S/h = 1$

It should be also noted that despite the considerable qualitative changes of the effective permittivity and the characteristic impedance shown in Figures 2.20–2.22, when the air gap emerges and increases, the relative variations of these parameters are not so significant. For example, the discussed jump of all curves in the initial area, when the air gap emerges, does not exceed 2–4%, and even twentyfold increase of the gap (from to $t/h_1 = 0.005$ to $t/h_1 = 0.1$) does not cause variation of curves by more than 2–6%.

Air Gap above the Microstrips

When the upper dielectric plate is mounted imprecisely for reasons explained in 2.4.1, the air gap of the DSM devices is further increased. The air gap exists between the dielectrics of the DSM line, but also there is air between the

conductors and the upper (covering) dielectric. The purpose of this set of modelling was to gain better knowledge of the influence of this air microlayer on the electrical characteristics of the DSML device.

The impact of this increased gap on the effective permittivity and characteristic impedance of the DSM transmission line, coupled lines and six-conductor line is presented in Figures 2.23–2.25.

It is seen in the graphs that the effective permittivity and characteristic impedance of the investigated devices varied monotonously when the air gap is changed – no fast abrupt changes or irregularities of curves have been noticed. However a quantitative change of the permittivity and impedance is greater than in the case of the gap caused by the non-zero microstrips thickness only. For example, for almost threefold increase of the total air gap the effective permittivity changes within 21–23% (Figs. 2.23 a), 2.24 a) and 2.25 a)), and the characteristic impedance – 13–14% (Figs. 2.23 b), 2.24 b) and 2.25 b)).

In case when air layer is between the conductors and the upper dielectric plate of the DSML, charactersitic impedance slightly increases, when the thickness of the said air layer is increased.

Such a significant change of the permittivity and impedance may be explained by the fact that in this case the layer of air is in contact not only with microstrips side walls but also is located between the microstrips plane and the upper dielectric plate, so part of the electric field is in the air layer, and the unit-length capacitance of the lines decreases.

2.5. Conclusions of Chapter 2

1. Models of asymmetrically coupled microstrip lines and multiconductor microstrip lines, based on the method of moments, have been created. Comparison with results obtained by the conformal mapping and spectral-domain analysis has shown good accuracy of less than 4% for the most of the practical ranges of physical dimensions. The models have also been used to evaluate the influence of constructional parameters: dielectric constant of the substrate, normalized width and gap size between the conductors, on the electrical characteristics: modal voltages, effective permittivity and characteristic impedance of the lines.
2. Models of coupled and multiconductor striplines in stratified dielectric medium, based on the finite difference method have been created. Difference of the results compared with published values obtained by other methods was less then 5%.

3. By analysing coupled microstrip line on a double layer dielectric substrate and the similar structure with an additional layer of dielectric above the conducting strips it was found, that for particular combinations of dielectric constants and thicknesses of layers, pahse velocities for both – even and odd mode were equal. Such property is useful redusing cross-talk betwwen the adjacent transmission lines.
4. The created model was used to evaluate the effect of air microlayer in double shielded microstrip structures. Two types of air microlayer types were analysed. In one case, air microlayer is present due to non-zero thickness of the conducting strips, and in other case, air microlayer is present between the conducting strips and the upper dielectric plate due to imprecise placement of the upper plate or non-uniform thickness of the conducting strips.
5. Analysis showed, that air microlayer above the conducting strips has more significant effect on the electrical characteristics of the lines that air microlayer between the dielectric plates. However the effects have to be taken into account when designing devices based on double shielded microstrip structures.

3

Synthesis Technique of Microstrip Slow Wave Devices in Stratified Dielectric Medium

In this chapter synthesis techniques, based on the models described in Chapter 2, of the multiconductor microstrip lines (MCML) are investigated. Multiconductor microstrip line is the simplest case of stratified dielectric medium, consisting of two dielectrics: dielectric substrate and the surrounding air. MCMLs are widely used as a basis for modelling periodic slow-wave devices (SWD) such as meander and helical delay lines.

Synthesis algorithm is described and results of the synthesis presented and analyzed.

Three articles have been published on the topic of this chapter: (Mikučionis, Urbanavičius 2010b; Mikučionis, Urbanavičius 2011; Mikučionis 2012)

3.1. Synthesis technique

3.1.1. General Aspects of Synthesis

Analysis techniques are useful for analyzing structures and general model research. However, synthesis – calculation parameters of the device for some specific characteristics is needed for design of the devices.

One of the ways of performing synthesis is iteration of analysis by changing parameters until the desired characteristics are obtained, i.e. optimization problem needs to be solved.

Since modelling procedures have high demands for computational resources, number of iterations must be the lowest possible. Therefore, thorough knowledge about analysis models and choice of iteration technique is necessary.

In general, synthesis algorithm is solving some equation:

$$f(x) = f_0, \tag{3.1}$$

where $f(x)$ is some characteristic dependent on variable x, and f_0 is the desired value of a characteristic. Or it can be rewritten as

$$f(x) - f_0 = 0. \tag{3.1a}$$

Since exact solutions are not possible using numerical techniques, the solution of the problem becomes looking for a value, which differs from a desired one by no more than error δ. In this case x satisfying the following inequality is to be found:

$$\left| f(x) - f_0 \right| < \delta. \tag{3.2}$$

The whole synthesis technique can be broken down to the following steps:

Step 1. Picking the initial value of x, and calculating value of the function $f(x)$.

Step 2. Checking if the error $\left| f(x) - f_0 \right|$ is less than the desired δ,

Step 3. If so calculations end, otherwise, proceed to Step 4.

Step 4. New value of x is chosen and the procedure is repeated.

The more complicated structures are synthesized, the more time it takes for the first step (calculation of the function $f(x)$ value) to complete, therefore it is critical to minimize the number of iterations to be able to synthesize complicated structures in reasonable amount of time.

Number of iterations highly depends on how fast x approaches the desired value x_0 during every iteration. This property of root finding algorithm is called convergence speed. Newton-Raphson method was chosen for this work due to its fast convergence and applicability of discrete derivatives. It proved to be effective while testing the algorithms.

3.1.2. The Newton-Raphson Method

The Newton-Raphson method is a method of finding successively better approximations of the roots of the equation of type (3.1a). The successive root is expressed as:

$$x_{i+1} = x_i - \frac{f(x_i)}{f'(x_i)}, \tag{3.3}$$

where x_i is a current root iteration, $f(x_i)$ is value of a function of a current root iteration and $f'(x_i)$ is a value of a derivative of a function at a current root iteration.

In cases when a function is a calculation algorithm, rather than an analytical epression, discrete derivative can be used:

$$f'(x_i) \approx \frac{f(x_i + \Delta x) - f(x_i)}{\Delta x}, \tag{3.4}$$

where Δx is sufficiently small change of the function argument. Therefore, Equation (3.3) for a numerical case is expressed as:

$$x_{i+1} = x_i - \frac{\Delta x \cdot f(x_i)}{f(x_i + \Delta x) - f(x_i)}. \tag{3.5}$$

In some cases Δx is chosen to be the difference between two successive root iterations $\Delta x = x_i - x_{i-1}$, and the method is then also called a secant method, and the successive root iteration is expressed as:

$$x_{i+1} = x_i - f(x_i)\frac{x_i - x_{i-1}}{f(x_i) - f(x_{i-1})}. \tag{3.6}$$

Both of the mentioned methods have been used in the calculations described in this dissertation.

3.2. Synthesis of Multiconductor Lines Operating in Normal Mode

As it was shown in Chapter 2, modal voltages are different for conductors of multiconductor microstrip line operating in normal mode, if widths of the conductors are equal, and gaps between the conductors are of the same size. However, it might be useful to design a microstrip multiconductor line for which absolute values of modal voltages for even or odd mode are equal. In order to solve this problem, synthesis procedure can be applied.

Microstrip multiconductor line is considered. Thickness and properties of the dielectric are fixed, so are the gaps between the conductors. Initial widths of the conductors are chosen. It is already known that in case widths of the conductors are equal, modal voltages of the conductors for even and odd modes are not equal. Therefore widths of the conductors must be modified in order to have modal voltages of the same absolute value.

In general case, modal voltage of every conductor can be considered as a function of widths of all conductors of an MCML:

$$\begin{aligned} V_1 &= f\left(W_1, W_2, ...W_N\right), \\ V_2 &= f\left(W_1, W_2, ...W_N\right), \\ &... \\ V_N &= f\left(W_1, W_2, ...W_N\right). \end{aligned} \tag{3.7}$$

Therefore, the problem to be solved is the equation:

$$V_1 = V_2 = ... = V_N .$$

It is also known that the line is symmetric, i.e. $W_1 = W_N$, $W_2 = W_{N-1}$ and so forth; and correspondingly $V_1 = V_N$, $V_2 = V_{N-1}$ etc. So number of equations and variables reduces in half.

It has also been noticed in calculations described in Chapter 2, that modal voltage of the conductor is highly dependent on its own width, and almost independent on widths of other conductors. Therefore Equation (3.7) can be expressed:

$$\begin{aligned} V_1 &= f\left(W_1\right), \\ V_2 &= f\left(W_2\right), \\ &... \\ V_N &= f\left(W_N\right). \end{aligned} \tag{3.7a}$$

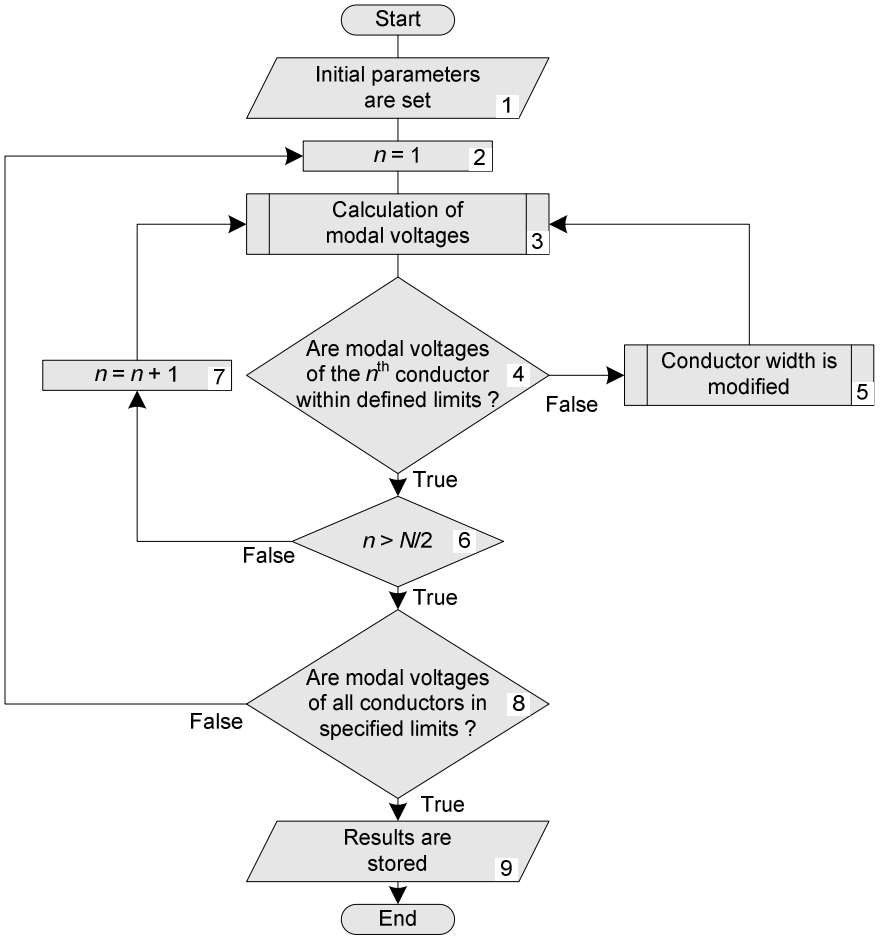

Fig. 3.1. Flowchart of synthesis algorithm

The synthesis procedure is best described by a flowchart diagram (Fig. 3.1). The description of the flowchart in Figure 3.1 is as follows:

Step 1. The initial parameters are set. These include widths of the conductors W_i and gaps between them S_i, thickness h and dielectric constant of the substrate ε_r.

Step 2. Synthesis starts at the first conductor.

Step 3. Modal voltages V_i are calculated as described in Chapter 2.

Step 4. It is checked, if voltages of the conductors are within defined limits, if not, Step 5 is performed, if true, calculation proceeds to Step 6.

Step 5. Widths W_i of the conductors are modified according to formula presented in Equation (3.5) or (3.6), proceed to Step 3.

Step 6. It is checked if all conductors have been calculated, if true, Step 8 is performed, if false, algorithm proceeds to Step 7.

Step 7. Conductor index is incremented, Step 3 is performed.

Step 8. It is checked if modal voltages for a specified mode of all conductors are within specified limits, if false, calculation proceeds to Step 2 and modal voltages of all conductors are synthesized again. If true, it is considered, that the required line is calculated, algorithm proceeds to Step 9.

Step 9. The resulting parameters and characteristics of the line are output and/or stored for further processing.

3.3. Results of Synthesis

Multiple syntheses were performed in order to estimate what constructional parameters of the MCML are required, so that modal voltages for some particular mode are equal for every conductor.

3.3.1. Synthesis of Four Conductor Line

The proposed technique for synthesis of symmetrically coupled MMCL, operating in normal mode, was investigated in the following order. Firstly, accuracy of the mathematical model (the analysis stage) used in the proposed technique was tested by comparing the results of the calculations with the results obtained by other research methods. Model verification results are presented in subchapter 2.52.

Further, the dependence of the width of the conductors W_i and the characteristic impedance Z_i on constructional parameters of an MCML: space between the conductors S and the dielectric constant of the substrate ε_r was investigated for the lines operating in particular modes.

The proposed technique was used to synthesize four-conductor MCML, operating in A- (even) and D- (odd) normal modes. These modes were selected due to their potential practical utility, applying to the conductors correspondently +1 V, +1 V, +1 V, +1 V or +1 V, –1 V, +1 V, –1 V voltages. During the synthesis procedure, accordingly to defined *S*/*h* ratio, dielectric constant of the substrate ε_r, and selected type of normal mode, the ratio of widths of adjacent

conductors W_1/W_2 (or W_4/W_3), which ensured propagation of single normal wave, was searched. Having found such a ratio the process of synthesis was finished, and the characteristic impedance $Z_{1\&4,2\&3\ e,o}$ of the conductors of the MCML and relative effective permittivity $\varepsilon_{r\ eff\ e,o}$ were calculated. The results of the synthesis of the MMCL, operating in even and odd normal mode are shown in Figures 3.2 to 3.4.

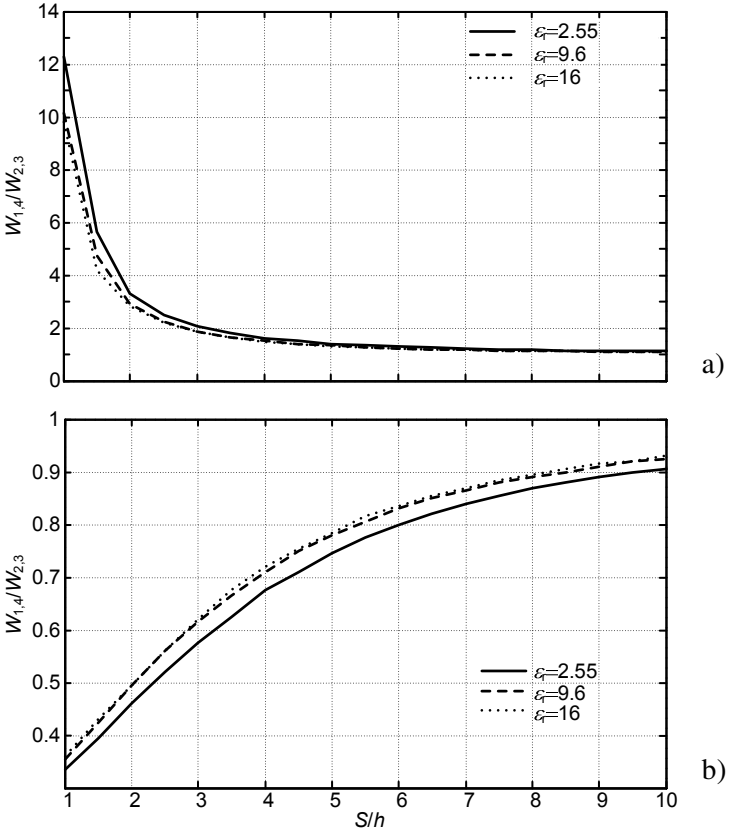

Fig. 3.2. Dependence of ratio of widths of conductors of the four conductor MCML on the size of gap between the conductors in case of a) even mode and b) odd mode, when $W_{2,3}/h = 1$

In order to ensure the propagation of the even normal wave, i.e. make phase velocities v_p equal along all conductors in the MCML, the widths of the external conductors W_1 and W_4 should be larger than that of the internal conductors ($W_{1\&4} > W_{2\&3}$). In case of the odd normal wave – the external conductors should be narrower than internal ($W_{2\&3} > W_{1\&4}$). It is necessary to note that at small

distances between the conductors ($S/h < 2$), the ratio of widths of neighbouring wide and narrow conductors W_1/W_2 for the even normal wave exceeds the same ratio (W_2/W_1) more than twice for the odd normal wave (Fig. 3.2).

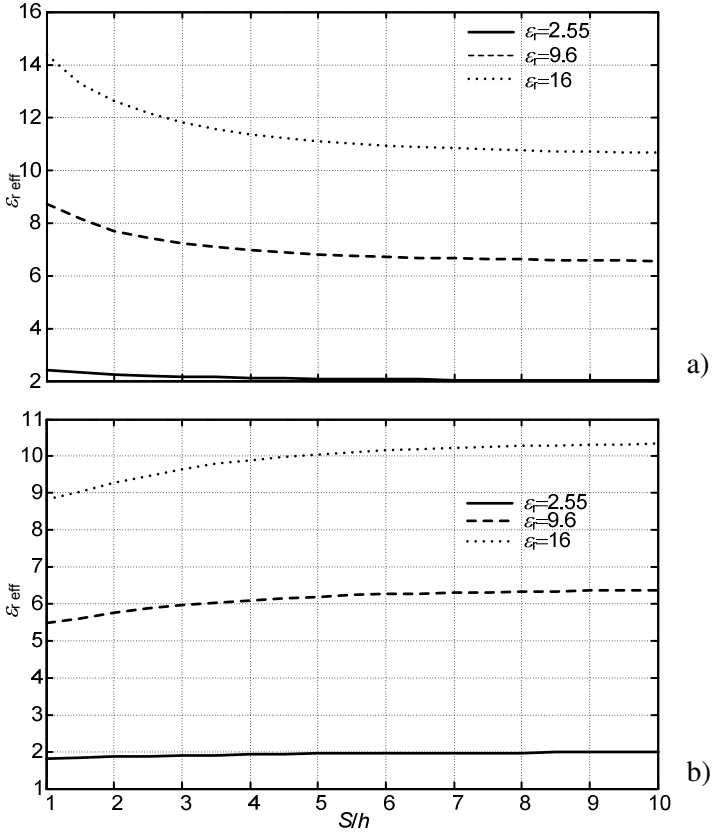

Fig. 3.3. Dependence of the effective permittivity of the four conductor MCML operating in a) even mode and b) odd mode on the size of gap between the conductors when $W_{2,3}/h = 1$

It is natural, that increasing the space between the conductors of an MCML, their intercoupling becomes negligible and the ratio of widths of the adjacent conductors (W_1/W_2) approaches unity for both: even normal wave, and odd normal wave, regardless of the permittivity of the dielectric substrate (Fig. 3.2).

The effective permittivity $\varepsilon_{r\,eff}$ of an MCML which characterizes the phase velocity of the wave propagating in the line, changes slightly, varying the space between conductors (Fig. 3.3). For example, at tenfold change of the space between the conductors, the effective permittivity $\varepsilon_{r\,eff}$ of the MCML, operating

in the even normal mode, changes, depending on the dielectric constant of the dielectric substrate ε_r, within 20–35%, and in the MCML, operating in the odd normal mode, under the same conditions, the change is even less: 10–17%.

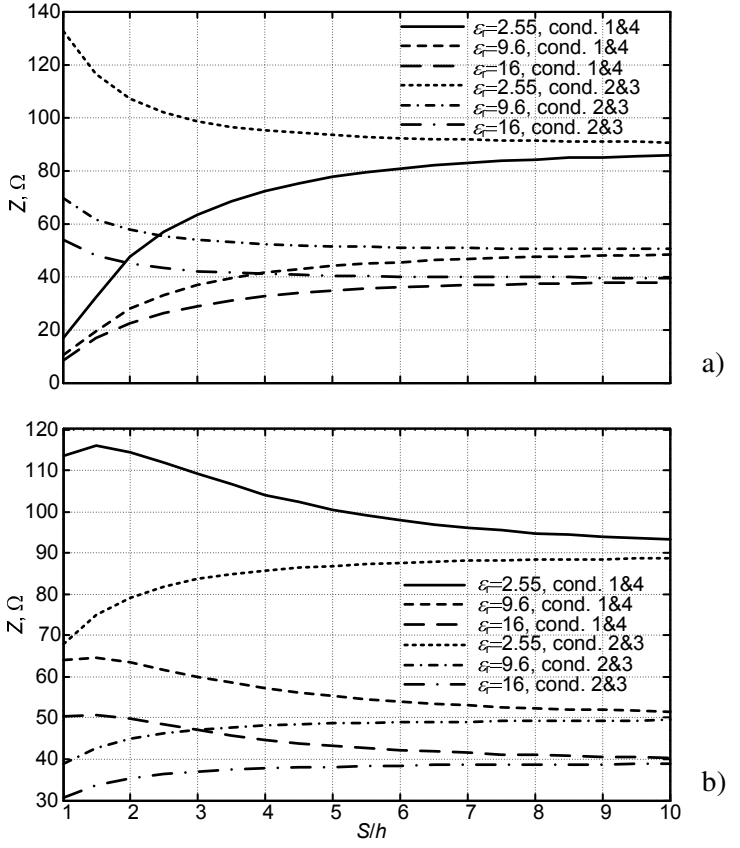

Fig. 3.4. Dependence of the characteristic impedance of the four conductor MCML operating in a) odd mode and b) even mode on the size of gap between the conductors when $W_{2,3}/h = 1$

Increasing the space between adjacent conductors of the MCML, causes their characteristic impedance to become comparable and the difference between MCML, operating in opposite normal modes, becomes negligible. E.g. when $S/h = 1$ the difference between $Z_{1\&4,\,e}$ and $Z_{2\&3,\,e}$ is 5–6 times, depending on permittivity of the dielectric substrate ε_r (the larger ε_r, the less difference). And when $S/h = 10$ the said difference is only 3–7% (Fig. 3.4). If an MCML operates in odd normal mode, the difference between $Z_{1\&4,\,o}$ and $Z_{2\&3,\,o}$, when $S/h = 1$, is

less than when the MCML operates in even normal mode, it is only 65–75%. And for S/h = 10, the said difference is 3–7% (Fig. 3.4).

3.3.2. Synthesis of Six Conductor Line

Further, the proposed technique was used to synthesize six-conductor MMCL, operating in even and odd normal modes, in order to investigate MMCL characteristics dependence on its constructive parameters. These modes were selected due to their potential practical utility, applying to the conductors correspondently equal voltages +1 V, … , +1 V or applying counter-phase voltages +1 V, –1 V,… , +1 V, –1 V.

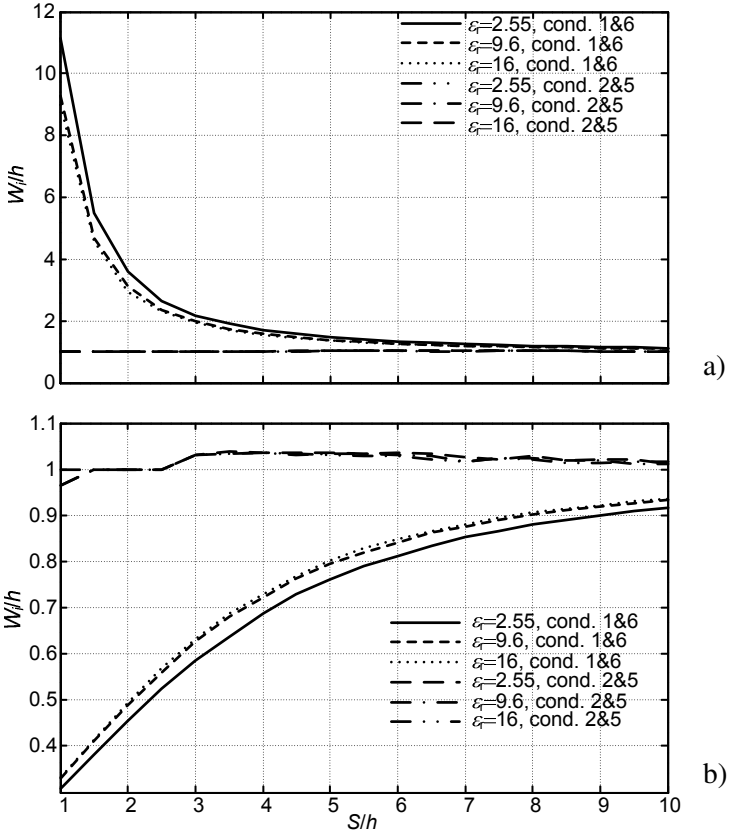

Fig. 3.5. Normalized width of conductors of synthesized six-conductor symmetrically coupled MCML, operating in a) even mode and b) odd mode, versus normalized space between conductors at different dielectric constants of the substrate, when $W_{3,4}/h$ = 1

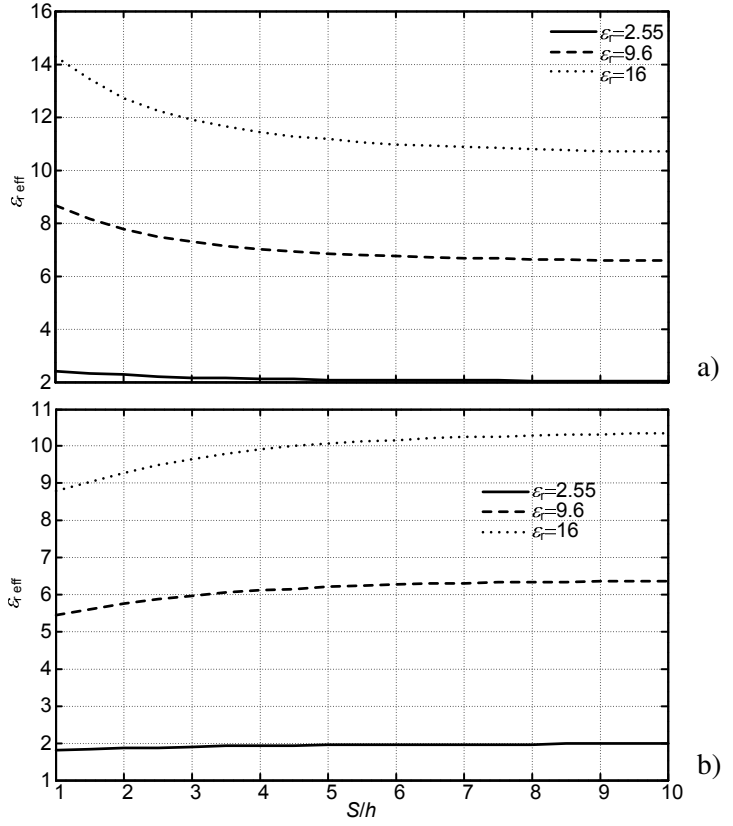

Fig. 3.6. Effective dielectric permittivity of synthesized symmetrically coupled six-conductor multiconductor microstrip line, operating in a) even and b) odd normal modes, versus normalized space between conductors and permittivity of the dielectric substrate, when $W_{3,4}/h = 1$

The widths of conductors, which ensured propagation of single normal wave, were searched during the synthesis procedure, accordingly to the defined S/h ratio, dielectric constant of the substrate ε_r, and the selected type of normal mode. After finding such widths, the process of synthesis was finished, and the characteristic impedance $Z_{i\,e,o}$ of the conductors of the MCML and the effective permittivity $\varepsilon_{r\,eff\,e,o}$ were calculated. The results of the synthesis of the MCML, operating in even and odd normal modes are shown in Figures 3.5–3.7.

Firstly, by examining these figures, it is necessary to note that all diagrams, submitted in Figures 3.5 a), 3.6 a), and 3.7 a), characterize the MCML, operating in the even normal mode, and there are inverse relationships in comparison with corresponding diagrams in Figures 3.5 b), 3.6 b) and 3.7 b), that characterize the

MCML, operating in the odd normal mode. By further, analyzing the curves presented in Figure 3.5, it can be assumed that a symmetrically coupled MCML, operating in a normal mode, is a regular multiconductor line in its middle part, i.e. only widths of the external conductors (in this case $W_{1\&6}$ see Figure 3.5 a) for the even mode and Figure 3.5 b) for the odd mode) should be changed for rough adjustment of an MCML.

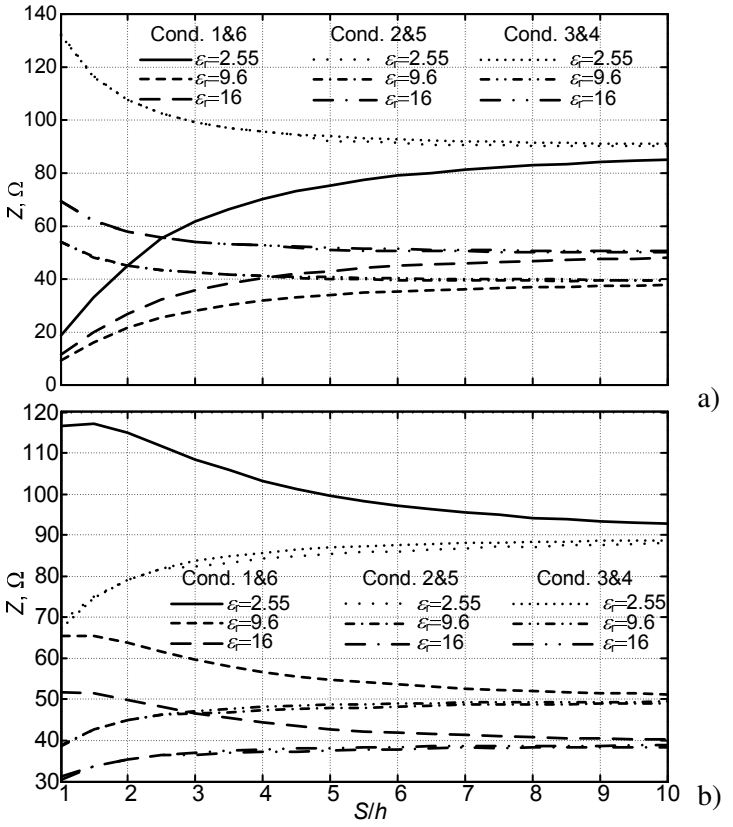

Fig. 3.7. Characteristic impedance of the synthesized symmetrically coupled six-conductor multiconductor microstrip line, operating in a) even and b) odd normal modes, versus normalized space between conductors and permittivity of the dielectric substrate, when $W_{3,4}/h = 1$

In order to ensure the even normal wave propagation in an MMCL, the width of the external conductors (in case under consideration these are conductors #1 and #6) should be greater than that of the internal conductors (Fig. 3.5 a)), and on the contrary, in case of odd normal wave (Fig. 3.5 b)) – the

external conductors should be narrower than internal ones. It is necessary to note that at small distances between the conductors (when $S/h < 2$), the ratio of widths of wide and narrow conductors W_1/W_2 for the even normal wave exceeds the same ratio (W_2/W_1) more than twice for the odd normal wave (Fig. 3.5 a) and Fig. 3.5 b)). By analyzing the curves presented in Figure 3.5 a) for the even mode, and Figure 3.5 b) for the odd mode, it is seen that the widths of the external conductors have the most influence on the propagation of normal waves in an MCML, while widths of internal conductors vary negligibly while changing S/h.

Diagrams presented in Figure 3.6 show that the effective permittivity $\varepsilon_{r\,eff}$ in case of both – even and odd modes, changes slightly, while changing the space between conductors. For example, at tenfold change of the space between the conductors, the effective permittivity $\varepsilon_{r\,eff}$ of the MCML changes, depending on the dielectric constant of the substrate ε_r, within 20–35%, and in the MCML, operating in the odd normal mode, under the same conditions, the change is even less: 10–17%.

Increasing the space between adjacent conductors of the MCML, causes their characteristic impedance to become comparable and the difference between MCML, operating in opposite normal modes, becomes negligible (Fig. 3.7). E.g. when $S/h = 1$ the ratio between $Z_{1\&6}$ and $Z_{2\&5,3\&4}$ is 5–6 times (Fig. 3.7 a)), depending on the dielectric constant of the substrate ε_r (the larger ε_r, the less the difference). And when $S/h = 10$, the said difference is only 3–7% (Fig. 3.6 b)). If an MCML operates in the odd normal mode, the difference between $Z_{1\&6}$ and $Z_{2\&5,3\&4}$ (Fig. 3.7 b)), when $S/h = 1$, is less than in case of the even normal mode, only 65–75%. And for $S/h = 10$, the said difference is 3–7% (Fig. 3.7 b)).

Conductors of the synthesized MMCL were divided into 2500–4500 sub-areas (for odd and even-mode respectively) during all calculations, and the synthesis procedure took 220–560 s (Pentium 4 CPU, 3 GHz clock frequency and 1 GB RAM).

3.4. Conclusions of Chapter 3

1. Synthesis technique of microstrip multiconductor lines operating in normal mode has been created ant implemented in software. Two cases were tested – four conductor MCML and six conductor MCML. In both cases it was noticed, that only widths of the outermost conductors have to be changed in order to ensure propagation of a single normal mode. In case of even mode, the outermost conductor width has to be increased, and in case of odd

mode, the outermost conductors have to be narrower than the rest. Modal voltages of the conductors differ by no more than 2% in this case.

2. In case of tightly coupled MCMLs ($S/h < 5$), in order to ensure propagation of normal modes with equal amplitudes of signals, ratio of the widths of the conductors can go as high as 12.
3. When dielectric constant of the substrate is lower, MCML operating in normal mode is more sensitive to change of conductor width and gap size between the conductors. For example, the ratio of the widths of the adjacent wide and narrow conductors for even mode exceeds the same ratio more than twice for the odd mode.
4. If an MCML is designed to operate in a normal mode with equal signal amplitudes, characteristic impedance is more dependent on the gap size between the conductors, when the dielectric constant of the substrate is lower. On the other hand, the effective permittivity of the lines is more dependent on the gap size between the conductors, when the dielectric constant of the substrate is higher.

4

Hybrid Models of Meander Microstrip Delay Line in Stratified Dielectric

In this section hybrid models of two delay lines in stratified dielectric medium, and results of investigation are presented. The first model is the meander microstrip delay line (MMDL), based on the multiconductor microstrip line (MCML) operating in even normal mode. The second one is the double shielded microstrip meander delay line (DSMMDL).

In general case hybrid model is based on at least two methods of analysis and/or synthesis. In the case described in this chapter, the model of an MCML is based on the method of multiconductor lines (synthesis of an MCML) and the method of moments (MoM) for the analysis of an MCML. The model of the DSMMDL is based on the method of finite differences (analysis of the double shielded microstrip structures and synthesis of the DSMMDL) and the *S*-parameter matrix method (analysis of the DSMMDL).

Three papers have been published on the topic of this chapter: (Krukonis *et al* 2013; Krukonis, Mikučionis 2014; Mikučionis *et al.* 2014).

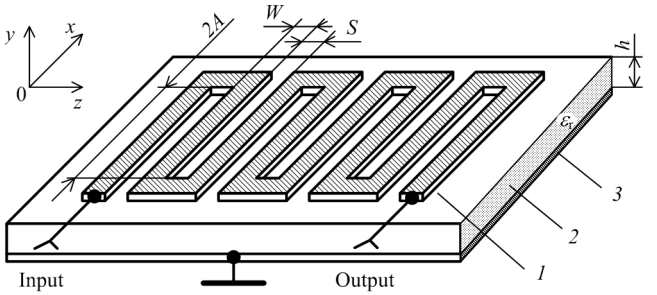

Fig. 4.1. The structure of the ordinary microstrip meander delay line, where 1 is a signal conductor in the form of meander; 2 is a dielectric substrate; 3 is a reference conductor

4.1. Microstrip Meander Delay Line, Based on the Multiconductor Line, Operating in Even Normal Mode

Delay of signals in electrodynamic delay lines (DLs) is caused by propagation of an electromagnetic wave through a predefined path for the prescribed finite time interval – delay time. In order to increase the delay time of the DLs without increasing their dimensions by significant amounts, the length of the path for the electromagnetic wave propagation is increased by shaping the transmission conductor of the DL into a longer line. In most cases meander or helical shapes are used. Thus electrodynamic DLs have a periodic structure with a specific repetition period of the meander strips or helical loops; therefore the multiconductor line method is applicable for the analysis and modelling of such lines.

The multiconductor line method is notable for its moderate demand of computational resources, which is very important for DL synthesis. According to this method the multiconductor line and the corresponding analysed DL are both periodic, therefore theoretically infinite, and consist of the infinite number of evenly spaced conductors of equal widths. However real DLs, which have finite dimensions, based on such infinite periodic multiconductor lines have non-uniform parameters at the side conductors caused by non-uniform electromagnetic field spread. The influence of non-uniformity of the multiconductor microstrip line (MCML) effective permittivity $\varepsilon_{r\ eff}$ on the frequency response of the meander microstrip delay line (MMDL) is studied in this subchapter.

4.1.1. Design and Modelling of the Meander Microstrip Delay Line

The generalized structure of the MMDL is presented in Figure 4.1. It consists of a dielectric substrate, on one side of which is a conductive layer, and a meander-shaped transmission conductor on the other. According to the multiconductor line method, such MMDL is modelled using the MCML, structure of which is shown in Figure 4.2 a). Thickness h and dielectric constant ε_r of the substrate of the MCML is the same as those of the MMDL substrate, moreover, width W of the conductors of the MCML and space S between them are also equal to the corresponding dimensions of the MMDL signal conductor.

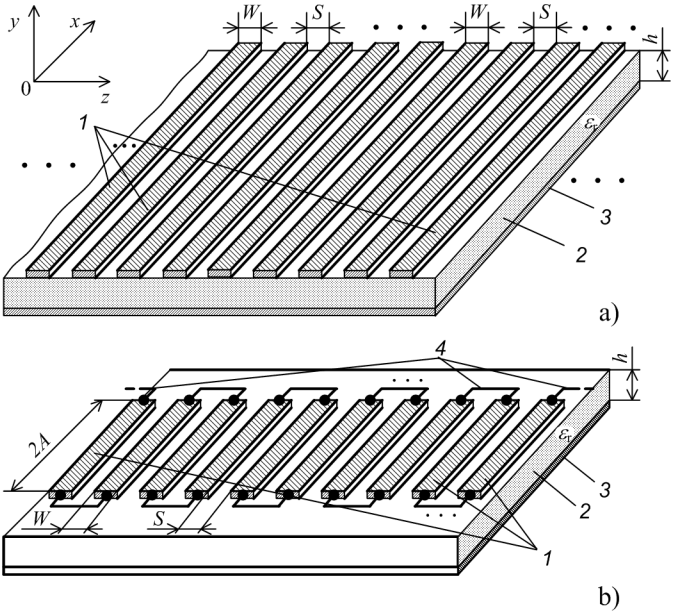

Fig. 4.2. Structure of a) multiconductor microstrip line and b) microstrip meander delay line model based on multiconductor microstrip line: *1* are the line conductors; *2* is a dielectric substrate; *3* is a shield; *4* are meander rod connections

For the mathematical model, MCML is considered infinite in both – x and z directions. A meander structure is derived from the MCML by separating the section of length $2A$ in x direction and accordingly connecting the ends of the obtained conductor strips (Fig. 4.2 b)).

In general two kinds of non-uniformity appear in real MMDLs based on the mathematical model of the MCMLs:

- non-uniformity of characteristic impedance $Z_i \neq Z_j$, and
- non-uniformity of effective permittivity $\varepsilon_{\text{r eff}\,i} \neq \varepsilon_{\text{r eff}\,j}$,

where i and j are numbers of conductors of the MMDL, and $i \neq j$ for both cases. These kinds of non-uniformity are caused by equal widths of all strips of the meander conductor according to widths of the conductors of the corresponding periodic MCML. The technique used to investigate the influence only of non-uniformity of effective permittivity $\varepsilon_{\text{r eff}\,i} \neq \varepsilon_{\text{r eff}\,j}$, of the MCML on responses of the MMDL is further described.

Two steps are included in the MMDL modelling. Firstly, the MCML, operating in even normal mode (hereafter referred to as the uniform permittivity MMDL) was synthesized using the technique described in Chapter 3. Further, the corresponding MMDL is created in the Sonnet® software environment, using dimensions of the synthesized MCML, and responses of this MMDL are calculated. The calculated responses are compared with those of the MMDL with equal widths of the conductors. The assumption is made that conductors and dielectric substrates of the synthesized MCMLs and investigated MMDLs are ideal lossless, and it is also assumed that the thickness of the conductors is zero.

4.1.2. Investigation of the Influence of Phase Velocity Differences on Frequency Characteristics of the Microstrip Meander Delay Line

In general, N modes can propagate in the MCML which consists of N signal conductors. However, only the even and odd modes are practically interesting when the MCML model is used for the design of the MMDL. The odd mode is used for analysis of the MMDL at high frequencies beyond the bandwidth, when the phase difference between adjacent meander strips voltages is equal to $(2k + 1)\pi$, where $k = 0, 1, 2, \ldots$ Therefore, when designing the MMDL, determination of the size of the meander topology and parameters of the dielectric substrate, it is sufficient to calculate the MCML parameters for the even mode only.

The even mode is possible in the MCML when phase velocities of electromagnetic waves propagating along the equipotential conductors of the MCML are equal, which in turn is only possible if the effective permittivities of the conductors are equal for the even mode. In case of periodic and infinite MCMLs this condition is satisfied naturally. In the MCMLs consisting of a finite number of conductors effective permeability is very irregular (Fig. 4.3). This irregular distribution of permittivity affects the determination of the delay time and the bandwidth of the designed MMDL (Fig. 4.4).

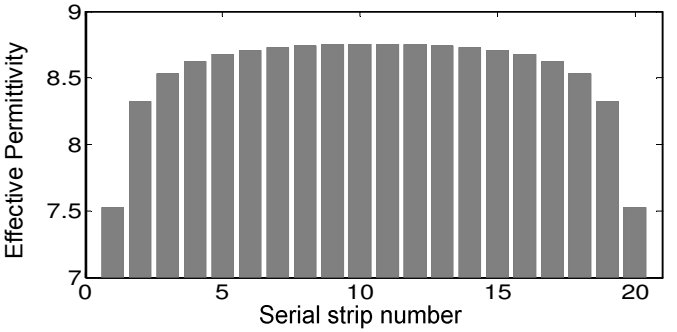

Fig. 4.3. Effective dielectric permittivity of the microstrip meander delay line based on the model of the microstrip multiconductor line, when $\varepsilon_r = 9.6$, $h = 0.5$ mm, $W = 0.6$ mm, $S = 0.5$ mm, $2A = 20$ mm, $N = 20$

Side conductors of the MCML should be wider than the inner ones in order to make its effective permittivity equal in all strips (i.e. to ensure the operation of even mode). However, characteristic impedance of such wide conductors differs significantly from the impedance of the regular part of the MCML as well as the rest of the signal transmission path, resulting in mismatch of the MMDL. For this reason, in addition to the resonances, frequencies of which are related to the wavelength of the electromagnetic wave propagating in the MMDL and may be approximated by the following equation:

$$f_k = \frac{c_0 k}{\sqrt{\varepsilon_{reff}}\left(2 \cdot 2A + S\right)}, \tag{4.1}$$

where c_0 is the velocity of light in free space, k is a serial number of resonance, $\varepsilon_{r\,eff}$ is effective permittivity of the MCML, $2A$ and S are dimensions of the meander topology (Fig. 4.1), the significant oscillations of amplitude greater than 3 dB appear in the magnitude response of S_{21} parameter of this MMDL (Fig. 4.4 a)). On the other hand phase distortion of the MMDL designed according to the even mode MCML model, is less than the phase distortion of the MMDL based on the multi-mode MCML (Fig. 4.4 b)). However, oscillations of magnitude response of S_{21} parameter lead to the fact that the bandwidth of the uniform effective permittivity MMDL is determined by the amplitude, rather than phase response.

Delay time t_d and bandwidth ΔF are those critical characteristics that determine the structure of the MMDL. The dielectric constant of the substrate ε_r, number of meander strips N and their length $2A$ have the most effect on these characteristics. It should also be noted, that the above mentioned characteristics

t_d and ΔF are inversely related, i.e. changing the design parameters of the MMDL in order to increase its delay time, the bandwidth is narrowed and vice versa. Therefore, in order to unambiguously determine the effect of design parameters on the characteristics of the MMDL it is preferable to use the integrated measure of the DL quality – so-called *D*-factor, which is calculated as the product of delay time of the MMDL and its bandwidth:

$$D_{(u,\,u\text{-}n)} = t_{d(u,\,u\text{-}n)} \cdot \Delta F_{(u,\,u\text{-}n)}, \tag{4.2}$$

where bottom index (u) means the uniform parameters MMDL (i.e. uniform effective permittivity of the MCML), and index (n-u) means the non-uniform parameters MMDL (i.e. non-uniform effective permittivity of the MCML).

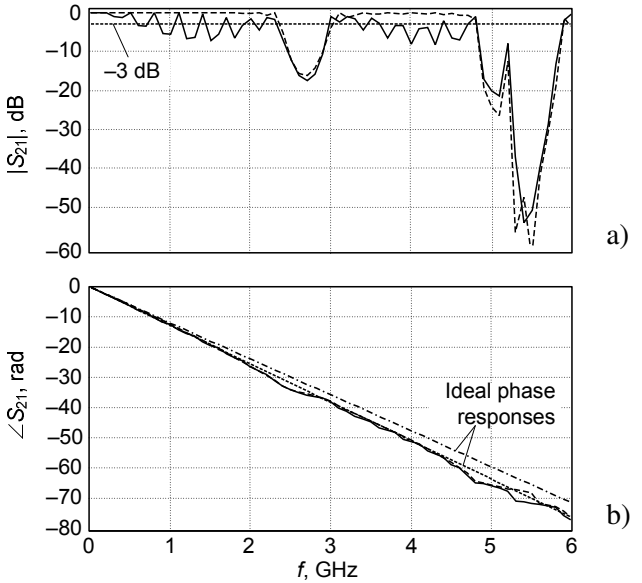

Fig. 4.4. Characteristics of the meander delay line design with equal phase velocities along the strips, when $\varepsilon_r = 9.6$, $h = 0.5$ mm, $S = 0.5$ mm, $2A = 20$ mm, $N = 10$

The results of the simulation of the MMDLs based on the model of the MCML, operating in the even mode are shown in Tables 4.1–4.4 with characteristics marked the subscript (u), which corresponds to the uniform effective permittivity MMDL. Characteristics of the MMDL based on the periodic MCML model, operating in the mixed modes are shown for comparison in the same tables; the subscript (n-u) marks these characteristics, i.e. the non-uniform effective permittivity MMDL. Relative differences between the

characteristics of the uniform and non-uniform impedance MMDLs are also presented. The differences are calculated as follows: delay time relative difference

$$\delta t_{\mathrm{d}} = \frac{t_{\mathrm{d(u)}} - t_{\mathrm{d(n\text{-}u)}}}{t_{\mathrm{d(n\text{-}u)}}} 100\% , \tag{4.3}$$

where $t_{\mathrm{d(u)}}$ is time delay of the uniform parameters MMDL, and $t_{\mathrm{d(n\text{-}u)}}$ is time delay of the non-uniform parameters MMDL; bandwidth relative difference

$$\delta \Delta F = \frac{\Delta F_{\mathrm{(u)}} - \Delta F_{\mathrm{(n\text{-}u)}}}{\Delta F_{\mathrm{(n\text{-}u)}}} 100\% , \tag{4.4}$$

where $\Delta F_{\mathrm{(u)}}$ is bandwidth of the uniform parameters MMDL, and $\Delta F_{\mathrm{(n\text{-}u)}}$ is bandwidth of the non-uniform parameters MMDL; MMDL D-factor relative difference

$$\delta D = \frac{D_{\mathrm{(u)}} - D_{\mathrm{(n\text{-}u)}}}{D_{\mathrm{(n\text{-}u)}}} 100\% , \tag{4.5}$$

where $D_{\mathrm{(u)}}$ is the D-factor of the uniform parameters MMDL, and $D_{\mathrm{(n\text{-}u)}}$ is the D-factor of the non-uniform parameters MMDL.

Table 4.1. Dependence of characteristics of the uniform and non-uniform effective permittivity in the microstrip meander delay line on the number of meander strips ($\varepsilon_{\mathrm{r}} = 9.6$; $h = 0.5$ mm; $2A = 20$ mm)

MMDL characteristic	Number of meander strips N			
	3	5	10	20
$t_{\mathrm{d(u)}}$, ns	0.706	1.05	2.01	3.64
$t_{\mathrm{d(n\text{-}u)}}$, ns	0.642	0.948	1.88	3.42
δt_{d}, %	10.0	11.0	6.9	6.4
$\Delta F_{\mathrm{(u)}}$, GHz	1.1	0.63	0.5	0.5
$\Delta F_{\mathrm{(n\text{-}u)}}$,GHz	1.5	1.2	0.91	0.6
δF, %	–27.0	–48.0	–45.0	–17.0
$D_{\mathrm{(u)}}$	0.777	0.662	1.005	1.82
$D_{\mathrm{(n\text{-}u)}}$	0.963	1.138	1.71	2.052
δD, %	–19.0	–42.0	–41.0	–11.0

Table 4.2. Dependence of characteristics of the uniform and non-uniform effective permittivity in a microstrip meander delay line on the height of meander strips ($\varepsilon_r = 9.6$; $h = 0.5$ mm; $N = 20$)

MMDL characteristic	Meander strip height $2A$, mm		
	10	20	40
$t_{d(u)}$, ns	2.12	3.64	6.91
$t_{d(n-u)}$, ns	2.04	3.42	6.63
δt_d, %	3.9	6.4	4.2
$\Delta F_{(u)}$, GHz	1.0	0.5	0.3
$\Delta F_{(n-u)}$,GHz	1.3	0.6	0.3
δF, %	–23.0	–17.0	0
$D_{(u)}$	2.12	1.82	2.073
$D_{(n-u)}$	2.652	2.052	1.989
δD, %	–20.0	–11.0	4.2

Table 4.3. Dependence of characteristics of the uniform and non-uniform effective permittivity in the microstrip meander delay line on the dielectric constant of the substrate ($h = 0.5$ mm; $2A = 20$ mm; $N = 20$)

MMDL characteristic	Relative dielectric permittivity of the substrate ε_r		
	4.5	9.6	16.0
$t_{d(u)}$, ns	2.62	3.64	5.1
$t_{d(n-u)}$, ns	2.61	3.42	4.78
δt_d, %	0.38	6.4	6.7
$\Delta F_{(u)}$, GHz	1.5	0.5	0.3
$\Delta F_{(n-u)}$,GHz	1.6	0.6	0.3
δF, %	–6.3	–17.0	0
$D_{(u)}$	3.93	1.82	1.53
$D_{(n-u)}$	4.176	2.052	1.434
δD, %	–5.9	–11.0	6.7

Analysis of the characteristics presented in Tables 4.1–4.4, shows that delay time of the uniform effective permittivity MMDL due to the greater width of the side meander strips in all investigated cases is larger than delay of the non-uniform effective permittivity MMDL. At the same time bandwidth $\Delta F_{(u)}$ of the uniform effective permittivity MMDL, due to the significant characteristic

impedance mismatch in most cases studied is narrower than bandwidth $\Delta F_{(u\text{-}n)}$ of the non-uniform effective permittivity MMDL.

Table 4.4. Dependence of characteristics of the uniform and non-uniform effective permittivity in the microstrip meander delay line on the gap size between meander strips ($\varepsilon_r = 9.6$; $h = 0.5$ mm; $2A = 20$ mm; $N = 20$)

MMDL characteristic	Gap size between strips S, mm		
	0.5	1.0	2.0
$t_{d(u)}$, ns	3.76	3.64	3.99
$t_{d(n\text{-}u)}$, ns	3.11	3.42	3.96
δt_d, %	21.0	6.4	0.76
$\Delta F_{(u)}$, GHz	0.2	0.5	1.1
$\Delta F_{(n\text{-}u)}$,GHz	0.6	0.6	1.0
δF, %	–67.0	–17.0	10.0
$D_{(u)}$	0.752	1.82	4.389
$D_{(n\text{-}u)}$	1.866	2.052	3.96
δD, %	–60.0	–11.0	11.0

Increasing the number of meander strips correspondingly increases delay time of the MMDL (Table 4.1). However, due to narrow bandwidth of the uniform effective permittivity MMDLs their D-factor is up to 42% less than the D-factor of the non-uniform effective permittivity MMDLs. Only at the largest of the investigated number of meander strips ($N = 20$) this difference was rather negligible – 11%.

Delay time of the MMDL can be changed also by varying the length of the meander strips (Table 4.2) and adopting dielectric constant of the substrate (Table 4.3).

The performed calculations have shown that varying the length of the meander strips $2A$ and dielectric constant of the substrate ε_r, characteristics of the MMDLs change in a similar way; i.e. increasing $2A$ or ε_r, the delay time increases also, however, the bandwidth becomes narrower. Again it was found that the bandwidth of the uniform effective permittivity MMDL in most cases is narrower than the bandwidth of the non-uniform effective permittivity MMDL. Only at $2A = 40$ mm (Table 4.2) and $\varepsilon_r = 16$ (Table 4.3), the bandwidth of both lines: of the uniform and non-uniform effective permittivity MMDL, is the same. D-factor of the investigated MMDLs varying $2A$ and ε_r has changed similarly.

The influence of the distance between the meander strips on the characteristics of the MMDL line is shown in Table 4.4. Increasing this space

the bandwidth of the MMDL increases proportionally and delay time remains almost unchanged. As in previous cases (Tables 4.1–4.3) bandwidth and *D*-factor of the uniform effective permittivity MMDL is lower than the same characteristics of the non-uniform effective permittivity MMDL. Only at a relatively large space between the strips (S = 2.0 mm) the uniform effective permittivity MMDL has better characteristics.

4.2. Investigation of the Double Shielded Meander Microstrip Delay Line

Microstrip devices are typically placed in a conductive package for protection against external electromagnetic fields. Top cover of such package becomes the second shield of the microstrip device. Beside that in case of microstrip delay devices, e.g. meander delay line, additional dielectric plate is placed between the top shield and a microstrip conductor, in order to reduce overall dimensions, while maintaining retarding properties. The design of such microstrip delay device becomes double-shielded (Fig. 4.5). The resulting structure of the double-shielded device is similar to a conventional stripline. However, one major difference is the presence of the air gap due to the non-zero thickness of the microstrip conductor. In order to distinguish such a structure from the conventional stripline, we call it double-shielded microstrip (DSM) structure. The said air gap makes the dielectric medium between the conductive shields inhomogeneous. In general, DSM device can be considered as a special case of a layered dielectric structure.

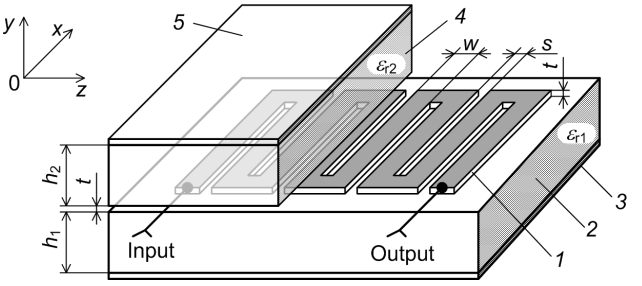

Fig. 4.5. The structure of the double shielded microstrip meander delay line, where *1* is a signal conductor in the shape of meander, *2* is a bottom dielectric substrate, *3* is a bottom shield, *4* is a dielectric plate, *5* is a top shield. A portion of the top plate is omitted in a picture for visual purposes

4.2.1. Model of Double Shielded Meander Microstrip Delay Line

In order to investigate the influence of the air gap on the frequency dependence of the phase delay (i.e., the dispersion characteristics) of the double shielded meander delay line (DSMMDL) two models were created. The first model (Fig. 4.5) takes into account the influence of the air gap caused by the non-zero thickness meander microstrips. The gap between the meander and upper dielectric plate is absent here. The second model imitates deviated mounting of dielectric plate on top of the DSMMDL resulting in an additional air gap above the meander conductor.

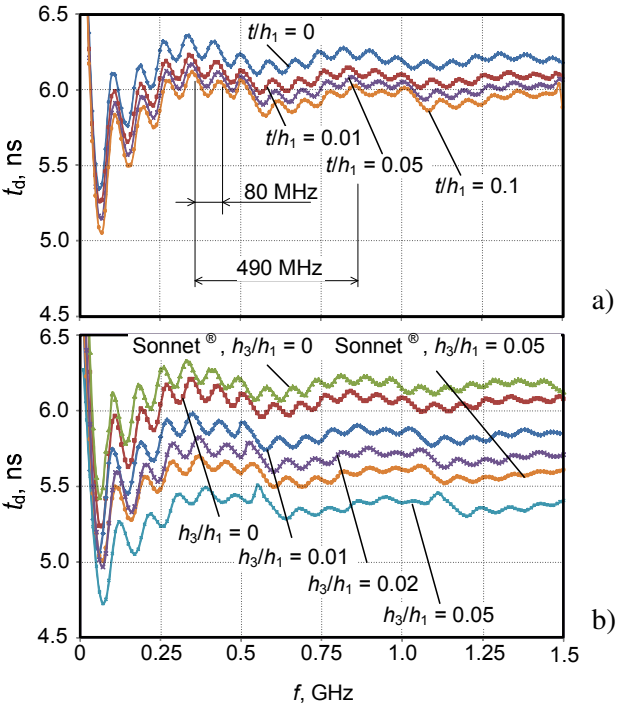

Fig. 4.6. Calculated and simulated dependencies of dispersion characteristics of the double shielded microstrip meander delay line on a) conductor thickness and b) thickness of the air gap, when $\varepsilon_{r1} = \varepsilon_{r2} = 9.6$, $w_t/w_1 = 1.0$, $w_1/h_1 = 2.0$, $s/h_1 = 1.0$, $t/h1 = 0.02$, $h_2/h_1 = 1.0$, $h_1 = 0.5$ mm

The calculated dispersion characteristics of the DSMMDL are presented in Figure 4.6. The DSMMDL models are formed from multiconductor line, parameters of which are shown in Figure 2.22. The length 2*A* of the meander

strips in this case is chosen to be equal to 100 mm. The calculations are performed in two ways: a hybrid method – a combination of the FDM and scattering matrices (Štaras *et al.* 2012), and using Sonnet® simulator. The curves in Figure 4.6 a) show the effect of the thickness of the air gap, which is caused by the non-zero thickness of meander microstrips on the dispersion characteristics of the DSMMDL. Figure 4.6 b) displayed the same characteristics, but their variation along the time axis due to changes of the air gap above the meander conductor. Chart analysis shows that at very low frequencies there is a significant rise of the dispersion characteristics inherent in all meander delay lines. However, despite the large absolute values of this rise, the ratio of the delay time with the period of the correspondent low frequency oscillation is only a fraction of a percent, and does not cause significant phase distortion. At all the dispersion characteristics of Figure 4.6 oscillations of two types are visible: of a rare repetition period along the frequency axis – about 0.5 GHz, and with the frequent repetition period – about 80 MHz. The assumption can be made that rare oscillations (~0.5 GHz) are caused by inhomogeneities of the signal path at the ends of the meander strips where neighbour strips are connected with each other (0.48–0.55 GHz, depending on the thickness of the air gap, is the frequency at which the coupled neighbour strips are a wavelength long).

$$f_{\text{rare}} = \frac{c_0}{2\sqrt{\varepsilon_{\text{reff}}}\,2A} = \frac{3\cdot 10^8}{2\sqrt{9.3}\cdot 0.1} \cong 491.9\cdot 10^6 \text{ Hz} \approx 490 \text{ MHz}.$$

Frequent oscillations are due to inhomogeneities on input and output terminals of the DSMMDL. Their repetition period corresponds to half the value of the resonant frequency of the entire DSMMDL (from 160/2 = 80 MHz till 180/2 = 90 MHz).

$$f_{\text{frequent}} = \frac{c_0}{2\sqrt{\varepsilon_{\text{reff}}}\left(6\cdot 2A + 5S\right)} = \frac{3\cdot 10^8}{2\sqrt{9.3}\cdot\left(6\cdot 0.1 + 5\cdot 10^{-3}\right)} \cong$$

$$\cong 81.3\cdot 10^6 \text{ Hz} \approx 80 \text{ MHz}.$$

Analysis of the dispersion characteristics (Fig. 4.6 a)) shows that when the air gap emerges in the stripline structure due to the finite microstrips thickness (i.e. stripline becomes DSM), delay time of the DSMMDL reduces by about 2.5%, and a further increase of this gap has almost no effect on the delay time. For example, when the thickness of this gap increases tenfold the delay time decreases by only 1.7%. The air gap above a meander conductor has more influence on the absolute values of the dispersion characteristics (Fig. 4.6 b)).

Here it is seen that a fivefold increase of the air gap (from $h_3/h_1 = 0.01$ till $h_3/h_1 = 0.05$) reduces the delay time of about 9%.

Fig. 4.6 b) also shows the dispersion characteristics calculated using Sonnet® simulator. Here it is seen that the difference between the characteristics obtained by hybrid method and the simulator do not exceed 3%.

4.2.2. Experimental Measurements

Prototype of the DSM meander delay line was designed, constructed (Fig. 4.7) and measured to confirm the adequacy of the proposed models of the DSM devices. The prototype was made on the dielectric substrate Rogers® 3006, its dimensions and topology of the meander are presented in the title of Figure 4.7.

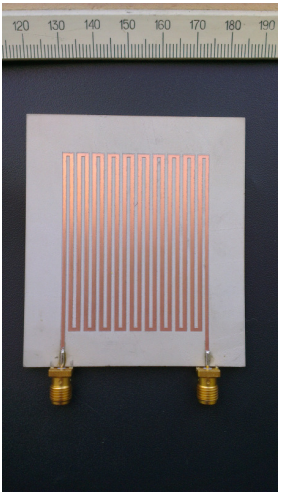

Fig. 4.7. Prototype of the double-shielded microstrip meander delay line (before the top dielectric plate mounting). Design parameters of the prototype are: $\varepsilon_{r1} = \varepsilon_{r2} = 6.15$, $W = 1.1$ mm, $h_1 = h_2 = 1.27$ mm, $S = 1.0$ mm, $t_1 = 0.035$ mm, $2A = 50$ mm, number of the meander strips $N = 20$

Calculated dispersion characteristic of the DSMMDL prototype is shown in Figure 4.8. The dispersion characteristic simulated by Sonnet® is shown here also. The relative difference between them does not exceed 6%. It is seen in Figure 4.8 that prototype bandwidth determined with the proviso that phase distortion does not exceed 0.35 rad, using the equation:

$$\Delta F = \frac{0.35}{2\pi\Delta t}, \tag{4.6}$$

where Δt is deviation of dispersion characteristic on the boundary of the bandwidth from its value in the middle of the bandwidth, is equal to 300 MHz. Phase delay of the DSMMDL, calculated according to proposed DSM device model, in the middle of the bandwidth equals 7.1 ns.

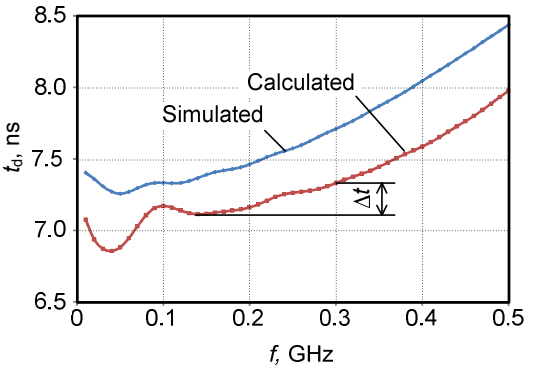

Fig. 4.8. Calculated using hybrid technique and simulated using Sonnet® simulator dispersive characteristics of the DSM meander delay line prototype

Prototype measurements were performed in the time domain using sampling oscilloscope PicoScope 9312 from Pico Technology Ltd. Waveforms of the input and output voltage transients of the measured DSMMDL prototype are shown in Figure 4.9.

Fig. 4.9. Measured transients on the input (top) and output (bottom) of the double-shielded microstrip meander delay line. Measured delay parameters, shown on the bottom are: “Current” – 7.074 ns, “Minimum” – 7.058 ns, “Maximum” – 7.11 ns, “Mean” – 7.094 ns, “Std. Deviation” – 7.158 ps

It is seen here that the rise time of the output transient between the levels of 0.1 and 0.9 is 1.2 ns and equivalent bandwidth of DSMMDL calculated according to equation:

$$\Delta F = \frac{0.35}{\tau_{\text{t}}}, \tag{4.7}$$

where τ_{t} is the rise time the output transient, corresponds to 300 MHz. Averaged measured delay time between input and output transients at 0.5 levels equals 7.094 ns, which demonstrates a very good agreement with the calculated phase delay (7.1 ns).

4.3. Conclusions of Chapter 4

1. An attempt to improve characteristics of the meander microstrip delay line was made by designing one based on the model of the multiconductor microstrip line (MCML) operating in even normal mode. An MCML operating in even mode was synthesized using the technique described in Chapter 3. The parameters were found, which ensured propagation of even normal wave along the line. Characteristics of the designed line were calculated by implementing the model in the Sonnet® software environment.
2. In general, characteristics of the designed line were worse, than those of the analogous MMDL with equal strip widths. The corresponding MCML operates in mixed mode, not single normal mode, i.e. effective permittivities, and therefore phase velocities of the electromagnetic wave in signal conductors are different. However, two parameters were improved. The delay time was increased by 0.38–11%. Amplitude distortions however, which occurred due to the characteristic impedance mismatch between the meander strips of different width, decreased the bandwidth of the device up to 48%.
3. Double shielded microstrip meander delay line MMDL was designed, modeled and produced. Results of models using different modelling techniques and results of measurements of the prototype device show good agreement. It can be stated, that the proposed hybrid technique using the finite difference method and S-matrix technique is applicable for the design of planar delay devices in complex stratified dielectric medium. The difference between the frequency characteristics obtained by the hybrid method and the simulator do not exceed 2%.

General Conclusions

1. Technique for evaluating influence of stratified medium on stripline devices has been created. Such technique is useful for design of stripline delay devices. This technique proved to be useful for finding a combination of dielectric layers (dielectric constants and thicknesses), for which effective permittivity (and hence the phase velocity) for even and odd normal modes is the same. This property is useful for transmission lines and delay lines. This technique was also used to evaluate the effect of the air microlayer in double shielded devices.
2. Synthesis technique for multiconductor lines operating in even or odd modes has been created. Normal mode operation can be achieved in two ways in multiconductor microstrip lines – by changing voltages of signals travelling along the conductors, or by modifying dimensions of the conductors, so that voltages for a particular mode are equal. The latter is more applicable in practical applications. The created synthesis technique calculates the required widths of the conductors, so that absolute values of voltages of a particular mode are equal.
3. Microstrip meander delay line, based on the model of the multiconductor microstrip line, operatingin even normal mode was

designed and modelled to check its characteristics. It was found that phase distortions in such line are less by up to 2%, comparing to the line of the same length with meander strips of equal widths, i.e. based on the model of multiconductor microstrip line operating in mixed mode.

4. Double shielded meander stripline delay line has been designed using hybrid technique, based on the created analysis technique and S-matrix method. The delay line was modelled using softwatre bassed on the method of moments. Also, prototype device has been produced and experimentally tested. It was found, that the results found by the described hybrid technique (multiconductor model and S-matrix method), the results of modelling using the proposed technique and commercial software differ by approximately 2% and the difference from the measured result is less than 1%.Therefore the suggested technique is adequate and applicable for design and analysis of stripline delay devices.

References

Acero, J.; Alonso, R. 2006. Modeling of Planar Spiral Inductors Between Two Multilayer Media for Induction Heating Applications. *IEEE Transactions on Magnetics* 42(11): 3719–3729.

Aschen, H. Von 2011. High Resolution Permittivity Reconstruction of One Dimensional Stratified Dielectric Media From Broadband Measurement Data in the W-band, in *8th European Radar Conference*, Oct. 12–14, 2010, Manchester, UK. 45–48.

Awasthi, S., Srivastava, K.V. & Biswas, A. 2005. Dispersion Properties of Four and Five Coupled Microstrip Lines in Suspended Substrate Structure Using Hybrid Mode Formulation, *Asia-Pacific Microwave Conference Proceedings, 2005,* 2.

Bauer, F., Menzel, W. 2010. A Wideband Transition from Substrate Integrated Waveguide to Differential Microstrip Lines in Multilayer Substrates. *Proceedings of the 40th European Microwave Conference*, 811–813.

Bedair, S.S. 1984. Characteristics of Some Asymmetrical Coupled Transmisssion Lines. *IEEE Transactions on Microwave Theory and Techniques* 32(1): 108–110.

Bhadauria, A.; Kumar, R. 2010. Simple and Highly Accurate Quasi-Static Model for High Speed MIS Microstrip Interconnects on Lossy Substrate in RF MEMS and Integrated Circuits. *Asia-Pacific Symposium on Electromagnetic Compatibility*, April 1216, 2010, Beijing, China. 1068–1071.

Bianconi, G. *et al.* 2010. A New Technique for Efficient Simulation of Microstrip Circuits Etched in Layered Media, *IEEE International Symposium on Antennas and Propagation*, July 11–17, 2010, Toronto, Canada. 1–4.

Braaten, B.D.; Nelson, R.M.; Rogers, D.A. 2009. Input Impedance and Resonant Frequency of a Printed Dipole with Arbitrary Length Embedded in Stratified Uniaxial Anisotropic Dielectrics, *IEEE Antennas and Wireless Propagation Letters* 8: 806–810.

Cangellaris, A.C.; Wu, H. 2008. A Finite-Element Domain-Decomposition Methodology for Electromagnetic Modeling of Multilayer High-Speed Interconnects, *IEEE Transactions on Advanced Packaging* 31(2): 339–350.

Chen, P.; Xu, X. 2012. Introduction of Oblique Incidence Plane Wave to Stratified Lossy Dispersive Media for FDTD Analysis, *IEEE Transaction on Antennas and Propagation* 60(8): 3693–3705.

Chirala, M.K.; Nguyen, C. 2006. Multilayer Design Techniques for Extremely Miniaturized CMOS Microwave and Millimeter-Wave Distributed Passive Circuits, *IEEE Transactions on Microwave Theory and Techniques* 54(12): 4218–4224.

Choubani, M. *et al.*, 2006. Analysis and Design of Antireflection and Frequency Selective Surfaces with Stratified and inhomogeneous media, *13th IEEE International Conference on Electronics, Circuits and Systems*, Dec. 10–13, 2006, Nice, France. 326–330.

Dembelov, M.G.; Bashkuev, Y.B.; Khaptanov, V.B. 2012. Electromagnetic Waves Over Stratified Media in Natural Conditions, *2012 International Conference on Mathematical Methods in Electromagnetic Theory*, Aug 28–30, 2012, Kyiv, Ukraine. 398–400.

Elsherbeni, A.Z. et al., 1993. Quasi-Static Characteristics of a Two-Conductor Multi-Layer Microstrip Transmission Line with Dielectric Overlay and a Notch between the Strips, *Journal of Electromagnetic Waves and Applications* 7(6): 769–789.

Engin, A. E., *et al.* 2006. Finite-Difference Modeling of Noise Coupling between Power/Ground Planes in Multilayered Packages and Boards. *56th Electronic Components and Technology Conference 2006*, May 30–Jun. 2, 2006, San Diego, California, USA. 1262–1267.

Evans, R.J.; Skafidas, E.; Yang, B. 2012. Slow-Wave Slot Microstrip Transmission Line and Bandpass Filter for Compact Millimetre-Wave Integrated Circuits on Bulk Complementary Metal Oxide Semiconductor, *IET Microwaves, Antennas & Propagation* 6(14): 1548–1555.

Fitzek, F.; Rasshofer, R.H. 2009. Automotive Radome Design – Reflection Reduction of Stratified Media. *IEEE Antennas and Wireless Propagation Letters* 8: 1076–1079.

Ge, Y.; Esselle, K. 2002. New Closed-Form Green's Functions for Microstrip Structures Theory and Results, *IEEE Transactions on Microwave Theory and Techniques* 50(6): 1556–1560.

Ghasr, M.; Zoughi, R. 2008. Multimodal Solution for a Rectangular Waveguide Radiating Into a Multilayered Dielectric Structure and its Application for Dielectric Property and Thickness Evaluation, *Instrumentation and Measurement Conference Proceedings*, May 12–15, 2008, Victoria BC, Canada. 552–556.

Gnilenko, A.B. 2007. Entire-Domain Method of Moments Analysis of Shielded Microstrip Transmission Line. *The Sixth International Kharkov Symposium on Physics and Engineering of Microwaves, Millimetre and Sub-Millimetre Waves*, June 2530, 2007, Kharkov, Ukraine. 295–297.

Guo, W.; Shiue, G. 2006. Comparisons Between Serpentine and Flat Spiral Delay Lines on Transient Reflection/Transmission Waveforms and Eye Diagrams, *IEEE Transactions on Microwave Theory and Techniques* 54(4): 1379–1387.

Gupta, S.; Sounas, D. 2012. CRLH–CRLH C-Section Dispersive Delay Structures With Enhanced Group-Delay Swing for Higher Analog Signal Processing Resolution, *IEEE Transactions on Microwave Theory and Techniques* 60(12): 3939–3949.

Han, L.; Wu, K.; Chen, X. 2009. Accurate synthesis of four-line interdigitated coupler, *IEEE Transactions on Microwave Theory and Techniques* 57(10): 2444–2455.

He, M. 2006. Accurate and Efficient Analysis of Aperture Coupled Cylindrically Conformal Microstrip Antennas. *7th International Symposium on Antennas, Propagation & EM Theory*, Oct. 26–29, 2006, Guilin, China. 1–4.

Hou, Q.; Gao, L. 2009. The Current Distribution of Microstrip Spiral Antenna in Biological Stratified Media. *2nd International Conference on Biomedical Engineering and Informatics*, Oct. 17–19, 2009, Tianjin, China. 2(2): 1–4.

Hsu, H.; Wen, J. 2007. Timing synchronization in ultra-wide band systems with delay line combination receivers, *IEEE Communications Letters* 11(3): 264–266.

Itoh, T.; Mittra, R. 1974. A Technique for Computing Dispersion Characteristics of Shielded Microstrip Lines. *IEEE Transactions on Microwave Theory and Techniques, Short Papers* 22(10): 896–898.

Yang, J.; Jeong, Y. 2006. A New Compact 3-D Hybrid Coupler Using Multi-Layer Microstrip Lines at 15 GHz, *36th European Microwave Conference*, Sep. 10–15, 2006, Manchester, UK. 25-28.

Ye, L.; Chai, S.; Zhang, H. 2013. Solving the Axial Line Problem for Fast Computation of Mixed Potential Green's Functions for Cylindrically Stratified Media. *IEEE Transactions on Microwave Theory and Techniques* 61(1): 23–37.

Janhsen, A.; Hansen, V. 1991. Determination of the Characteristic Impedance of Single and Coupled Lines in Layered Dielectric Media, *IEEE MTT-S International Microwave Symposium Digest* vol. 2, Jul. 10–14, 1991, Boston, MA, USA. 765–768.

Jiang, H.; Ruimin, X. 2009. X-band 3D Meander Stripline Delay Line Using Multilayer LTCC. *IEEE MTT-S International Microwave Symposium Digest*, Jun. 7–12, 2009, Boston, MA, USA. 345–348.

Jin, Y. Q.; Fa, W. 2010. The Modeling Analysis of Microwave Emission From Stratified Media of Nonuniform Lunar Cratered Terrain Surface for Chinese Chang-E 1 Observation, *IEEE Geoscience and Remote Sensing Letters* 7(3): 530–534.

Karan, S.; Erturk, V.; Altintas, A. 2009. Closed-form Green's Function Representations in Cylindrically Stratified Media for Method of Moments Applications, *IEEE Transactions on Antennas and Propagation* 57(4): 1158–1168.

Khalil, A. I.; Yakovlev, A. B.; Steer, M. B. 1999. Efficient Method-of-Moments Formulation for the Modeling of Planar Conductive Layers in a Shielded Guided-Wave Structure, *IEEE Transactions on Microwave Theory and Techniques* 47(9): 1730–1736.

Kim, G. 2008. Mode-Impedance Method for Modelling and Analysis of Crosstalk in Differential Meander Delay Lines, *Electrical Design of Advanced Packaging and Systems Symposium*, Dec. 1012, 2008, Seoul, South Korea. 93–96.

Kim, S.; Myoung, S. 2005. Multilayer Meander Parallel Coupled-Line Microstrip Bandpass Filter, *2005 Asia-Pacific Microwave Conference Proceedings* vol. 4.

Kleiza, A.; Staras, S. 1999. Calculation of Characteristic Impedances of Multiconductor. *Electronics and Electrical Engineering* 4: 41–44.

Li, G.; Tousi, Y. M.; Hassibi, A.; Afshari, E. 2009. Delay-Line Based Analog-to-Digital Converters, *IEEE Transactions on Circuits and Systems II: Express Briefs* 56(6): 464–468.

Liang, Q., *et al.* 2009. A Modified FDTD Implementation for EM Scattering by Stratified Medium for Oblique Incidence by TM Wave, *International Conference on Microwave Technology and Computational Electromagnetics*, Nov. 3–6, 2009, Beijing, China. 399–402.

Liao, S.-H.; Nguyen, C. 2007. A New CMOS Multilayer Electromagnetic Band-Gap Microstrip Line and Experimental Investigation of UWB Pulse Propagation, *IEEE Microwave and Wireless Components Letters* 17(7): 522–524.

Ling, F.; Jin, J. 2000. Discrete Complex Image Method for Green's Functions of General Multilayer Media, *IEEE Microwave and Guided Wave Letters* 10(10): 400–402.

Lucido M. 2012, A New High-Efficient Spectral-Domain Analysis of Single and Multiple Coupled Microstrip Lines in Planarly Layered Media, *IEEE Transactions on Microwave Theory and Techniques* 60(7): 2025–2034.

Musa, S. M.; Sadiku, M. N. O. 2008. Application of the Finite Element Method in Calculating the Capacitance and Inductance of Multiconductor Transmission Lines, *IEEE SoutheastCon*, Apr. 3–6, 2008, Huntsville, AL, USA. 300–304.

Muthana, P. & Kroger, H., 2007. Behavior of Short Pulses on Tightly Coupled Microstrip Lines and Reduction of Crosstalk by Using Overlying Dielectric. *IEEE Transactions on Advanced Packaging* 30(3), 511–520.

Nayyeri, V.; Soleimani, M.; Dehmollaian, M. 2011. Analytical and Numerical Calculation of Reflection from a Stratified Structure Backed by a PEMC, *11th Mediterranean Microwave Symposium*, Sep. 8–10, 2011. 134–137.

Nannapaneni Narayana Rao 2004. *Elements of Engineering Electromagnetics*, Pearson Prentice Hall.

Park, S.; Jeon, S. 2013. A 15–40 GHz CMOS True-Time Delay Circuit for UWB Multi-Antenna Systems, *IEEE Microwave and Wireless Components Letters* vol. 23(3): 149–151.

Pozar, D.M. 2011. *Microwave Engineering* Fourth Edition, Wiley Global Education.

Prasad, M., *et al*. 2008. Dispersion and Attenuation Characteristics of Suspended Microstrip Line on Multilayer Lossy Silicon Substrate at 60 GHz, *33rd International Conference on Infrared, Millimeter and Terahertz Waves*, Sep. 15–19, 2008, Pasadena, CA, USA. 1–2.

Scarlatos, A.; Schuhmann, R.; and Weiland, T. 2005. Solution of Radiation and Scattering Problems in Complex Environments Using a Hybrid Finite Integration Technique. Uniform Theory of Diffraction Approach. *IEEE Transactions on Antennas and Propagation* 53(10): 3347–3356.

Sileikis, A.; Gurskas, A.; Kirvaitis, R. 2000. Analysis of Electrodynamic Systems Using Finite-Difference and Finite-Element Methods, *Electronics and Electrical Engineering* 5(28): 38–42.

Silvester, P. P.; Ferrari, R.R. 1996. Finite Elements for Electrical Engineers, 3rd Edition. Cambridge University Press.

Staras, S. 2008. Introduction into Numerical Methods in Electrodynamics and their Applications. Vilnius, Lithuania: Technika, 185.

Staras, S. *et al*. 2012. Wide-Band Slow-Wave Systems: Simulation and Applications. New York: Taylor&Francis Group. 460 p.

Steer, M. B.; Bandler, J. W.; and Snowden, C. M. 2002. Computer Aided Design of RF and Microwave Circuits and Systems. *IEEE Transactions on Microwave Theory and Technique* 50(3): 996–1005.

Su, T. *et al.* 2012. Computation for Electromagnetic Scattering from Electrically Large 3-D PEC Objects Buried in a Lossy Stratified Medium, *International Conference on Microwave and Milimeter Wave Technology*, May 5–8, 2012, Shenzhen, China. 1–4.

Urbanavicius, V.; Martavicius, R. 2006. Model of the Microstrip Line with Nonuniform Dielectric. *Electronics and Electrical Engineering* 3(67): 55–60.

Urbanavicius, V.; Pomarnacki, R. 2008. Models of Multiconductor Line with non-Homogeneous Dielectric. *Proceedings EMD the XVIII International Conference on Electromagnetic Disturbances*. Vilnius, Lithuania, Sep. 25–26, 2008, 203–208.

Vendik, I. *et al.* 2003. Full-Wave 2D and 3D Spectral Domain Analysis of HTS Multistrip Multilayer Lossy Structure, *IEEE Transactions on Applied Superconductivity* 13(2): 269–271.

Verma, A.; Sharma, E. 2004. Analysis and Circuit Model of a Multilayer Semiconductor Slow-Wave Microstrip Line, *IEE Proceedings on Microwaves, Antennas and Propagation* 151(5): 441–449.

Vo, H.; Davidson, C.; Shi, F. 2002. New Effective Dielectric Constant Model for Ultra-high Speed Microstrip Lines on Multilayer Dielectric Substrates: Effect of Conductor-Dielectric Interphase, *Proceedings on 52nd Electronic Components and Technology Conference*. 86–89.

Wei-Tsung, L.; Yun-Chieh, C.; Jeng-Han, T.; Hong-Yuan, Y.; Jen-Hao, C.; Tian-Wei, H. 2013. 60-GHz 5-bit phase shifter with integrated VGA phase-errorcompensation, *IEEE Transactionson Microwave Theory and Techniques* 61(3): 1224–1235.

Weiss, S.; Kilic, O. 2010. A Vector Transform Solution Procedure for Solving Electromagnetic Problems in Cartesian Coordinates, *IEEE Antennas and Wireless Propagation Letters* 9(1): pp.291–294.

Wu, X.; Kishk, A.; Glisson, A. 2006. A Transmission Line Method to Compute the Far-field Radiation of Arbitrarily Directed Hertzian Dipoles in a Multilayer Dielectric Structure: Theory and Applications, *IEEE Transactions on Antennas and Propagation* 54(10): 2731–2741.

Xiang, B.; Kopa, A.; Fu, Z.; Apsel, A. B. 2012. Theoretical Analysis and Practical Considerations for the Integrated Time-Stretching System Using Dispersive Delay Line (DDL), *IEEE Transactions on Microwave Theory and Techniques* 60(11): 3449–3457.

Xu, J.; Chen, R. 2011. Meandered Microstrip Transmission Line Based ID Generation Circuit for Chipless RFID Tag, *IEEE Electrical Design of Advanced Packaging and Systems Symposium*, Dec. 12–14, 2011. 1–4.

Zeng, Q.; Delisle, G. 2010. Transient Analysis of Electromagnetic Wave Reflection From a Stratified Medium, *Asia-Pacific Symposium on Electromagnetic Compatibility*, Apr. 12–16, 2010, Beijing, China. 881–884.

Zhang, L.; Song, J. 2005. Dispersion Characteristics of Multilayer Microstrip Lines with Thin Metal Ground, *IEEE Antennas and Propagation Society Internationl Symposium* vol. 2B: 642–645.

Zhang, L.; Song, J. 2007. Slow Wave Effects Induced by the Thin-film Metal Ground in On-chip Multilayer Microstrip Lines, *IEEE Antennas and Propagation Society International Symposium*, Jun. 9–15, 2007. 469–472.

Zhou, E.; Xu, S. 2005. A New Approach for Leakage Suppression of Microstrip Line Structure with Multilayer Substrates, *2005 Asia-Pacific Microwave Conference Proceedings* vol. 1: 1–3.

List of Author's Scientific Publications on the Topic of the Dissertation

Papers in the reviewed periodic scientific journals

Urbanavičius, V.; Mikučionis, Š.; Martavičius, R. 2007. Model of the Coupled Transmission Lines with a non-uniform Dielectric, *Electronics and Electrical Engineering* 5(77): 28–31. (ISI Web of Science, CSA, EBSCO, INSPEC, VINITI)

Mikučionis, Š.; Urbanavičius, V. 2010a. Investigation of Normal Modes in Microstrip Multiconductor Line Using the MoM, *Electronics and Electrical Engineering* 4(100): 94–97. (ISI Web of Science, CSA, EBSCO, INSPEC, VINITI)

Mikučionis, Š.; Urbanavičius, V. 2011. Synthesis of Six-Conductors Symmetrically Coupled Microstrip Line, Operating in a Normal Mode, *Electronics and Electrical Engineering* 4(110): 47–52. (ISI Web of Science, CSA, EBSCO, INSPEC, VINITI)

Mikučionis, Š. 2012. Synthesis of Multiconductor Microstrip Lines Operating in Normal Modes, *Science – Future of Lithuania: Electronics and Electrical Engineering*. 4(1): 71–76. (ICONDA, Gale®, ProQuest)

Krukonis, A.; Mikučionis, Š. 2013. Susietųjų mikrojuostelinių linijų dažninės charakteristikos [The Frequency Characteristics of Coupled Microstrip Lines], *Science – Future of Lithuania: Electronics and Electrical Engineering* 5(2), 173–180. (ICONDA, Gale®, ProQuest)

Krukonis, A.; Mikučionis, Š.; Urbanavičius, V. 2013. The Influence of Non-Uniformity of the MultiConductor Line Parameters on Frequency Responses of the Meander Delay Line, *Electronics and Electrical Engineering* 6(19), 81–86. (ISI Web of Science, CSA, EBSCO, INSPEC, VINITI)

Krukonis, A.; Mikučionis, Š. 2014. Effect of Non-Uniformity of the Multiconductor Line Constructional Parameters on the Frequency Characteristics of the Meander Microstrip Delay Line, *Science – Future of Lithuania: Electronics and Electrical Engineering* 6(2), 211–217. (Academic Search Complete, IndexCopernicus, ProQuest)

Mikucionis, Š.; Urbanavicius, V.; Gurskas, A.; Krukonis, A. 2014. The Influence of the Air Gap on the Characteristics of the Double-Shielded Microstrip Delay Devices, *Przegląd Elektrotechniczny* 90(6), 275–279. (INSPEC, SCOPUS)

Other papers

Mikučionis, Š.; Urbanavičius, V. 2010b. Synthesis of Microstrip Multiconductor Lines, Operating in Normal Mode, in *18th International Conference on Microwaves, Radar and Wireless Communications MIKON-2010:* June 14–16, 2010, Vilnius, Lithuania, Proceedings, Vols. 1–2, 353–356. (Conference Proceedings Citation Index, IEEE/IEE)

Mikučionis, Š.; Urbanavičius, V. 2012. Quasi-tem analysis of coupled microstrip lines on multilayered dielectric, in *The 22nd International Conference "Electromagnetic disturbances EMD'2012"*: September 20–21, 2012, Vilnius, Lithuania. Vilnius, Technika, 91–86.

Summary in Lithuanian

Įvadas

Problemos formulavimas

Vėlinimo įtaisai (VĮ) plačiai taikomi šiuolaikinėje elektroninėje įrangoje. Dažniausiai pasitaikanti šių įtaisų struktūra iki XXI a. pradžios buvo planarinė, t. y. signaliniai laidininkai išdėstyti vienoje plokštumoje. Tačiau pastaraisiais dešimtmečiais vis dažniau taikoma erdvinė, arba trimatė tokių įtaisų struktūra. Trimačių struktūrų privalumai yra mažesni gabaritai ir masė, trumpesni signaliniai traktai ir dėl to didesnė veikimo sparta. Taip pat taikant trimatę struktūrą siekiama gauti naujas funkcines galimybes.

Trimačiuose įtaisuose laidininkai išdėstomi tarp įvairių dielektrikų sluoksnių, tokiu būdu sukuriant sluoksniuotą dielektrikų ir laidininkų struktūrą.

Ryšys tarp laidininkų skirtinguose sluoksniuose, ir sluoksniuotos dielektrinės terpės įtaka elektromagnetinės bangos sklidimui yra mažai ištirti.

Sluoksniuotos dielektrinės terpės vėlinimo įtaisai nėra detaliai išnagrinėti. Taip pat nėra pasiūlyta daugialaidžių linijų, veikiančių normaliųjų bangų režimu sintezės metodika. Tokių linijų modeliai taikomi kaip pagrindas vėlinimo įtaisų projektavimui.

Šioje disertacijoje formuluojamos hipotezės, kad taikant skaitinius elektromagnetizmo modeliavimo metodus galima:

- rasti sąlygas, kurioms esant elektromagnetinės bangos faziniai greičiai vėlinimo įtaisų laidininkuose nevienalyčiame dielektrike yra vienodi,

- rasti sluoksniuotos dielektrinės terpės vėlinimo įtaiso elektrines charakteristikas taikant kvazi-TEM artinį,
- įvertinti sluoksniuotos dielektrinės terpės įtaką įtaisų dažninėms charakteristikoms.

Darbo aktualumas

Elektronikos įtaisuose vėlinimo įtaisai taikomi įvairiose elektroninėse grandinėse. Viena panaudojimo sritis yra grįžtamojo ryšio vėlinimas signalų generatoriuose. Antenų gardelių kryptingumui nustatyti būtinas tikslus signalo vėlinimas į kiekvieną gardelės elementą. Kai kurių skaitmeninių perdavimo linijų patikimam veikimui būtinas tikslus signalo atsiradimo laikas, todėl esant skirtingo elektrinio ilgio keliams, siekiant juos suvienodinti taikomos vėlinimo linijos.

Vėlinimo linijų (VL) yra įvairių tipų ir konstrukcijų. Pagal veikimo principą, vėlinimo linijos gali būti skirstomo į dvi kategorijas: aktyviosios ir elektrodinaminės. Aktyviosiose VL signalas užlaikomas aktyviaisiais elementais (tranzistoriais, integriniais stiprintuvais). Šiuo metu tokios VL taikomos plačiausiai. Elektrodinaminių VL veikimas grįstas ilgesniu signalo nueinamu elektriniu keliu. Paprasčiausias tokios VL atvejis yra nenulinio ilgio perdavimo linija (juostelinė, mikrojuostelinė, koaksialinė ir kt.). Tačiau daugeliu atveju reikalinga vėlinimo trukmė yra tokia, kad tokios perdavimo linijos dydis būtų nepraktiškas. Todėl laidininkas formuojamas į kompaktiškesnę struktūrą. Praktikoje dažniausiai naudojamos meandrinės ir spiralinės.

Tokių formų vėlinimo linijose yra didesni faziniai iškraipymai, taip pat pasireiškia užtvarinio filtro savybės, t. y. smarkiai slopinami tam tikro dažnių ruožo signalai ir ženkliai sumažinama įtaiso pralaidumo juosta. Prieš taikant tokią VL būtina žinoti ne tik jos vėlinimo trukmę, bet ir pralaidumo juostą. Atsirandant vis naujiems VL taikymams, būtina sukurti efektyvią VĮ projektavimo metodiką kuri leistų sukurti norimos vėlinimo trukmės ir pralaidumo juostos mažiausių gabaritų VL.

Vienas iš svarbiausių projektavimo uždavinių yra įtaiso sintezė, t. y. konstrukcinių parametrų radimas pagal norimas elektrines charakteristikas. Jei tiesioginės sintezės metodikos nėra, tenka kartoti analizės iteracijas keičiant parametrus tol, kol gaunamos reikiamos elektrinės charakteristikos.

VĮ struktūra dažniausiai yra planarinė, tačiau taikomos ir daugiasluoksnės struktūros, kai planariniai įtaisai išdėstomi vienas virš kito. Tokių struktūrų svarba ir plačios pritaikymo galimybės yra dažnai minimos, tačiau analizės ir sintezės metodų pasiūlyta mažai.

Tyrimų objektas

Pagrindiniai tyrimo objektai yra daugialaidės juostelinės ir mikrojuostelinės struktūros sluoksniuotoje dielektrinėje terpėje, meandrinė vėlinimo linija sluoksniuotoje dielektrinėje terpėje, grįsta daugialaide juosteline arba mikrojuosteline linija.

Darbo tikslas

Išnagrinėti sluoksniuotos dielektrinės terpės įtaką vėlinimo įtaisų elektrinėms charakteristikoms sukuriant ir įgyvendinant skaitiniais metodais grįstą daugiasluoksnės dielektrinės terpės įtakos vėlinimo įtaisų charakteristikoms įvertinimo metodiką.

Darbo uždaviniai

Toliau išvardinti uždaviniai reikalingi darbo tikslui pasiekti.

1. Sukūrus matematinį modelį, ir jį įgyvendinus programiškai, išnagrinėti normaliųjų bangų daugialaidėse juostelinėse linijose sužadinimo sąlygas ir galimybę suvienodinti lyginės ir nelyginės normaliųjų bangų fazinius greičius susietosiose linijose sluoksniuotame dielektrike.
2. Sudarius daugialaidžių mikrojuostelinių linijų, veikiančių normaliųjų bangų režimu, sintezės metodiką, ir įgyvendinus ją programiškai išnagrinėti konstrukcinių parametrų įtaką linijų elektrinėms charakteristikoms.
3. Išnagrinėti meandrinės vėlinimo linijos, grįstos daugialaidės mikrojuostelinės linijos, veikiančios lyginių normaliųjų bangų režimu, modeliu, charakteristikas.
4. Išnagrinėti oro sluoksnio įtaką dviekranės meandrinės vėlinimo linijos charakteristikoms.

Tyrimų metodika

Darbe taikomas skaitinis elektromagnetinių laukų modeliavimas nagrinėjamose struktūrose. Naudojami du skaitiniai metodai – momentų metodas ir baigtinių skirtumų metodas. Kvazi-TEM artinys taikomas supaprastinti užduotis iš trimatęs į dvimatę, taip sumažinant skaičiavimų apimtis. Normaliųjų bangų sąlygos susietosiose ir daugialaidėse linijose nagrinėjamos ir taikomos meandrinei vėlinimo linijai projektuoti. S-parametrų matricų metodas ir komercinė momentų metodu grįsta programinė įranga (Sonnet®) yra taikomi sukurtiems vėlinimo linijų modeliams analizuoti. Suprojektuota ir pagaminta vėlinimo linija išmatuota osciloskopu PicoScope 9312 pagamintu „Pico Technology Ltd.“ Modeliavimo rezultatai lyginami su publikuojamais, kitų tyrėjų gautais rezultatais, ir vienu atveju palyginti su eksperimentiniais matavimais.

Darbo mokslinis naujumas

Nepaisant to, kad planariniai vėlinimo įtaisai mikrobangų elektronikoje taikomi jau seniai, naujos projektavimo ir gamybos technologijos reikalauja gerai žinomų įtaisų naudojimo naujoviškose struktūrose. Minėtiems uždaviniams įgyvendinti reikalinga efektyvi ir tiksli projektavimo metodika. Dėl sudėtingų sluoksniuotų dielektrikų struktūrų tokios metodikos nėra sukurtos. Šiame darbe siūlomi nauji sluoksniuotos terpės įtakos elektrinėms vėlinimo įtaisų charakteristikoms įvertinimo metodai.

Atliekant darbe aprašytus tyrimus buvo gauti šie elektros ir elektronikos inžinerijos mokslui nauji rezultatai:

1. Pasiūlytas naujas matematinis modelis, tinkamas analizuoti daugialaidę juostelinę liniją sluoksniuotame dielektrike.

2. Sukurta daugialaidės mikrojuostelinės linijos, veikiančios lyginės arba nelyginės normaliosios bangos režimu, sintezės metodika.
3. Pasiūlyta susietųjų linijų sluoksniuotame dielektrike normaliųjų bangų fazinių greičių vienodumo sąlygų nustatymo metodika.

Rezultatų praktinė reikšmė

Šiuolaikinė komunikacijos įranga grįsta sudėtinga įvairių mikrobangų įtaisų sąveika. Signalų vėlinimo įtaisai yra itin svarbūs mikrobangų grandynuose. Dauguma šiuolaikinių įtaisų formuojami integriniuose grandynuose ir montažinėse plokštėse (sluoksniuotos terpės atvejai). Išsamesnės žinios apie vėlinimo įtaisus sluoksniuotoje terpėje gali būti naudingos kuriant efektyvesnius įtaisus.

1. Sukurta daugialaidžių mikrojuostelinių linijų, veikiančių normaliųjų bangų režimu, sintezės metodika. Sintezės rezultatai yra pritaikomi daugialaidėmis linijomis grįstų vėlinimo įtaisų projektavimui.
2. Sukurta daugiasluoksnio dielektriko susietųjų juostelinių linijų, kurių faziniai greičiai lyginei ir nelyginei normaliosioms bangoms yra vienodi. Tokiose perdavimo linijose mažesni tarpusavio trukdžiai, be to vėlinimo linijų, grįstų tokių susietųjų linijų modeliais, faziniai iškraipymai mažesni. Tokia savybė tai pat naudinga filtrų, šakotuvų ir kitų mikrobangų įtaisų projektavime.
3. Įvertinta oro mikrosluoksnio dviekranėse struktūrose įtaka elektriniams juostelinių įtaisų parametrams.

Sukurti susietųjų, daugialaidžių ir vėlinimo linijų modeliai gali būti taikomi kompiuterinio projektavimo programinėje įrangoje vėlinimo linijų sluoksniuotoje terpėje projektavimui.

Ginamieji teiginiai

1. Taikant iteracinį analizės algoritmą grįstą Niutono-Rapsono metodu, galima parinkti daugialaidės mikrojuostelinės perdavimo linijos kraštinių laidininkų pločius taip, kad lyginės arba nelyginės modų įtampų moduliai skirtųsi ne daugiau 2%, o bangų faziniai greičiai skirtųsi ne daugiau 3%.
2. Parenkant dielektrinių sluoksnių storius ir dielektrines skvarbas galima suvienodinti susietųjų juostelinių linijų daugiasluoksniame dielektrike lyginės ir nelyginės modų fazinius greičius.
3. Projektuojant meandrinę vėlinimo liniją pagal daugialaidės mikrojuostelinės linijos, veikiančios lyginės normaliosios modos režimu, modelį, faziniai iškraipymai sumažinami iki 2%.
4. Oro mikrosluoksnio, atsiradusio dėl baigtinio laidininko storio, normuotojo storio padidėjimas dviekranėje meandrinėje juostelinėje vėlinimo linijoje nuo 0 iki 0,1 sumažina jos vėlinimo trukmę iki 5%. Oro mikrosluoksnio, atsiradusio dėl netikslios viršutinio ekrano padėties, normuotojo storio padidėjimas nuo 0 iki 0,05 sumažina jos vėlinimo trukmę iki 20%.

Darbo rezultatų aprobavimas

Darbo tema publikuota 10 straipsnių Lietuvos ir užsienio moksliniuose leidiniuose: 4 straipsniai Thomson Reuters ISI Web of Science duomenų bazės recenzuojamuose mokslo žurnaluose su citavimo indeksu: (Martavičius *et al.* 2007; Mikučionis, Urbanavičius 2010a; Mikučionis, Urbanavičius 2011, Krukonis *et al.* 2013), 6 – kituose recenzuojamuose mokslo leidiniuose: (Mikučionis 2012; Krukonis, Mikučionis 2013) įtraukti į ICONDA, Gale®: Academic OneFile, InfoTrac Custom; ProQuest: Ulrichsweb™, Summon™; EBSCOhost: Academic Search Complete; IndexCopernicus duomenų bazėse; (Mikučionis *et al.* 2014) indeksuojami INSPEC ir SCOPUS duomenų bazėse; (Mikučionis, Urbanavičius 2010b) indeksuojamas IEEE duomenų bazėje. Disertacijos rezultatai buvo pristatyti 10 konferencijų: 1 tarptautinėje užsienyje (Varšuva, Lenkija), 5 tarptautinėse Lietuvoje, 4 kitose konferencijose.

Disertacijos struktūra

Diseraciją sudaro įvadas, 4 skyriai, bendrosios išvados, šaltinių ir literatūros sąrašas, autoriaus mokslinių publikacijų disertacijos tema sąrašas ir santrauka lietuvių kalba. Disertacijos apimtis – 119 puslapių be priedų. Disertacijoje yra 47 paveikslai, 8 lentelės ir 62 numeruotos formulės, disertacijoje panaudota 70 šaltinių.

1. Juostelinių vėlinimo ir kitų mikrobangų įtaisų sluoksniuotame dielektrike ir jų tyrimų metodų apžvalga

Sluoksniuotos dielektrinės terpės įtakos įvertinimo mikrobangų įtaisams problema aktuali įvairių įtaisų projektavime. Vienais atvejais sluoksniuoti dielektrikai yra neišvengiami: mikrobangų įtaisai turi būti suformuoti daugiasluoksniame integruotajame grandyne, daugiasluoksnėje spausdintinėje plokštėje. Kitais atvejais sluoksniuota struktūra leidžia gauti reikiamas charakteristikas – mažesnį ryšį tarp gretimų perdavimo linijų, mažesnius fazinius iškraipymus, sumažinti įtaiso gabaritus, panaikinti elektromagnetinės bangos atspindžius nuo paviršių.

Sluoksniuotos dielektrinės terpės vėlinimo įtaisų taikymas nėra plačiai išnagrinėtas, tai taikoma siekiant sumažinti vėlinimo įtaiso gabaritus išlaikant vėlinimo trukmę ir pralaidumo juostą.

Mikrobangų įtaisų analizės ir modeliavimo metodus galima suskirstyti į keturias grupes: analitiniai, skaitiniai, hibridiniai ir empiriniai.

Taikant analitinius metodus norimos charakteristikos skaičiuojamos taikant tiesiogines algebrines išraiškas. Šie metodai labai spartūs, tačiau apsiriboja paprasčiausiomis struktūromis, be to dėl taikomų aproksimacijų gali būti netikslūs.

Skaitiniai metodai – tai skaitinis integralinių arba diferencialinių lygčių sprendimas. Dažniausiai taikant šiuos metodus diskretizuojama nagrinėjama sritis arba jos dalis, ir ieškomas laukas skaičiuojamas iteraciniu algoritmu arba kitokiais algebriniais metodais.

Hibridiniai metodai – tai analitinių ir skaitinių metodų kombinacija.

Empiriniai metodai – tai interpoliuoti ir/arba ekstrapoliuoti eksperimentų duomenys. Šie metodai dažnai yra tikslūs, tačiau pagrindinis jų trūkumas – dideli duomenų gavimo ir jų patikimumo įvertinimo kaštai.

Darbe nagrinėjamos struktūros, kurioms galima taikyti kvazi-TEM artinį, tokiu būdu trimatis dinaminis uždavinys sprendžiamas kaip dvimatis statinis. Taikant šį artinį norint rasti nagrinėjamų struktūrų elektrines charakteristikas užtenka rasti statinius dydžius – atskirų laidininkų ilgio vieneto talpas.

Išanalizavus metodus, taikomus nagrinėjamoms struktūroms analizuoti, pasirinkti du skaitiniai metodai: momentų metodas ir baigtinių skirtumų metodas. Momentų metodo pagrindinis pranašumas yra tai, kad nereikia diskretizuoti visos analizuojamos erdvės, diskretizuojamas tik krūvis laidininke. Taikant šį metodą mikrojuostelinėms struktūroms, dviejų dielektrinių erdvių (pagrindo ir oro) įtaka įvertinama taikant dalinių atvaizdų metodą. Norint taikyti momentų metodą didesniam sluoksnių skaičiui reikalingi sudėtingi pradiniai skaičiavimai. Todėl daugiasluoksnėms struktūroms modeliuoti buvo pasirinktas baigtinių skirtumų metodas. Šis metodas reiklesnis skaičiavimo pajėgumams, tačiau jo įgyvendinimas, ypač sudėtingai dielektrinės terpės struktūrai yra paprastesnis.

Darbe tai pat taikoma modų arba normaliųjų bangų analizė. Normaliųjų bangų režimas – tai daugialaidės linijos veikimas, kai ties kiekvienu laidininku sklindančių elektromagnetinių bangų greičiai yra vienodi. Taikant kvazi-TEM artinį tai atitinka vienodą efektyviąją dielektrinę skvarbą visiems laidininkams. Moda šiame darbe vadinamas daugialaide linija sklindančių signalų amplitudžių dydžiai, kurie reikalingi siekiant užtikrinti normaliosios bangos režimą.

Projektuojant daugialaidės linijos modeliu grįstą meandrinę vėlinimo liniją būtina žinoti laidininkų elektrines charakteristikas lyginei ir nelyginei modoms. Lyginės (sinfazinės) modos atveju visų laidininkų poliarumas yra vienodas, nelyginės (priešfazinės) modos atveju gretimų laidininkų poliarumai priešingi.

2. Juostelinių vėlinimo įtaisų sluoksniuotame dielektrike modeliavimas

Sukurti ir išbandyti dviejų mikrojuostelinių struktūrų modeliai – nesimetrinių susietųjų linijų ir keturių laidininkų daugialaidės linijos modeliai (S1 pav.). Gauti rezultatai palyginti su publikuojamais, kitų tyrėjų ir kitais metodais gautais rezultatais. Skirtumas tarp gautų ir publikuojamų rezultatų neviršijo 4 %.

Naudojant darbe sukurtus, momentų metodu ir dalinių atspindžių metodais grįstus modelius, buvo išnagrinėtos susietųjų ir daugialaidžių linijų (S1 pav.) konstrukcinių parametrų (laidininkų pločio, tarpo tarp laidininkų dydžio, pagrindo dielektrinės konstantos) įtaka elektrinėms charakteristikoms – efektyviajai skvarbai, charakteringajam impedansui, modų įtampoms. Nustatyta, kad lyginės modos atveju kraštinių daugialaidės linijos laidininkų įtampų moduliai yra didesni, o nelyginės modos atveju atvirkščiai – mažesni nei kitų laidininkų. Tuo tarpu laidininkuose esant vienodoms įtampoms efektyvioji dielektrinė skvarba kiekvienam laidininkui yra skirtingos.

Taip pat pastebėta, kad esant mažesniems tarpams tarp laidininkų, kraštinių laidininkų modų įtampos nuo vidinių skiriasi daugiau, nei esant didesniems tarpams.

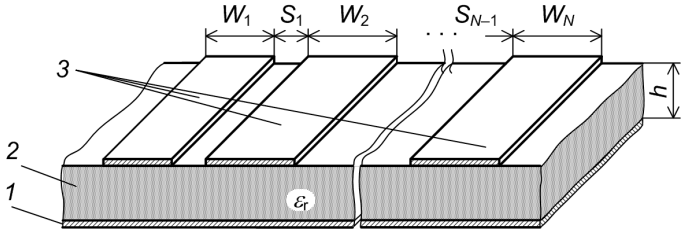

S1 pav. Apibendrintas daugialaidės mikrojuostelinės linijos struktūros eskizas: 1 – atskaitos laidininkas, 2 – dielektrinis pagrindas, 3 – signaliniai laidininkai

Taikant baigtinių skirtumų metodą sukurtas modelis susietųjų ir daugialaidžių juostelinių ir mikrojuostelinių linijų daugiasluoksniame dielektrike modeliavimui. Susietųjų mikrojuostelinių linijų ant dvisluoksnio dielektrinio pagrindo rezultatai, gauti sukurtais modeliais palyginti su publikuojamais, kitais metodais gautais rezultatais, skirtumas neviršijo 4,5%.

Naudojant sukurtus modelius išnagrinėtos susietųjų mikrojuostelinių linijų ant dvisluoksnio dielektriko (S2 pav. a)) elektrinių charakteristikų – efektyviosios skvarbos ir laidininkų charakteringųjų impedansų priklausomybės nuo konstrukcinių parametrų: dielektrikų skvarbų ir storių santykių. Taip pat analogiškai išnagrinėta papildomo dielektriko, esančio virš laidininkų (S2 pav. b)), sluoksnio storio ir dielektrinės skvarbos įtaka susietųjų juostelinių linijų elektrinėms charakteristikoms.

Analizuojant susietąsias mikrojuostelines linijas ant dvisluoksnio dielektriko, pastebėta, kad dielektriko esančio arčiau laidininkų (ε_{r2}) dielektrinė skvarba turi daugiau įtakos linijų elektrinėms charakteristikoms tiek lyginės tiek nelyginės modos atveju, nei dielektriko sluoksnio prie ekrano (ε_{r1}).

Analizuojant daugiasluoksnes susietąsias linijas su papildomu dielektriko sluoksniu virš signalinių laidininkų buvo pastebėta, kad esant tam tikroms papildomo sluoksnio dielektrinės skvarbos ε_{r3} ir storio h_3 kombinacijoms (S2 pav.), efektyvioji skvarba ε_{reff} lyginei ir nelyginei modoms tampa vienodos (S3 pav.). Ši savybė naudinga taikant susietųjų linijų modelį vėlinimo linijoms projektuoti, mažinant trukdžių įtaką perdavimo linijose, projektuojant filtrus.

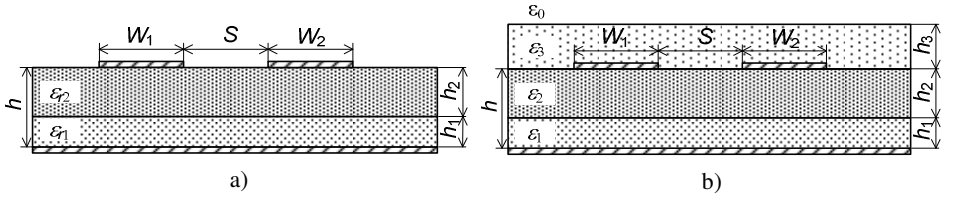

S2 pav. Susietosios mikrojuostelinės linijos: a) ant dvisluoksnio dielektriko ir b) susietosios mikrojuostelinės linijos ant dvisluoksnio dielektriko su papildomu dielektriko sluoksniu virš laidininkų

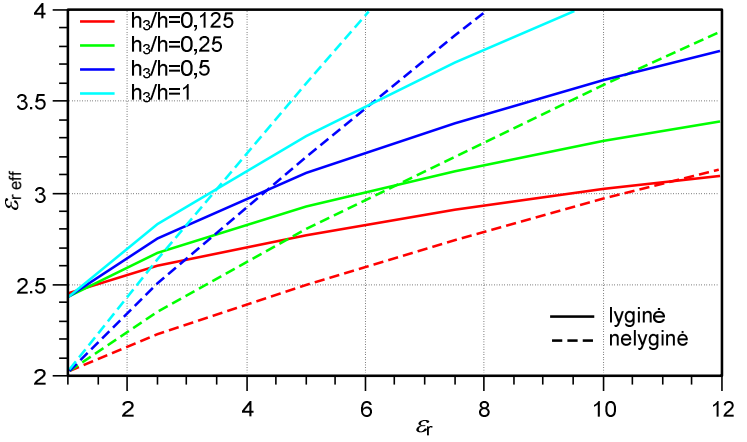

S3 pav. Susietųjų juostelinių linijų efektyviosios dielektrinės skvarbos priklausomybė nuo papildomo sluoksnio dielektrinės skvarbos ir storio, kai $W_1/h = W_2/h = 1$, $S/h = 1$, $h_1/h = h_2/h = 0{,}5$, $\varepsilon_{r1} = 9{,}6$ and $\varepsilon_{r2} = 2{,}2$

Sukurtas modelis taip pat panaudotas oro mikrosluoksnio įtakai dviekranių juostelinių struktūrų charakteristikoms tirti. Oro mikrosluoksnio atsiradimo priežastys yra dvi. Pirmuoju atveju tarp viršutinio ir apatinio dielektrikų sluoksnių yra oro tarpas dėl nenulinio laidininkų storio (S4 pav. a), c) ir e)). Antruoju atveju, dėl netikslios konstrukcijos gali atsirasti oro tarpas tarp laidininko ir viršutinės dielektrinės plokštelės (S4 pav. a), c) ir e)).

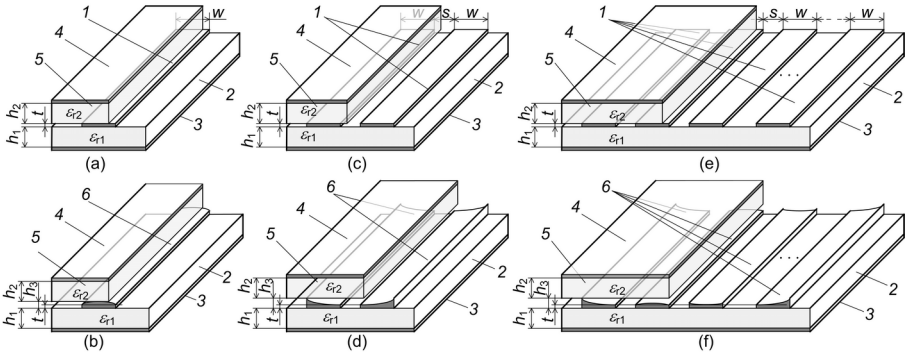

S4 pav. Apibendrinta dviekranių mikrojuostelinių įtaisų struktūra: a) – perdavimo linija, b) – perdavimo linija su netaisyklingos formos skerspjūviu, c) – susietosios linijos, d) – susietosios linijos su netaisyklingos skerspjūvio formos laidininkais, e) – daugialaidė linija, f) – daugialaidė linija su netaisyklingos formos skerspjūvio laidininkais; čia 1 – laidininkai, 2 ir 5 – atitinkamai apatinis ir viršutinis dielektrikai, 3 ir 4 – atitinkamai apatinis ir viršutinis ekranai, 6 – netaisyklingos skerspjūvio formos laidininkai. Dalis viršutinių dielektrikų eskizuose neparodyti

Abiems atvejams išnagrinėtos elektrinių charakteristikų priklausomybės nuo oro mikrosluoksnio storio pavienėms, susietosioms ir daugialaidėms juostelinėms linijoms. Nustatyta, kad oro sluoksnis esantis tarp laidininko ir viršutinės dielektrinės plokštelės daugiau veikia elektrines įtaiso charakteristikas, nei oro tarpas tarp dielektrinių plokštelių esantis dėl baigtinio laidininkų storio.

3. Mikrojuostelinių vėlinimo įtaisų sluoksniuotame dielektrike sintezės metodika

Remiantis 2-ajame skyriuje aprašytais modeliais, sukurta sintezės metodika. Sukurta metodika kurią taikant randami daugialaidės mikrojuostelinės linijos konstrukciniai parametrai, kuriems esant lyginės arba nelyginės normaliosios bangos atveju modų įtampų moduliai būtų vienodi. Kitaip tariant, vienodos amplitudės ties laidininkais sklindančių bangų faziniai greičiai turi būti vienodi. Siekiant užtikrinti tam tikros modos režimą reikalinga parinkti laidininkų pločius.

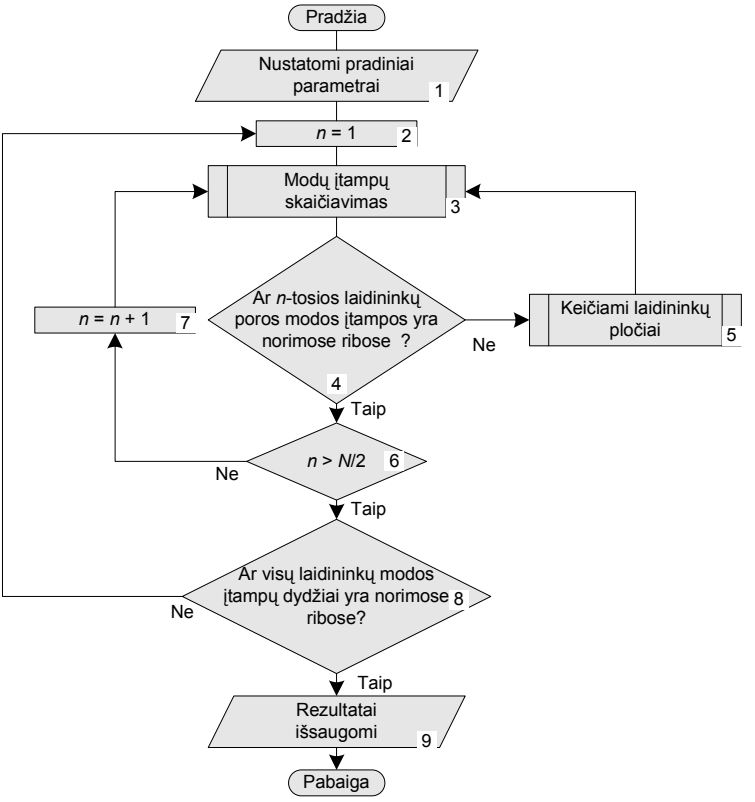

S5 pav. Sintezės algoritmo blokinė diagrama

Sudaryta metodika grįsta 2-ajame skyriuje aprašyto analizės modelio iteraciniu skaičiavimu keičiant parametrus – laidininkų pločius iki pasiekiamas reikiamas rezultatas – lyginės arba nelyginės modos įtampų moduliai skiriasi ne daugiau nei norimas skirtumas. Parametrų parinkimui kiekvienai skaičiavimo iteracijai pasirinktas Niutono-Rapsono metodas, skaitiniu atveju dar vadinamas sekantų metodu. Sintezės algoritmo blokinė diagrama pateikta S5 paveiksle. Kadangi linija simetriška, laidininkų pločiai parinkinėjami poromis. Taikant analizę buvo nustatyta, kad didžiausią įtaką turi kraštinių laidininkų pora, todėl skaičiavimai pradedami nuo jos. Paprastumo dėlei, pirmai iteraciją laidininkų pločiai parenkami vienodi. Nepakitusi lieka tik centrinė laidininkų pora, arba, jei laidininkų skaičius nelyginis – centrinis laidininkas. Modų įtampos normuojamos pagal centrinių laidininko(-ų) įtampą(-as).

Algoritmą sudaro devyni žingsniai.

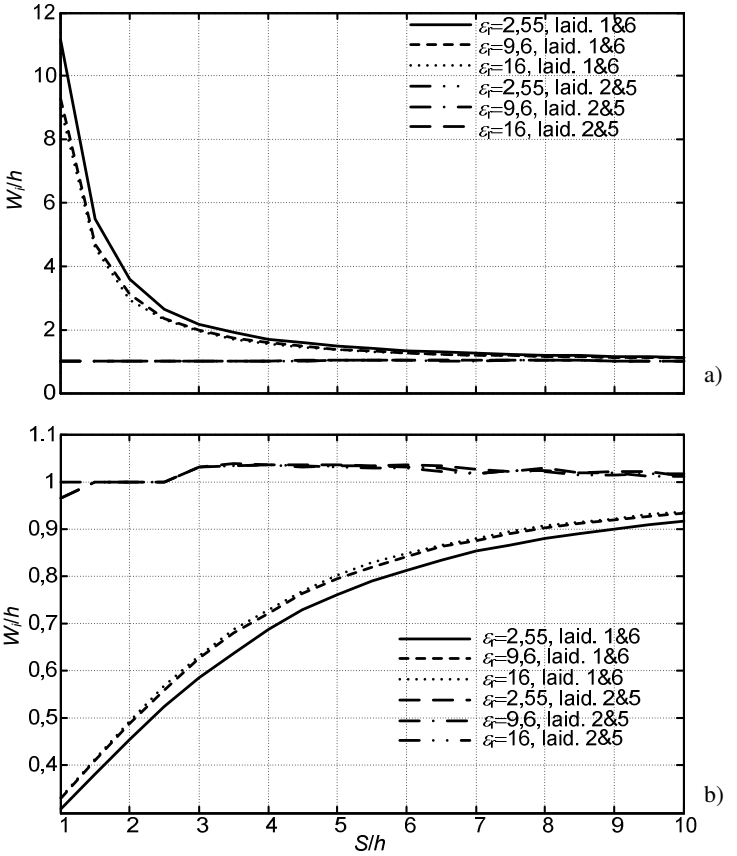

S6 pav. Normuotųjų laidininkų pločių priklausomybė nuo tarpo tarp laidininkų dydžio esant skirtingoms pagrindo santykinėms dielektrinėms skvarboms: a) lyginės bangos ir b) nelyginės bangos atvejais

1. Nustatomi pradiniai daugialaidės linijos parametrai: laidininkų pločiai W_i, tarpai tarp laidininkų S_i, pagrindo storis h ir dielektrinė konstanta ε_r.
2. Sintezė pradedama nuo pirmosios laidininkų poros.
3. Skaičiuojamos modos įtampos (kaip aprašyta 2-ajame skyriuje).
4. Tikrinama, ar n-tosios laidininkų poros modos įtampos yra norimose ribose, jei ne atliekas 5-asis žingsnis, jei taip, pereinama į 6-ąjį žingsį.
5. n-tosios poros laidininkų pločiai keičiami pagal (3.5) arba (3.6) išraiškas ir pereinama į 3-iąjį žingsnį.
6. Tikrinama, ar visos laidininkų poros perskaičiuotos, jei taip, pereinama į 8-ąjį žingsni, jei ne –pereinama į 7-ąjį žingsnį.
7. Laidininkų poros rodiklis n padidinamas 1 ir grįžtama į 3-ąjį žingsnį.
8. Tikrinama, ar visų laidininkų modos įtampos yra norimose ribose. Jei ne – visi laidininkai yra skaičiuojami nuo 2-ojo žingsnio, jei taip – laikoma, kad linijos sintezė baigta ir pereinama į 9-ąjį žingsnį.
9. Rezultatai išsaugojami ir skaičiavimas baigiamas.

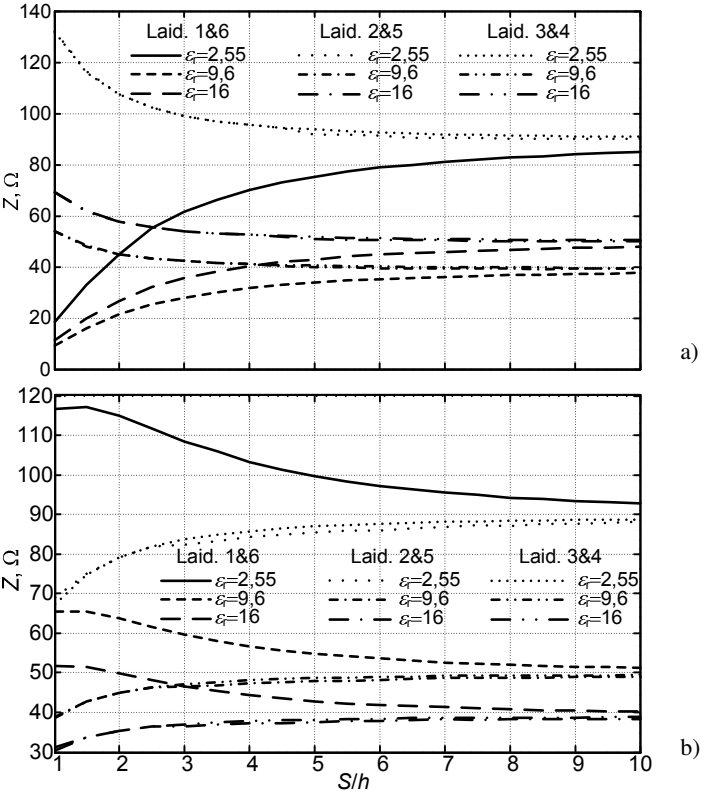

S7 pav. Sintezuotųjų simetrinių šešių laidininkų mikrojuostelinių linijų, veikiančių a) lyginės ir b) nelyginės normaliosios bangos režimu laidininkų charakteringieji impedansai, kai $W_{3,4}/h = 1$

5-ajame žingsnyje numatytas laidininkų pločių keitimas atliekamas remiantis Niutono-Rapsono metodu, pagal išraišką:

$$x_{i+1} = x_i - f(x_i)\frac{x_i - x_{i-1}}{f(x_i) - f(x_{i-1})}, \quad \text{(S1)}$$

čia x_{i+1} – kita ieškomo parametro reikšmė, x_i ir x_{i-1} – atitinkamai paskutinė ir priešpaskutinė bandyta (iteruota) parametro reikšmės, $f(x_i)$ ir $f(x_{i-1})$ – atitinkamai paskutinė ir priešpaskutinė funkcijos (charakteristikos) reikšmės.

Taikant sukurtą metodiką atliktos 4-ių ir 6-ių laidininkų daugialaidžių linijų sintezės. Išnagrinėta, kiek turi būti keičiami laidininkų pločiai esant įvairiam tarpų tarp laidininkų dydžiui ir skirtingoms pagrindo dielektrinėms konstantoms (S6 pav.).

Taip pat visiems atvejams rastos efektyviosios skvarbos ir laidininkų charakteringieji impedansai.

Nustatyta, kad didžiausią įtaką modų įtampoms turi kraštiniai laidininkai. Siekiant suvienodinti lyginės modos įtampas kraštinius laidininkus reikia platinti, siekiant suvienodinti nelyginės modos įtampas, kraštinius laidininkus reikia siaurinti. Kuo tarpai tarp laidininkų mažesni, tuo daugiau reikia keisti kraštinius laidininkus. Keičiant tik kraštinių laidininkų pločius galima pasiekti modų įtampų skirtumus ne didesnius nei 2%.

Modeliuojant taip pat apskaičiuotos daugialaidės linijos elektrinės charakteristikos. S7 paveiksle pateiktos laidininkų charakteringųjų impedansų priklausomybės nuo tarpo tarp laidininkų. Iš grafikų matyti, kad kraštinių laidininkų charakteringieji impedansai ženkliai skiriasi nuo likusiųjų. Lyginės modos atveju, kraštinių laidininkų pločiai yra didesni nei likusiųjų, todėl jų ilgio vieneto talpos yra didesnės, ir atitinkamai charakteringieji impedansai mažesni. Apskaičiavus laidininkų pločius, reikalingus užtikrinti vienodus fazinius greičius nelyginei modai, išorinių laidininkų pločiai yra mažesni, nei likusiųjų. Tokiu atveju šių laidininkų ilgio vieneto talpos yra mažesnės, ir atitinkamai charakteringieji impedansai didesni. Analizuojant grafikus S7 paveiksle matyti, kad šis skirtumas mažėja didinant tarpą tarp laidininkų. Šis skirtumas didesnis esant mažesnei pagrindo dielektrinei skvarbai.

4. Hibridiniai meandrinės mikrojuostelinės vėlinimo linijos sluoksniuotame dielektrike modeliai

Remiantis sukurta sintezės metodika ir daugialaidžių linijų metodu, suprojektuota meandrinė vėlinimo linija, grįsta daugialaide mikrojuosteline linija, veikiančia lyginių normaliųjų bangų režimu. Projektuojant meandrinę vėlinimo liniją daugialaidžių linijų metodu, iš pradžių sintezuojama daugialaidė mikrojuostelinė linija veikianti lyginės normaliosios bangos režimu (S8 pav. a)). Iš norimo ilgio sintezuotos linijos segmento suformuojama meandrinė linija (S8 pav. b)).

Siekiant patikrinti tokios linijos charakteristikas, suprojektuota linija sumodeliuota Sonnet® programa.

Siekiant patikrinti oro mikrosluoksnio įtakos dviekranių vėlinimo įtaisų sluoksniuotame dielektrike elektrinėms charakteristikoms, remiantis daugialaidžių linijų sluoksniuotoje dielektrinėje terpėje modeliu ir S-parametrų matricų metodu

suprojektuota dviekranė meandrinė vėlinimo linija (S9 pav.). Oro mikrosluoksnio įtaka šioje linijoje įvertinta pagal 2-ajame skyriuje siūlomą metodiką, ir charakteristikos apskaičiuotos S-parametrų matricų metodu bei palyginimui momentų metodu grįsta programa Sonnet®.

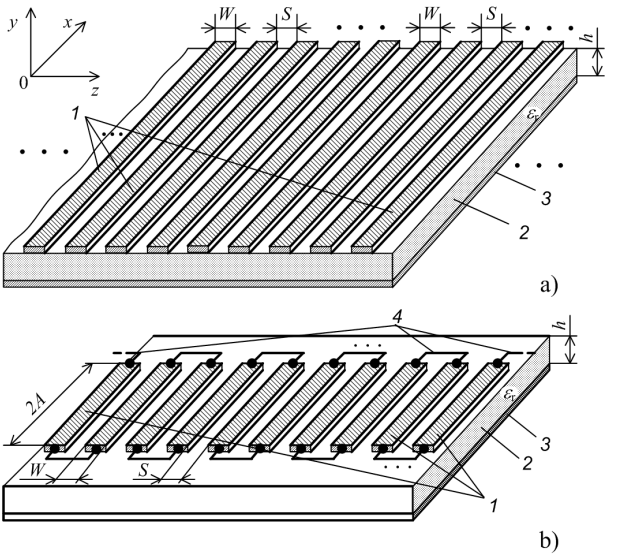

S8 pav. Meandrinės linijos modelio sudarymas: a) Mikrojuostelinės daugialaidės linijos struktūra, ir b) mikrojuostelinės meandrinės vėlinimo linijos, grįstos daugialaide linija, modelis: 1 – signaliniai laidininkai, 2 – dielektrinis pagrindas, 3 – ekranas, 4 – meandro strypų sujungimai

S-parametrų matricų metodų gauta vėlinimo trukmė t_d = 7,1 ns, o programa Sonnet® – $t_d \approx 7{,}4$ ns.

Rezultatų adekvatumas parodė, kad siūloma metodika taikytina projektuojant tokius įtaisus.

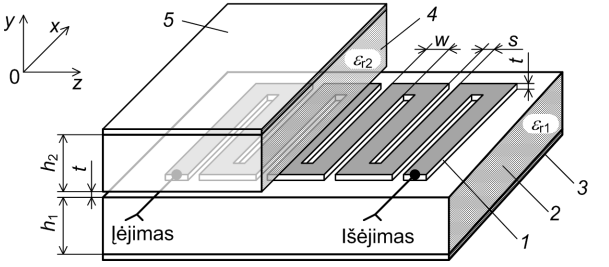

S9 pav. Dviekranės mikrojuostelinės meandrinės vėlinimo linijos struktūra: 1 – meandro formos signalinis laidininkas, 2 – apatinė dielektrinė plokštelė, 3 – apatinis ekranas, 4 – viršutinė dielektrinė plokštelė, 5 – viršutinis ekranas; vaizdumo dėlei dalis viršutinio ekrano nepavaizduota

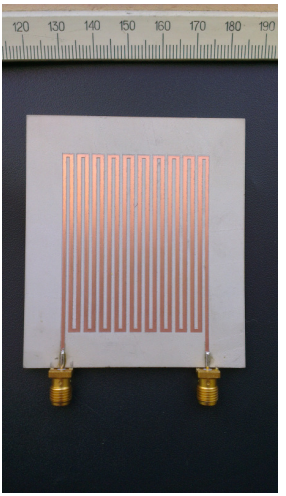

S10 pav. Dviekranės meandrinės mikrojuostelinės vėlinimo linijos maketas (prieš surinkimą); maketo parametrai: $\varepsilon_{r1} = \varepsilon_{r2} = 6{,}15$, $W = 1{,}1$ mm, $h_1 = h_2 = 1{,}27$ mm, $S = 1{,}0$ mm, $t_1 = 0{,}035$ mm, $2A = 50$ mm, meandro strypų skaičius $N = 20$

Taip pat siekiant patikrinti modelio adekvatumą, buvo pagamintas ir ištirtas dviekranės meandrinės vėlinimo linijos eksperimentinis maketas (S10 pav.).

Vėlinimo linijos charakteristikos išmatuotos osciloskopu PicoScope 9312 padedant UAB „Eltesta“ inžinieriams. Matavimų oscilogramos pateiktos S11 paveiksle.

Siekiant išmatuoti linijos vėlinimo trukmę, į vėlinimo linijos įėjimą buvo siunčiamas žingsnio formos signalas ir matuojamas laikas, po kurio signalas išėjime pasiekia 0,5 nusistovėjimo įtampos vertės.

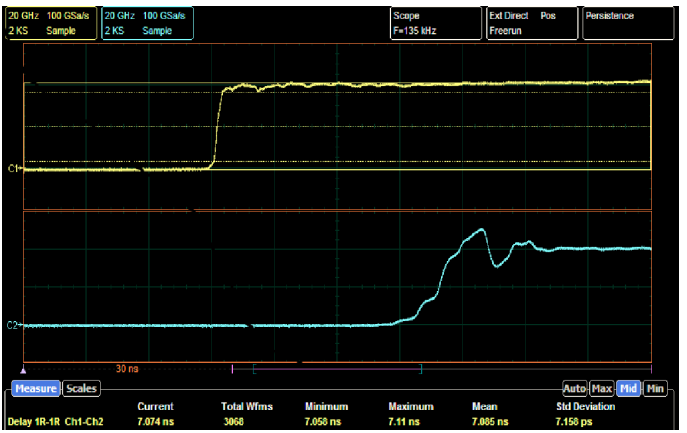

S11 pav. Pereinamųjų procesų vėlinimo linijos įėjime (viršutinė kreivė) ir išėjime (apatinė kreivė) oscilogramos

Matuojant gautos tokios vėlinimo trukmės reikšmės: vidutinė vėlinimo trukmė – 7,094 ns, didžiausia išmatuota – 7,11 ns, mažiausia išmatuota – 7,058 ns, vidutinis nuokrypis – 7,158 ps. Gauti matavimo rezultatai yra artimi S-parametrų matricų metodu apskaičiuotais rezultatais – 7,1 ns.

Laikant, kad faziniai iškraipymai neturi viršyti 0,35 rad, vėlinimo linijos pralaidumo juosta randama pagal išraišką:

$$\Delta F = \frac{0{,}35}{2\pi\Delta t}, \tag{S2}$$

čia Δt – vėlinimo trukmės dispersijos nuokrypis nuo vidutinės vėlinimo trukmės reikšmės, iki vėlinimo trukmės reikšmės esant fazinės charakteristikos nuokrypiui nuo idealios 0,35 rad. Pagal apskaičiuotas charakteristikas ir išraišką (S2) gauta apie $\Delta F \approx 300$ MHz. pralaidumo juosta.

Pagal išėjimo signalo pereinamojo proceso formą (S11 pav.) matyti, kad įtampa nuo 0,1 iki 0,9 pastovios vertės pakyla per 1,2 ns. Linijos pralaidumo juosta ΔF remiantis šiais parametrais skaičiuojama pagal išraišką:

$$\Delta F = \frac{0{,}35}{\tau_{\mathrm{t}}}, \tag{S3}$$

čia τ_{t} yra išėjimo signalo pakilimo laikas nuo 0,1 iki 0,9 pastovios vertės. Pagal išraišką (S3) apskaičiuota pralaidumo juosta yra apie $\Delta F \approx 300$ MHz.

Remiantis sukurtos, sluoksniuotos dielektrinės terpės įtakos įvertinimo elektrinėms vėlinimo linijų charakteristikoms, metodikos taikymo rezultatais ir pagaminto maketo matavimo rezultatais matyti, kad sukurta metodika yra adekvati ir taikytina tokių įtaisų projektavime.

Bendrosios išvados

1. Sukurta sluoksniuotos dielektrinės terpės įtakos juosteliniams įtaisams įvertinimo metodika. Ši metodika naudinga projektuojant juostelinius vėlinimo įtaisus. Taikant šią metodiką galima parinkti sluoksnių dielektrines skvarbas ir storius taip, kad susietųjų juostelinių linijų efektyviosios dielektrinės skvarbos lyginei ir nelyginei normaliosioms bangoms būtų vienodos. Ši savybė naudinga projektuojant perdavimo ir vėlinimo linijas. Minėtoji metodika taip pat pritaikyta oro mikrosluoksnio įtakai dviekranių juostelinių įtaisų elektrinėms charakteristikoms įvertinti.
2. Sukurta daugialaidžių mikrojuostelinių linijų, veikiančių lyginių arba nelyginių normaliųjų bangų režimu metodika. Normaliosios bangos režimas pasiekiamas dviem būdais – pirmuoju, keičiant laidininkais sklindančių signalų įtampas, antruoju – keičiant laidininkų gabaritus taip, kad konkrečiai vienai normaliajai bangai įtampų moduliai būtų vienodi. Pastarasis yra labiau praktiškai pritaikomas. Taikant sukurtą

sintezės metodiką randami daugialaidės mikrojuostelinės vėlinimo linijos laidininkų pločiai, kuriems esant laidininkų įtampų moduliai konkrečiai modai yra vienodi.

3. Suprojektuota mikrojuostelinė meandrinė vėlinimo linija, grįsta daugialaidės mikrojuostelinės linijos, veikiančios lyginių normaliųjų bangų režimu, modeliu ir modeliuojant rastos linijos charakteristikos. Nustatyta, kad tokios linijos faziniai iškraipymai sumažinami 2%, lyginant su analogiška vėlinimo liniją, grįsta daugialaidės mikrojuostelinės linijos, veikiančios mišriųjų bangu režimu (t. y. tokios, kurios visi laidininkai vienodo pločio), modeliu.
4. Naudojant hibridinį metodą, grįstą sukurta daugiasluoksnės terpės įtakos juostelinių įtaisų charakteristikoms įvertinimo metodika ir S-parametrų matricų metodu, suprojektuota dviekranė meandrinė juostelinė vėlinimo linija. Linija modeliuota momentų metodu grįsta programine įranga, taip pat pagamintas ir eksperimentiškai ištirtas linijos prototipas. Nustatyta, kad vėlinimo trukmės vertė, gauta darbe sukurtu metodu, nuo gautos komercine, momentų metodu grįsta, programine įranga, skiriasi apie 2%, o nuo išmatuotos skiriasi apie 1%. Siūloma metodika yra adekvati ir taikytina tokių įtaisų projektavime.

Annexes[1]

Annex A. The co-authors agreement to present publications material in the dissertation.
Annex B. Copies of scientific publications by the author on the topic of the dissertation.

[1] Annexes are available in the CD attached to the dissertation.

Šarūnas MIKUČIONIS

MODELLING OF STRATIFIED DIELECTRIC MEDIUM STRIPLINE DELAY DEVICES

Doctoral Dissertation

Technological Sciences,
Electrical and Electronic Engineering (01T)

SLUOKSNIUOTOS DIELEKTRINĖS TERPĖS JUOSTELINIŲ VĖLINIMO ĮTAISŲ MODELIAVIMAS

Daktaro disertacija

Technologijos mokslai,
elektros ir elektronikos inžinerija (01T)

2014 12 15. 11,0 sp. l. Tiražas 20 egz.
Vilniaus Gedimino technikos universiteto
leidykla „Technika“,
Saulėtekio al. 11, 10223 Vilnius,
http://leidykla.vgtu.lt
Spausdino UAB „Ciklonas“
J. Jasinskio g. 15, 01111 Vilnius.